UNIVERSITÀ POLITECNICA DELLE MARCHE

FACOLTÀ DI INGEGNERIA

Corso di Laurea Magistrale in Biomedical Engineering

Study and development of algorithms for the home assessment of gait parameters related to fall risk in Parkinsonian patients through a single wearable sensor

Relatore:

Dott. Lorenzo Palma

Correlatore:

Dott.ssa Paola Pierleoni

Candidato:

Luca Lorusso

Anno Accademico 2020/2021

INDEX

Introduction I

CHAPTER 1: PARKINSON'S DISEASE AND ITS EFFECTS ON POSTURAL STABILITY 1

1.1 GENERAL DESCRIPTION OF PARKINSON'S DISEASE 1

1.2 HOW PARKINSON'S DISEASE AFFECTS THE POSTURAL STABILITY 2

1.3 MEASUREMENT SYSTEMS TO EVALUATE THE POSTURAL STABILITY 4

1.3.1 RATING SCALES AND GOLD STANDARD TECHNIQUES 4

1.3.2 WEARABLE SENSORS 7

1.4 FOCUS ON GAIT ANALYSIS AND GAIT CYCLE 8

CHAPTER 2: STATE OF THE ART 12

2.1 WORKS CARRIED OUT IN LABORATORY SETTING 12

2.1.1 THE STUDY OF THE MAIN DOMAINS OF MOTOR DYSFUNCTIONS 12

2.1.1 SWAY, ANTICIPATORY POSTURAL ADJUSTEMENTS AND POSTURAL RESPONSES 13

2.1.2 GAIT 16

2.2 WORKS CARRIED OUT IN HOME SETTING 17

2.2.1 FREEZING OF GAIT 17

2.2.2 FALL RISK, FALL DETECTION AND FALL PREVENTION 23

2.3 FINAL CONSIDERATIONS ABOUT THE STATE OF THE ART 38

CHAPTER 3: THE NEXT GENERATION INERTIAL MEASUREMENT UNIT DEVICE 44

3.1 GENERAL DESCRIPTION OF THE DEVICE 44

3.2 TECHNICAL CHARACTERISTICS OF THE DEVICE 45

3.3 ACCELEROMETER 49

3.4 ROTATION MATRICES, EULER ANGLES, AND QUATERNIONS 50

CHAPTER 4: EXPERIMENTAL TRIALS 55

4.1 LABORATORY TRIALS 55

4.2 HOME TRIALS 57

CHAPTER 5: DATA ACQUISITION AND SOFTWARE IMPLEMENTATION 59

5.1 DATA ACQUISITION 59

5.2 SOFTWARE IMPLEMENTATION 60

5.2.1 PRE-PROCESSING 63

5.2.2 EXTRACTION OF ACTIVITY SEGMENTS 67

5.2.3 EXTRACTION OF WALKING SEGMENTS 71

5.2.4 QUATERNIONS 74

5.2.5 EXTRACTION OF WALKING SEGMENTS WITH "REAL" STEPS 77

5.2.6 EXTRACTION OF PARAMETERS 85

5.2.7 GRAPHICAL USER INTERFACE 90

CHAPTER 6: RESULTS 92
6.1 EXPLANATION OF THE FINAL OUTPUTS 92
6.2 RESULTS FROM LABORATORY RECORDINGS 94
6.3 RESULTS FROM HOME RECORDINGS 103
6.4 THE PERCENTAGE ERROR OF THE ALGORITHM 136
Discussions III
Conclusions X
REFERENCES XII

Introduction

Parkinson's disease is a widespread neurodegenerative disorder that is estimated to affect almost ten million people in the world [1], [2]. Although the real cause of this pathology is still unknown, it certainly compromises the quality of life of people suffering from it, since it entails serious motor and cognitive disorders. Tremor, rigidity, akinesia, bradykinesia, postural instability, and gait difficulties are the most common motor symptoms that appear with Parkinson's disease [3], [4]. These manifestations are accompanied by cognitive problems (memory loss and concentration difficulties), depression, sleep disturbances, autonomic dysfunction, psychiatric changes, and sensory symptoms. As a consequence, the capacity to maintain balance while performing simple activities of daily living, like walking, is generally impaired in parkinsonian subjects. This fact dramatically increases the probability to experience loss of balance episodes like falls. This, in turn, can lead to physical and mental consequences on victims like serious injuries due to falls and the continuous anxiety due to the "fear of falling". Moreover, the disease deterioration due to the aging process causes a progressive worsening of these motor symptoms and this inevitably augments the fall risk [5]–[7]. Since the elderly population and the problems related to falls have been constantly increasing in recent years, the development of new technologies and systems able to study balance and gait characteristics related to fall risk is becoming a topic of primary interest. Traditional methods to assess the severity of the disease, the level of autonomy of patients, and in general to treat people affected by Parkinson's disease are rating scales based on questionnaires or based on the observation of the subject [8]. Although they must satisfy certain standards of reliability, appropriateness, sensibility, and validity, they do not provide an objective tool able to define the actual status of the disease [7], [9]. For this reason, objective recordings obtained from stereophotogrammetry, dynamometric force platforms, and electromyography are frequently adopted. They are the gold standard techniques that are used to perform the gait analysis, which is the systematic study of the human motion in people affected by compromised ability to walk. Gait analysis performed through these instruments allows to obtain the values of some meaningful parameters related to balance while walking, freezing of gait, and fall risk. What's more, these tools ensure the highest performances in terms of accuracy and reliability, but they are expensive and uncomfortable for

patients. In addition, both scales and gold standards are time consuming and difficult to be applied since they require lab examinations and specialized personnel to be executed [10]. During these examinations, patients are asked to simulate some activities of daily living, like simple walking, or specific motor tasks that are known to induce loss of balance events [9], [11]. It means that this approach is not the best in terms of "real validity" of the results because patients perform activities in a different manner and context with respect to their daily life. Indeed, either patients are more concentrated in the execution of the task, or their walks are more compromised than normal. Wearable devices based on inertial measurement units represent the near future in the study of human motion since they can overcome the above-mentioned limitations [12]. These devices usually include three or more sensors, which are tri-axial accelerometer, gyroscope, and magnetometer and eventually barometer or other visionary or ambient sensors [13]. They can be comfortably positioned in different body segments and used to obtain objective recordings for real-time or offline applications. Furthermore, they are cheap, lightweight, and can be easily used in home settings. Thus, they allow to estimate parameters associated with balance while walking and fall risk without the necessity that patients leave their preferred environments. This can give clinicians a "realistic" picture of the walking capacity of patients since metrics are extracted from long-term recordings while subjects perform daily activities in their usual manners. However, the major limitations that prevent the diffusion of these tools are their performances which, in many cases, are unknown or lower compared to gold standards [14]. In literature, there are several works (from 2013 to 2021) that present systems based on wearable sensors to perform gait analysis, to study freezing of gait and fall risk, but also to detect or prevent falls in parkinsonian subjects. At the same time, there is no wide consensus about the optimal type, number, and location of sensors, features to be extracted, motor tasks to be performed, and validation procedure. This thesis tries to solve this problem by proposing a solid method which combines some of the most promising approaches seen in literature with new solutions to obtain the best result. In fact, the aim of this work is to study and develop algorithms for the home assessment of gait parameters related to fall risk in parkinsonian people using a single wearable sensor. Once this methodology will be improved, doctors will be able to investigate how the postural stability is compromised for each patient and optimize the medical therapy

for each of them. This could potentially lead to the reduction or prevention of dangerous situations like falls, finally improving the quality of life of people affected by Parkinson's disease.

CHAPTER 1: PARKINSON'S DISEASE AND ITS EFFECTS ON POSTURAL STABILITY

1.1 GENERAL DESCRIPTION OF PARKINSON'S DISEASE

Parkinson's Disease (PD) is a very common neurodegenerative progressive disorder that is characterized by motor and non-motor symptoms [1], [2]. PD is the second most widespread neurological disorder as it is estimated to affect one million people in the United States and seven to ten million people in the world. The causes of PD are still unknown but some risk factors that increase the chances of having this disease are related to age, genetic, and gender. When PD occurs, dopamine producing neurons, that live in an area of the basal ganglia called substantia nigra, die and/or become impaired and Lewy bodies are present in the remaining dopaminergic neurons [3]. This area of the midbrain is associated with the control of movements. Thus, the reduction in the amount of dopamine in the brain causes the typical motor signs of PD which are rest tremor, rigidity, akinesia, bradykinesia, postural instability, and gait difficulties [4]. Tremor is one of the first symptoms to appear, and it is initially unilateral but then progresses to bilateral over the years. Tremor can be classified based on the frequency domain in rest tremor (frequencies lower than 6 Hz), postural tremor (frequencies between 6 and 9 Hz), kinetic tremor (frequencies higher than 6 Hz) and can be detected by means of a bracelet attached to the patient wrist. Rigidity is the raised resistance opposed to passive joint movement that is more pronounced in presence of tremor. Akinesia is the absence of movement, while bradykinesia is the slowness of movement that causes difficulties in initiating a movement or in performing a fine motor task. Postural instability and gait difficulties are related to loss of balance and increased risk of fall. The gait becomes slower, with decrease in arm swing and reduction in stride length followed by shuffling steps, stooped posture and "en bloc" turning. Freezing refers to an intermittent inability to move that occurs during gait initiation or when there is hesitation in avoiding an obstacle since the person moves forward the Centre of Mass (COM), the point equivalent of the total body mass, while the foot is like "iced" to the soil. The Freezing of Gait (FoG) is associated with fluctuations or variability of motor capacity of a person during the day since in parkinsonian subjects there are moments of the day in which they are stable and moments in which they lose balance. FoG can be studied to detect the fall risk by means of sensors positioned on the chest and on the

feet of the subject. At the same time, there are also non-motor symptoms that appear in case of PD, like cognitive problems (memory loss and concentration difficulties), depression, sleep disturbances, autonomic dysfunction, psychiatric changes, and sensory symptoms. The motor and non-motor symptoms of PD are shown in Figure 1. The most used therapy to treat PD and to improve the quality of life of affected people is the levodopa administration, which is a dopamine precursor that can induce the dopaminergic neurons to produce more dopamine. PD cannot be diagnosed with traditional laboratory or blood tests. Instead, diagnosis is generally based on neurological examination or personal history. Also the gradual progression of motor and non-motor symptoms together with the patient "positive" reaction to drug therapy with levodopa, is considered the hallmark for PD diagnosis.

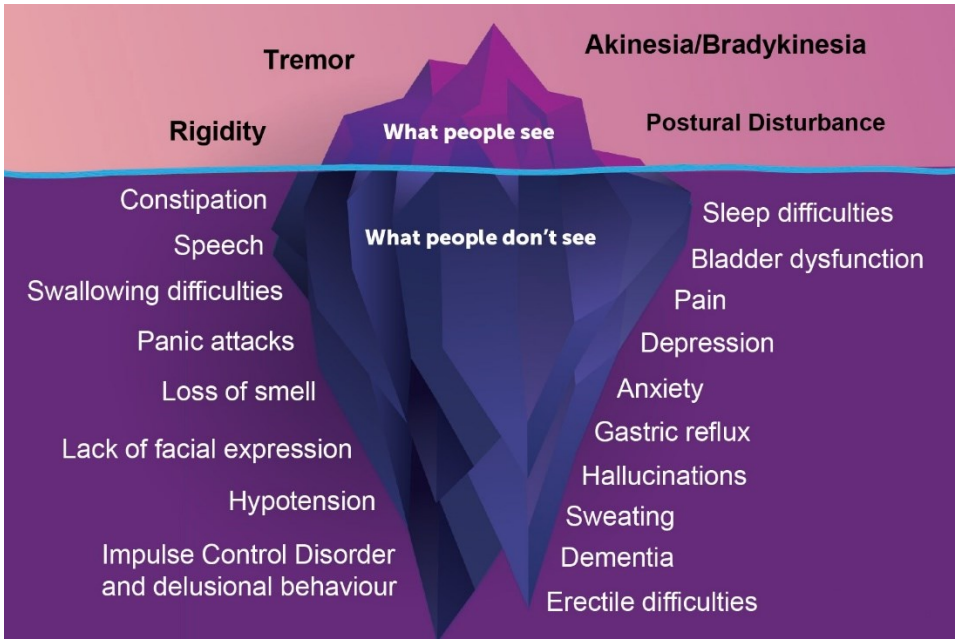

Figure 1: this figure shows the Parkinson's iceberg in which the main motor and non-motor symptoms of PD are illustrated. In the upper part the "visible" symptoms can be appreciated, while in the lower part the "non-visible" symptoms are reported [15].

1.2 HOW PARKINSON'S DISEASE AFFECTS THE POSTURAL STABILITY

In pathological conditions like PD, motor and cognitive deteriorations of the disease increase the risk of falls[5]. Additionally, the aging process in parkinsonian subjects but also in healthy people is associated with a progressive decrease in the capacity of performing daily motor skills and with an increased risk of falling [6], [7]. The constant

increase of the elderly population and of dangers related to falls is causing the development of new technologies, systems, and measurement instruments able to assess posture, balance, and to detect the risk of falling. Posture describes the orientation of any body segment relative to the gravitational vector, with correct alignment of axial body parts in the medio-lateral (ML) and anterior-posterior (AP) plane. Postural stability or postural control or balance are generic terms that describe the dynamics of body posture to prevent falling. They are the ability to maintain the body's COM over its base of support under static and dynamic conditions by adjusting the position of the body's Centre of Pressure (COP), the point location of the vertical ground reaction force that represents the weighted average of all the pressures over the surface of the area in contact with the ground. The location of the COP under each foot is governed by the muscular activity (mainly due to muscles at the trunk and at the lower limbs), ligamentous tension, and body weight that all together are responsible for the maintenance of stability. Static posturography, also known as static balance, is the dynamics of the postural control system associated with the maintaining balance during quiet standing. On the other hand, dynamic posturography or dynamic balance is the ability of postural control system to maintain balance when some body parts are in movement, like during walking or in response to applied or volitional perturbations. Gait or walking is the rhythmic alternation of leg movements to move the body forward. Both static and dynamic balance depend on several aspects regarding the characteristics of the subject, the task to be performed and the environment. The maintenance of balance is guaranteed by a complex sensorimotor system which integrates information from the visual, vestibular, and somatosensory systems, as shown in Figure 2. Vision is the system involved in the planning of locomotion and avoiding obstacles along the way. Vestibular system senses linear and angular accelerations, while somatosensory system is a multitude of sensors that sense position and velocity of all body segments, their contact with external objects, and the orientation of gravity. Dysfunctions at any of these components, as in the case of PD, or environmental factors, or changes in the task, can compromise the balance and enhance the risk of fall. Falls are involuntarily and sudden events during which the subject loses balance and reaches the ground. Falls can lead to severe injuries and even cause mortality. Thus, it is very important to predict and prevent these kinds of situations or at least to detect them in real-time to alert in short

time help centres or healthcare providers. Unobtrusive and precise technologies that allow a long-term monitoring or gait analysis in home settings of elderly people or subjects affected by balance disorders pathologies like PD are required.

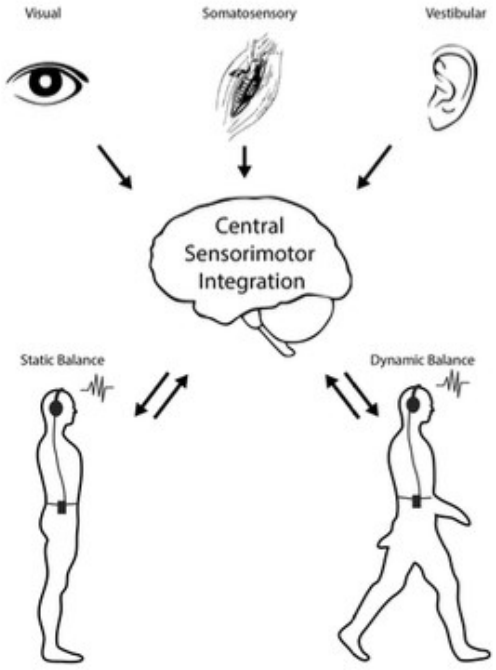

Figure 2: this figure illustrates the sensorimotor integration of visual, somatosensory, and vestibular systems that are responsible for the maintenance of balance and postural stability [16].

1.3 MEASUREMENT SYSTEMS TO EVALUATE THE POSTURAL STABILITY

1.3.1 RATING SCALES AND GOLD STANDARD TECHNIQUES

To assess the severity of the disease and to evaluate the level of autonomy of the patient in performing Activity of Daily Living (ADL), rating scales based on questionnaires or based on observation of the patient are generally used [8]. In scales based on questionnaires, clinicians give a score depending on the answers of the patients about their ability in performing specific motor tasks. For example, the Activities-specific Balance Confidence scale (ABC) to assess the fear of falling of parkinsonian patients. In scales based on observation of the patient, clinicians assign a score to each item of the scale itself while the patient is executing specific motor tasks. For example, the Unified Parkinson's Disease Rating Scale (UPDRS) that is the most widespread rating scale for PD and is divided in subscales in which the symptoms of PD and the status of the patients

are quantified with a scoring system [17]. Although these scales (reported in Figure 3) must guarantee certain levels of appropriateness, reliability, validity and, sensibility (or resolution), they do not utilize an objective criterion to define the actual status of the disease [7], [9]. In fact, both types of the scales depend on the patients' self-awareness and on the examiners' experience since the scoring is subjective and results difficult to be interpreted. Indeed, examiners and patients' scores to grade the same motor task are generally different. Moreover, there is no scale that can be used to assess information about gait, balance, and posture at the same time, because of the heterogeneity of these aspects. This means that more than one scale must be simultaneously used to obtain a complete overview of the patient's status and disease's stage. This procedure requires a certain compatibility in the scoring system among different scales which is still a real challenge in biomedical field. Most importantly, although these scales provide useful information about impaired balance capacity and consequent fall risk, they do not offer real-time monitoring on the patient's loss of balance events (like falls). Due to the above considerations, these scales are usually adopted as evaluation tools and not as diagnostic tools for the identification of the general clinical manifestations of parkinsonian subjects without specific consideration about pathophysiology of the condition.

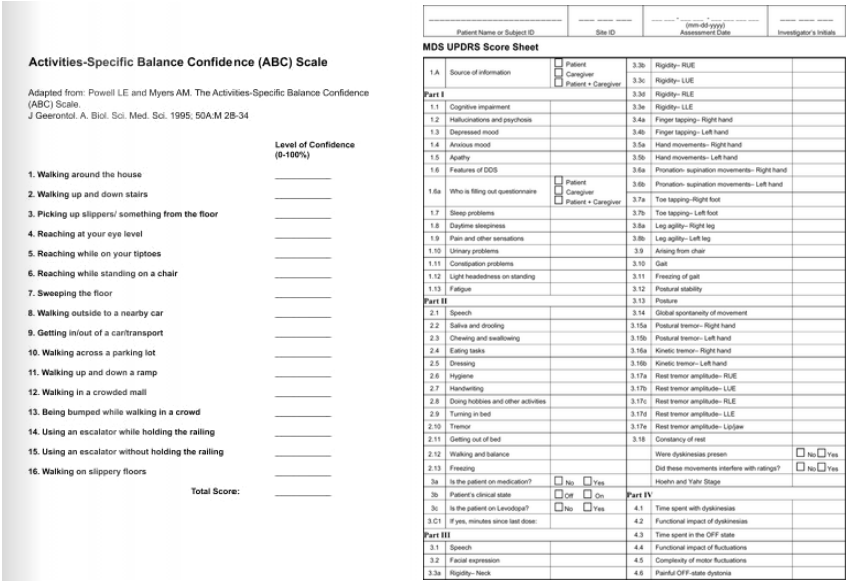

Activities-Specific Balance Confidence (ABC) Scale

Adapted from: Powell LE and Myers AM. The Activities-Specific Balance Confidence (ABC) Scale.
J Geerontol. A. Biol. Sci. Med. Sci. 1995; 50A:M 28-34

	Level of Confidence (0-100%)
1. Walking around the house	
2. Walking up and down stairs	
3. Picking up slippers/ something from the floor	
4. Reaching at your eye level	
5. Reaching while on your tiptoes	
6. Reaching while standing on a chair	
7. Sweeping the floor	
8. Walking outside to a nearby car	
9. Getting in/out of a car/transport	
10. Walking across a parking lot	
11. Walking up and down a ramp	
12. Walking in a crowded mall	
13. Being bumped while walking in a crowd	
14. Using an escalator while holding the railing	
15. Using an escalator without holding the railing	
16. Walking on slippery floors	
Total Score:	

Patient Name or Subject ID | Site ID | (mm-dd-yyyy) Assessment Date | Investigator's Initials

MDS UPDRS Score Sheet

1.A	Source of information	☐ Patient ☐ Caregiver ☐ Patient + Caregiver	3.3b	Rigidity– RUE	
			3.3c	Rigidity– LUE	
Part I			3.3d	Rigidity– RLE	
1.1	Cognitive impairment		3.3e	Rigidity– LLE	
1.2	Hallucinations and psychosis		3.4a	Finger tapping– Right hand	
1.3	Depressed mood		3.4b	Finger tapping– Left hand	
1.4	Anxious mood		3.5a	Hand movements– Right hand	
1.5	Apathy		3.5b	Hand movements– Left hand	
1.6	Features of DDS		3.6a	Pronation- supination movements– Right hand	
1.6a	Who is filling out questionnaire	☐ Patient ☐ Caregiver ☐ Patient + Caregiver	3.6b	Pronation- supination movements– Left hand	
			3.7a	Toe tapping–Right foot	
1.7	Sleep problems		3.7b	Toe tapping– Left foot	
1.8	Daytime sleepiness		3.8a	Leg agility– Right leg	
1.9	Pain and other sensations		3.8b	Leg agility– Left leg	
1.10	Urinary problems		3.9	Arising from chair	
1.11	Constipation problems		3.10	Gait	
1.12	Light headedness on standing		3.11	Freezing of gait	
1.13	Fatigue		3.12	Postural stability	
Part II			3.13	Posture	
2.1	Speech		3.14	Global spontaneity of movement	
2.2	Saliva and drooling		3.15a	Postural tremor– Right hand	
2.3	Chewing and swallowing		3.15b	Postural tremor– Left hand	
2.4	Eating tasks		3.16a	Kinetic tremor– Right hand	
2.5	Dressing		3.16b	Kinetic tremor– Left hand	
2.6	Hygiene		3.17a	Rest tremor amplitude– RUE	
2.7	Handwriting		3.17b	Rest tremor amplitude– LUE	
2.8	Doing hobbies and other activities		3.17c	Rest tremor amplitude– RLE	
2.9	Turning in bed		3.17d	Rest tremor amplitude– LLE	
2.10	Tremor		3.17e	Rest tremor amplitude– Lip/jaw	
2.11	Getting out of bed		3.18	Constancy of rest	
2.12	Walking and balance			Were dyskinesias presen	☐ No ☐ Yes
2.13	Freezing			Did these movements interfere with ratings?	☐ No ☐ Yes
3a	Is the patient on medication?	☐ No ☐ Yes		Hoehn and Yahr Stage	
3b	Patient's clinical state	☐ Off ☐ On	**Part IV**		
3c	Is the patient on Levodopa?	☐ No ☐ Yes	4.1	Time spent with dyskinesias	
3.C1	If yes, minutes since last dose:		4.2	Functional impact of dyskinesias	
Part III			4.3	Time spent in the OFF state	
3.1	Speech		4.4	Functional impact of fluctuations	
3.2	Facial expression		4.5	Complexity of motor fluctuations	
3.3a	Rigidity– Neck		4.6	Painful OFF-state dystonia	

Figure 3: on the left the ABC scale is shown, while on the right the UPDRS scale is reported [18], [19].

These factors introduce the need for measurement tools (e.g., wearable sensors) which provide objective and automated assessments, and that can be used not only in laboratories while the subject is performing specific motor tasks but also in patient's homes, to allow precise and prolonged monitoring of the patient's motor symptoms during daily life. Objective recordings by means of wearable sensors can help extract meaningful data with lower quantity of errors as compared to scales, in a comfortable and easy way. Some events like FoG, falls, or night-time disability are caused by PD and randomly occur during the day, while are absent during routine clinical visits. Through the usage of wearable tools, such situations can be revealed since they enable the assessment in home setting of the patient during a common day. In addition, small changes in the conditions of the patients due to the disease or to the effects of a therapy cannot be detected by means of classical scales but only using the wearable devices. At the same time, scales can be used to verify the clinical validity of these sensors. Despite the potential health benefits and improvements in patients' management and quality of life, the objectivity of the recordings, the possible cooperation with a team of clinicians, and the increased acceptance of the patients since the measurements are performed in their preferred environments, further scientific progress is needed to improve the performances of these sensors.

Indeed, the gold standard techniques for the quantitative estimation of the human balance to evaluate the risk of fall and the balance-related disabilities due to PD are stereophotogrammetry, electromyography, and dynamometric force plates. Stereophotogrammetry estimates three-dimensional coordinates of points which belong to an object by means of some cameras that acquire simultaneous images from different locations. Therefore, it requires a specific motion laboratory to be applied. Electromyography aims at recording the electrical activity of skeletal muscles and it is generally executed by clinicians or technicians. Force platforms are used to reconstruct the trajectory of the COP when the subject stands quietly or while executing a specific motor task [14], [20]. The above-mentioned techniques reveal higher performances in terms of accuracy and reliability with respect to wearable sensors. However, wearable devices represent the near future in the monitoring and treatment of subjects affected by disease-induced balance disorders like PD [12]. In fact, they are cheaper and easier

to use as compared to gold standard techniques, and applicable to all the patients. Moreover, they are lightweight, small, fast to be applied, and they do not require specialized personnel or any specific location (they can be easily used in home settings).

1.3.2 WEARABLE SENSORS

In recent years, wearable sensors based on Inertial Measurement Unit (IMU), or Magneto inertial Measurement Unit (MIMU), are undergoing a constant development and are trying to substitute the traditional cumbersome, inconvenient, and expensive devices. These devices can be comfortably positioned on different body segments depending on what is required for that examination. A wearable IMU generally includes one or more accelerometers, gyroscopes, and magnetometers, as illustrated in Figure 4. The accelerometer is a triaxial sensor that measures the linear acceleration along each axis in a three-dimensional (3D) reference frame fixed on the sensor itself, considering both motion and gravity components. The gyroscope is a triaxial sensor that measure the angular velocity around each axis of a 3D reference frame fixed on the sensor and the conventional rotations around the axes are known as Euler angles. The magnetometer measures the magnitude and direction of the magnetic field around the body in a 3D space. In some cases, also a barometer is added to the other sensors to measure the changes in altitude that occur during any fall on the ground. All the sensors provide measurements in the same 3D frame that is fixed to the sensor itself. Once the subject has performed a specific motor task or ADL, the data acquired from all the sensors are then combined through specific fusion-algorithms to identify the balance properties (orientation and altitude) of the subject or to detect or prevent a fall event. Finally, the performances of the proposed protocol are evaluated in terms of statistical parameters like sensitivity, specificity, and accuracy comparing the obtained outcomes with the outcomes of the gold-standard techniques.

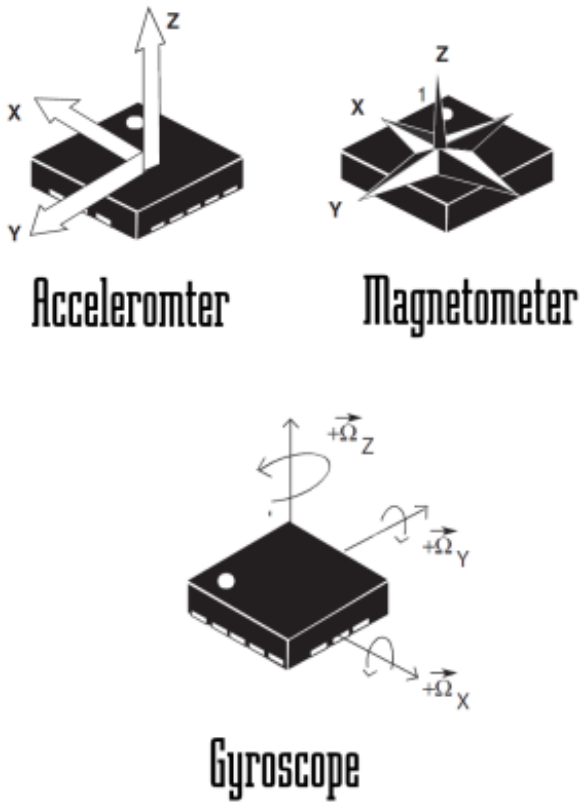

Figure 4: this figure illustrates the three main devices which are generally embedded in the wearable IMU sensors. They are tri-axial accelerometer, tri-axial magnetometer, and tri-axial gyroscope [21].

1.4 FOCUS ON GAIT ANALYSIS AND GAIT CYCLE

Gait analysis is the systematic study of human motion, using the instrumentation for measuring body movements. This type of analysis is used to assess and treat individuals with compromised ability to walk, like in PD. Gait analysis includes quantification which means the computation of measurable parameters of gait, as well as the interpretation of them, to give an overview of the gait pattern of the individual. It is necessary to highlight that the gait analysis is considered as an evaluation tool and not a diagnostic tool. Normally, only a single gait cycle of the patient is analysed. The gait cycle is defined as the time interval between two successive occurrences of one of the repetitive events of walking. Generally, it is considered the period between two successive initial contacts of the same foot on the ground [22]. The stance phase (about 60% of the gait cycle) is the period during which the foot is in contact with the ground, and it is bearing the body weight. The swing phase (about 40% of the gait cycle) is the period in which the foot

leaves the ground to allow the movement of the limb in forward direction. The following terms are used to identify the major events that occur during gait cycle, which are: initial contact (IC), opposite toe off (OT), heel rise (HR), opposite initial contact (OI), toe off (TO), feet adjacent (FA), and tibia vertical (TV). These events (IC, OT, HR, OI, TO, FA, TV, next IC) subdivide the cycle into seven periods. The first four events occur during the stance phase when one foot is in contact with the ground, while the last three events occur during the swing phase, when the same foot is moving forward through the air. The IC (0-2% of the gait cycle) is the phase in which the heel of one foot strikes the ground and marks the beginning of support (or stance) phase. The loading response (0-10% of gait cycle) is the phase that occurs between IC and OT, during which the impact absorption and the stability under load must be guaranteed. The midstance (10-30% of the gait cycle) occurs between OT and HR and guarantees the progression of the support foot and the stability of the limb and of the trunk. The terminal stance (30-50% of the gait cycle) occurs between HR and OI and ensures the progression of the body beyond the support foot. During the pre-swing phase (50-60 % of the gait cycle), in between the OI and TO, the foot is ready to leave the ground and signs the end of the stance phase. During the initial swing (60-73% of the gait cycle), between TO and FA, the foot is raised from the ground and the relative limb moves in forward direction and demarcates the beginning of the swing phase. The mid swing (73-87% of the gait cycle), which occurs between FA and TV, has the same function of the pervious phase. The terminal swing (87-100% of the gait cycle), between TV and IC, occurs to complete the progression of the limb and to prepare it for the next strike with the ground. The double support phase (about 20% of the gait cycle), during which both feet are in contact with the ground, includes the IC, the loading response, and the pre-swing phases. While the single support phase (about 80% of the gait cycle) includes the mid stance and the terminal stance phases, during which only one foot is in contact with the ground. The following figure 5 illustrates the phases of the gait cycle and the relative durations.

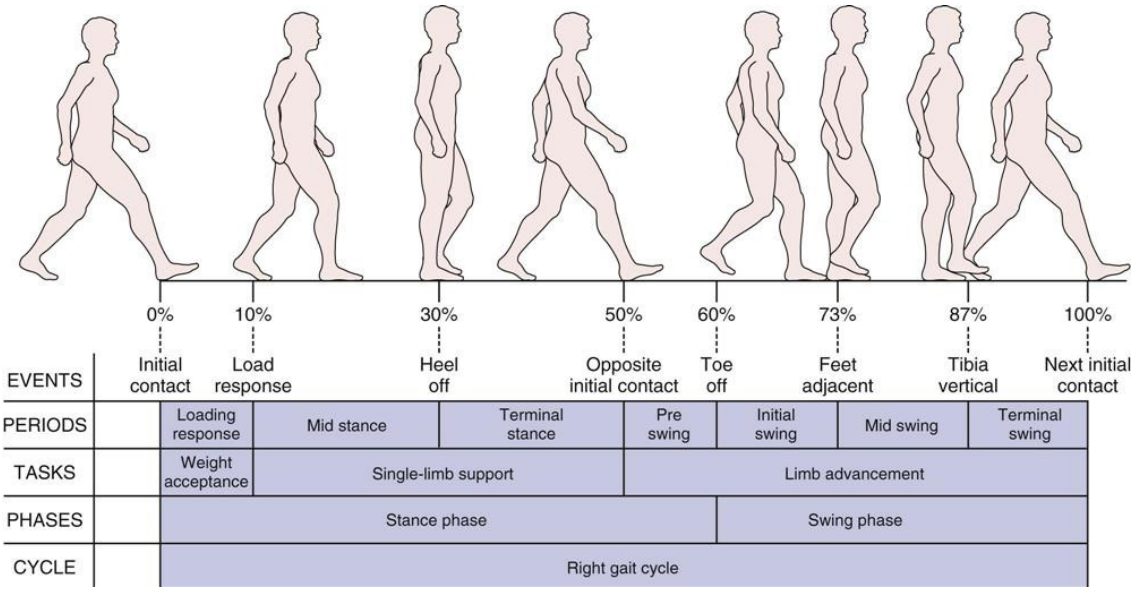

Figure 5: the image represents the phases of the gait cycle with the correspondence duration [22].

The parameters that characterize the gait can be used to analyse the capacity of an individual to maintain posture, in particular for people that suffer from pathologies that affect the balance like PD [6], [23]. Some parameters were found to be strictly correlated with motor dysfunctions typical of PD, like bradykinesia, FoG, impaired walking, and consequent fall. The most common parameters are the cadence, the stride length, the speed, the step time, the stride time, the stance time, the swing time, and the stride width [22]. First, the stride represents the sequence of events between successive heel strikes of the same foot, while the step represents the sequence of events between successive heel strikes of opposite feet. The cadence is the number of steps completed in one minute. The stride length is the distance between two successive heel strikes of the same foot. The step length is the distance between successive heel strikes of two different feet. The stride time is the time of a full gait cycle. The step time is the time for completion of heel strike of right foot to heel strike of left foot. The gait speed is the distance covered in a given amount of time. The base width is the lateral distance between the heel centres of two consecutive foot contacts. The mentioned spatio-temporal parameters are only a part of the gait descriptors that can be considered. Other parameters that can be added to these are frequency derived measures (like harmonic ratio) or step and stride regularity, step, and time asymmetry. The identification of a mismatch between some of these parameters and the normal ranges

defined for a particular category of people, can indicate the level of motor dysfunction of the individual and can be useful for doctors to decide the correct medical therapy to be applied.

CHAPTER 2: STATE OF THE ART

2.1 WORKS CARRIED OUT IN LABORATORY SETTING

2.1.1 THE STUDY OF THE MAIN DOMAINS OF MOTOR DYSFUNCTIONS

Since loss of balance episodes, like falls or FoG, can be related to the continuous oscillation (sway) of the body and movements of body's COM and COP to maintain the equilibrium during quiet standing, static balance evaluations are generally performed. They generally include both eyes-open and eyes-closed trials with arms along both sides also to estimate the role of the visual system in the maintenance of balance. However, they show limited capacity in revealing the mechanisms of balance and in pinpointing deficits of this system. Moreover, compromised balance events occur mostly during dynamic postural actions, such as walking. Thus, studies of dynamic balance during gait or with perturbations to the postural control system can be used to falls-related information or to isolate the role of visual, vestibular, and somatosensory system. Dynamic balance tests require patients to perform ADLs or specific motor tasks like six-minute walk test, time up and go test, or simple walking in their homes or in specialized laboratories. Internal perturbations aim at testing the anticipatory and proactive actions of the Central Nervous System (CNS) that commands the execution of motor programs to avoid destabilization of the body equilibrium in response to voluntary movements like gait initiation or arms, legs movements. On the other hand, external perturbations test the reactive responses of the CNS by means of translating or tilting platforms or muscle vibrators. The main parameters used to assess the balance deficits in people with PD, relative to the main control mechanisms, can be extracted by using wearable IMU devices. The domains in which balance dysfunctions can be grouped are: static postural sway, anticipatory postural adjustments (APA) due to internal disturbances like gait initiation or volitional movements, postural responses (PR) due to external disturbances, and dynamic balance during gait. For each of these systems, it is possible to extract some useful parameters to identify the maintenance of equilibrium and the risk of fall. In the following part, studies relative to sway, APA, PR, and gait parameters extracted through wearable IMU systems, and the way in which they influence the balance control in PD are reported. These studies (from 2013 to 2019) were conducted in laboratory settings while the PD subjects were asked to perform specific movements. Later, studies relative to FoG events, and studies relative to fall risk assessment, fall prediction and detection

(with a particular emphasis on systems used for home assessment) are pointed out. In these studies, subjects (PD or healthy young or elderly people) performed ADLs and real or simulated falls.

2.1.1 SWAY, ANTICIPATORY POSTURAL ADJUSTEMENTS AND POSTURAL RESPONSES

The sway represents the angle (oscillation) of the body with respect to the vertical direction and generally it is assumed that less resting sway means better balance performance, even though this is true only under certain circumstances. In the study conducted by Hasegawa et al., sway patterns were extracted from a IMU (tri-axial accelerometers, tri-axial gyroscopes and tri-axial magnetometers) placed on the lumbar region, while PD or healthy subjects were asked to stand quietly for 30 seconds in different conditions (firm or foam surface with eyes open or closed) [12]. Standardized mean difference (SMD) and random forest methods were used to highlight the most discriminating parameters between PD and healthy subjects, revealing an accuracy of 82.4 ± 12.0% (as mean ± standard deviation). The most sensitive measure to assess the sway domain was found to be the root mean square (RMS) of acceleration in ML and AP directions, while the subject was standing on foam surface with eyes open. Indeed, PD people showed higher RMS values than control subjects, underling the increased risk of falls under unstable conditions with eyes open, but not closed. Bonora et al. work evaluated body sway through information acquired from three wearable inertial devices (3D accelerometers and 3D gyroscopes) located at posterior trunk at the level of L4-L5 and on the tibias [24]. Healthy, parkinsonian subjects performed the One Leg Stance test (OLS), as a part of the mini-BESTest, and the results among different groups (healthy elderly and PD people) were compared. The mini-BESTest one-foot standing score, the Anticipatory sub score, and total score showed high sensitivity in distinguishing among different groups. RMS of acceleration in AP and ML directions were used as indicators of sway while standing on a single leg and reveal higher values of RMS in parkinsonian subjects, reflecting their poor control of posture. The concurrent clinical validity was confirmed by looking at the strong correlation between balance duration through wearable sensors and test duration by means of a stopwatch. The study of Curtze et al. assessed sway patterns of parkinsonian subjects during the execution of the

Instrumented Stand and Walk Test (ISWT) [25]. Also, in this case, the main indicators of sway were RMS acceleration in AP and ML directions, extracted by placing a wearable IMU (3D accelerometers and 3D gyroscopes) attached to the lumbar (L5) region. As already highlighted, postural sway parameters were found to be higher in PD than in control subjects. Clinical validity was assessed by measuring the correlation between objective measures of patients' mobility through wearable sensors and patient perception of mobility disability with ABC scale and disease severity with motor UPDRS, part III. In the work of Gago et al. a wearable IMU (tri-axial accelerometer and tri-axial gyroscope) was attached to the trunk, and both thighs of parkinsonian subjects while performing normal comfortable standing and Romberg test with open or closed eyes [26]. The total sway length, the range of ML and AP sway, and maximal distance of sway in AP and ML directions with respect to the origin were extracted as the most distinctive kinematic parameters to describe the postural sway mechanisms to maintain balance. A marked increase in these values was found after levodopa administration probably because this drug reduces the rigidity but does not improve the control of posture. In addition, AP and ML range of sway can be used as indicator of fall risk: the higher the value of this parameter, the higher the risk of fall. The correlation between the Postural Instability Gait Disorder (PIGD) score derived from Movement Disorder Society MDS-UPDRS scale part III, and the wearable sensors measurements confirmed the clinical validity of the method. In the study of Rigoberto et al. a IMU (3D accelerometer and 3D gyroscope) was placed on the low back (near L3 vertebra) to measure the sway of healthy young and elderly subjects [27]. They were asked to stand quietly in upright position with arms at the sides and feet at the width of the shoulders. The average acceleration in AP direction was used to differentiate between young and elderly people since it is higher in the latter. These changes were hypothesized to have a "similar" dynamic also in case of PD because both elderly and parkinsonian people generally suffer from "similar" kinds of balance disorders. Ozinga et al. research group collected sway data from iPad's built-in accelerometer and gyroscope wore at the level of the sacrum [28]. The sway acceleration range (P2P) in multiple movement directions was extracted while healthy and parkinsonian subjects were performing tasks with different complexities. Postural instability was greater for PD group than for control group as stressed by the increased values of P2P parameter in all directions (AP and ML).

Moreover, the higher is the complexity of the task, the higher is the P2P increase as observed in double-leg stance on foam surface with closed eyes. Also, in this case, the concurrent clinical validity was demonstrated by looking at the correlation between the proposed Cleveland Clinic-Postural Stability Index (CC-PSI) and the PIDG sub scores of MDS-UPDRS part III.

APA and PR represent the postural movements performed to recover the equilibrium after internal or external perturbations and are found to be reduced in PD people, resulting in lower responses to these kinds of stimuli. In the study of Hasegawa et al., APA and PR signals were extracted from one wearable IMU at the trunk while the subject was first performing the Push and Release Manoeuvre (PRM) (external stimulus) and then the Instrumented Stand and Walk test (ISW) (internal stimulus) [12]. For APA, peak acceleration in ML direction and first step range of motion (ROM) were found to be smaller in PD people than healthy controls. Moreover, these parameters can be used as trackers for the progression of the disease as in its early stages they have lower entities. For PR, length of compensatory stepping did not reveal a particular clinical instability in parkinsonian subjects. In fact, APA due to internal perturbations were more discriminant than PR due to external perturbations. In the Bonora et al. study, APA were evaluated by means of ML peak acceleration acquired via three IMUs on the trunk and on the frontal face of the tibias to describe the initial dynamic balance phase [24]. The ML peak acceleration was found to be decreased in PD than in healthy subjects, pointing out the balance difficulties prior to volitional movements. Moreover, the subsequent static balance phase was computed as the one-foot balance time, revealing reduced values for parkinsonian subjects with and without FoG events, and so increased fall risk. Also Curtze et al. described as the most discriminative APA parameters due to gait initiation were ROM first step and peak acceleration in ML direction acquired through one IMU on the lumbar region [25]. They revealed lower results in PD than in healthy subjects. Postural sway parameters were less discriminative than APA or gait parameters, which instead can be used to monitor the progress of the disease or the effects of drug therapy (levodopa administration) in diseased people. In the study of Rigoberto et al., to detect the behaviour of APA a wearable IMU device was placed near the L3 vertebrae while healthy young and elderly subjects were asked to walk starting from a comfortable

upright position [27]. Angular velocity signals were extracted revealing increased values for healthy young people, for whom balance control system is supposed to work well, with respect to healthy elderly people, for whom balance control is generally impaired as in case of PD.

2.1.2 GAIT

About gait, in the study of Hasegawa et al. PD participants walked back and forth in a comfortable way while performing a single or a dual task while wearing two IMUs on the feet [12]. The gait spatio-temporal parameters were extracted from accelerometer, gyroscope, and magnetometer placed on the feet. Turn velocity, foot strike angle, and gait speed were higher in PD than in control subjects and were found to be the most discriminative metrics to recognize dynamic balance dysfunction in PD people. The work of Curtze et al. aimed to pointing out the most discriminative measures of gait and balance for recognize motor impairments in PD while participants wearing two IMUs on the feet [25]. Features like turning peak velocity, gait speed, and stride length were strictly related to disease severity, patient balance confidence, and motor functions. In fact, changes in these gait parameters were found to be the main indicators of disease's progresses or patients' motor disabilities. Muthukrishnan et al. generated a system to measure step-based parameters in PD subjects [29]. PD and healthy participants wore two wearable IMUs (tri-axial accelerometer, tri-axial gyroscope, and tri-axial magnetometer) on the feet while performing walking in a straight line. Gait-related parameters, like step length and step time were extracted from the acquired data and were used as indicators of gait patterns of diseased people since they reached higher values in PD when compared to control subjects. The accuracy of the used algorithm was verified comparing the acquired parameters with results of a validated lab-based experiments. Hua et al. proposed a model to predict fall risk in PD older women starting from data of straight-line walking [30]. Participants were asked to wear a tri-axial accelerometer at the hip while performing 400 meters walk. Traditional gait features like step time, stride time, and cadence together with frequency and linear acceleration features were used as input of a random forest classifier to study the gait quality and associated fall risk of the subject. These parameters were found to be strong correlated with fall risk and can be used to obtain useful information like the time to first fall.

However, this study has a small sample size and women probably altered their walks in laboratory condition under supervision.

Despite the good performances and clinical validities obtained in these studies, the main limitations are their "ecological" validity and the offline computations of their results [10]. In fact, they were performed in supervised laboratory settings which are time-consuming and require patients to leave their preferred environments (generally homes) increasing their stress. Moreover, these methodologies do not allow real-time continuous monitoring of the patients while performing ADLs. This can be helpful for doctors to decide the correct medical therapy based on the disease severity and on the patient's motor disabilities. At the same time, patients can be helped in preventing or reducing as much as possible injuries due to dangerous situations like loss of balance due to FoG and fall.

2.2 WORKS CARRIED OUT IN HOME SETTING

2.2.1 FREEZING OF GAIT

As already mentioned, FoG is one of the most problematic and disabling motor symptoms of PD as it compromises the mobility of the subject and can lead to falls and fall-related injuries [31]. It is defined as a moment of inability to move a step forward since the feet are like "glued" to the floor, as shown in Figure 6. FoG is typically present in gait initiation, turning, walking while performing a dual task, and walking through narrow space. It is difficult to be assessed by using the standard clinical approach as it disappears when patient is deeply focused on walking and as the corridors of hospitals and laboratories are typically free of obstacles. Thus, the best solution to detect FoG events and the fall risk is the home assessment by means of wearable IMU devices that are able to quantitatively measure static and dynamic balance, as well as walking and postural adjustments. At the same time, there is no common consensus about the most effective sensors' configuration as their number, type, and positioning are not uniquely defined. Additionally, there are only few studies that were performed in home environments with IMU sensors and in some cases their performances are not good enough in terms of accuracy, sensibility, and specificity or their latency time is too much. In fact, it is always necessary to find the correct compromise between the complexity of

the algorithms to detect FoG events and fall risk, which require time and computational efforts, and the performances of these systems.

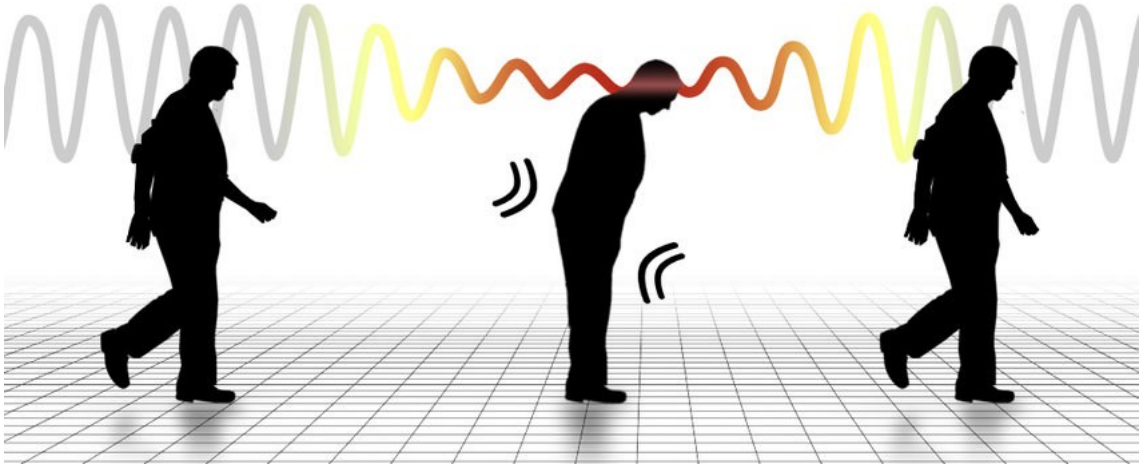

Figure 6: this figure shows an episode of FoG in which the subject is walking and experiences a moment of inability to move a step forward since the feet are like "glued" to the floor [32].

In this section, studies (from 2014 to 2021) relative to FoG detection in PD patients' home are described. The study of Sam et al. presented a method to detect FoG at patients' home in which parkinsonian subjects performed several ADLs like crossing a doorway, turning back, and executing dual task with and without medication [33]. Then, also false positive protocol activity for FoG was done in which patients performed fast and short activities whose frequency content resembles the ones of FoG episodes. The recorded signal was acceleration along 3 axes captured by means of a wearable IMU (accelerometer) positioned at the level of the left side of the waist together with a video recorder synchronized to the signal to create a gold standard for the occurrence of FoG events. The signal was pre-processed and windowed with the extraction of several features from each window, like the mean value of accelerometer axis to get the orientation of the system when no movement is present or the standard deviation of each axis to get the movement in a window time. A generic and a personalized model to each patient were elaborated by applying support vector machine (SVM) as a machine-learning classifier to distinguish between FoG and no-FoG events revealing an average sensitivity and specificity of 79.03% and 74.67% for generic model and 88.09% and

80.09% for the personalized one. Although the high sensitivity and specificity in detecting FoG episodes of this machine-learning approach (especially in the personalized model) and the “ecological” home measurement, the high computational complexity, the requirement of video recorders, and the choice on the position of the sensor represented the main limitations of this study. Indeed, sensors located on the feet generally allow to obtain higher performances for FoG detection than the ones located at the waist. The work of Nutt et al. aimed at assessing objective FoG measures of parkinsonian subjects by seven days monitoring through wearable IMUs (accelerometer, gyroscope, magnetometer) [34]. Subjects wore three inertial units on the lower back and on right and left foot and performed ADLs during the days of data collection. The average time spent freezing and its variability were extracted and demonstrated the clinical validity of this approach since they were found to be related to the freezing severity (assessed through New FoG Questionnaire) and balance perception (assessed through ABC scale). Moreover, they provided a measure of the turning and walking features of the subjects and investigated their association with the freezing features. They found that the average turning and pitch angles at the initial contact with the floor were smaller in freezers than in non-freezers. In fact, freezers have to avoid large turning angles that can induce more FoG events and have a more shuffling gait than non-freezers. However, the sample size of this study was small and so the number of subjects should be increased to verify the validity of this approach. In addition, they planned to add a camera pointed towards the feet of the subjects to create a gold standard to be compared with the proposed measurement method. In the study of Sigcha et al. FoG events in PD were detected by deep learning approach through single acceleration sensor (accelerometer) wore by the subjects at the level of the waist [35]. The patients were asked to perform some ADLs in their homes. Features related to FoG were extracted from the inertial signal, including hand-made features, Mel frequency cepstral coefficients, and Fast Fourier transform (FFT) which were supposed to be higher in presence of FoG events than in normal gait. Several approaches for FoG-detection in home environment were reproduced by using deep learning and machine learning algorithms in order to increase the ability of the system to detect FoG episodes while reducing the latency time. In this way, it was possible to provide precise monitoring of the patient freezing symptoms during their daily life and possibly aid them

in reducing the number of these events with the use of external cues. Among all the proposed methods, spectral features from previous windows and a classifier based on convolutional neural networks and long short-term memory layers (CNN-LSTM) was found to be compliant with the above-mentioned requirements, resulted in very high sensitivity (87.1%), and specificity (87.1%), obtained comparing the measurements with the video recordings of the subjects, together with low latency time. Also, in this case, a larger number of subjects with different FoG patterns is required to improve the validity of the proposed model. Another study conducted by Mancini et al. analysed FoG episodes in parkinsonian people in laboratory and also in home settings [36]. They wore three IMUs (tri-axial accelerometer, tri-axial gyroscope, tri-axial magnetometer) on the feet and over the lumbar area for a week while performing ADLs. A threshold-based algorithm was generated to detect number of FoG events, percentage of time spent freezing and its variability by using accelerations in AP direction from the lumbar sensor and rotations in ML direction from the sensors worn on the feet. Also turning-related features like average turn angle and average turn duration and walking features like gait speed and pitch angle of the foot at initial contact were extracted. The percentage of time spent freezing was higher in freezer people than in non-freezers because of certain quantity of FoG events during the day. While its variability was smaller in freezers than in non-freezers, possibly due to a false positive rate in non-freezers. In addition, the variability of time spent freezing and freezing severity (assessed through MDS-UPDRS part III) were found to be correlated. The average pitch angle at initial contact of foot with the ground and the average turning angle were smaller in freezers compared to non-freezers for the same reasons described in the previous study. Also in this case, further studies with larger dataset to increase the validity of objective freezing measures and the introduction of a mini camera to be used as a gold standard comparison medium with the IMUs are required improvements. The experiment conducted by Pierleoni et al. developed a system based on a wearable IMU (tri-axial accelerometer, a tri-axial gyroscope, and a tri-axial magnetometer) and data fusion algorithm to detect tremor and freezing events in parkinsonian subjects [37]. The device used for freezing classification was placed at the chest while subjects performed ADLs. The RMS of acceleration along AP and ML axes was extracted and band-pass-filtered and then the freeze index (the ratio between the power contained in the freezing and locomotion

frequency bands) was estimated to discriminate between FoG and no-FoG events through a threshold comparison in each observation window. The features extraction and classification process were executed in the web service platform so that clinicians could assess information about intensity and duration of FoG, allowing remote monitoring of the patients with the consequent adoption of the correct medical therapy to be applied. Validation of the model was done by means of video recordings for confirmation of the FoG event. The study of Borzì et al. proposed a method to quantitatively assess the motor conditions of PD patients in home environment [38]. They proposed a smartphone-based system to acquire data from accelerometer and gyroscope sensors, embedded in the smartphone itself, which was fixed at the waist. The sensors are passed as input of a machine learning classifier to detect FoG or other kinds of motor fluctuations. Subsequently, they executed a monitoring of PD people at home while performing ADLs through Sensor-Tile module. This wearable device embedded accelerometers, gyroscopes, magnetometers, and also environmental sensors (barometers, temperature sensors). For gait analysis, it was placed on the ankle, while for balance analysis on the trunk. The registered signals were orientation, acceleration, and angular velocity from which gait- and postural-related features were extracted and processed on the SD card of the device to detect FoG events or other PD's motor signs. The results and users' feedbacks demonstrated a higher sensitivity, comfortability, and ease-of-use of the inertial sensor when compared to the smartphone. In fact, SensorTile could be used to better follow PD motor symptoms, to adjust the medical therapy, and to improve the patient's quality of life. The main disadvantage of this device is its high cost. The research of Dorfman et al. underlined as the main useful features to analyse FoG were freeze index, FFT, time, frequency, and statistical features [39]. At the same time, they proposed a wearable FoG assistant system, called GaitAssist to help people with PD in detecting FoG episodes in real time. Subjects were asked to wear one or two IMUs (3D acceleration, 3D gyroscope, and 3D magnetometer) attached to the ankles and to switch on the GaitAssist while performing specific motor exercises known to induce FoG and then ADLs. The acceleration signal was windowed and from each window a set of FFT-based features was extracted. Successively, also statistical features from accelerometer and gyroscope data were considered. The entire set of features was used as input of machine learning classifier

to obtain a FoG-detection machine able to recognize FoG events in real time. When such events were detected, a cueing signal was generated for improving the gait performance of the freezer. Also in this case, the raw sensing data and the FoG-detection system outputs were sent to a cloud server in which doctors could evaluate the number of FoG during the day and their duration in order to adapt pharmacological or physical treatment of the patient. The user feedback about the GaitAssist device revealed the positive impact of this methodology in the gait of the subjects, helping them in reducing the number and duration of FoG events. The main limitations were in the number of subjects and in the uncomfortable sensors' positioning since they were located at the ankle using straps. Also in this case, the identification of FoG episodes was confirmed with a video recorder synchronized with the sensors. The experiment done by Ahlrichs et al. aimed to evaluate three approaches to detect FoG events in parkinsonian patients by means of a wearable accelerometer sensor positioned at the waist [40]. Participants performed activities of general nature while being at home. The acceleration signal was recorded and split into equally sized windows, from which several features relative to FoG are extracted. FFT, a set of features in time and frequency domains, and freeze index are used as input to a support vector machine for training or classification. The FoG detection system revealed high accuracy (higher than 90%), sensibility, and sensitivity in all the proposed approaches (obtained comparing the results with video recordings synchronized with the sensors) and frequency features were found to enable a reliable monitoring of FoG. However, the main drawback of this work is represented by the fact that these methods cannot be used in real time because of latency time required to detect FoG event. Tzallas et al. developed the PERFORM system to allow remote monitoring of the health status of parkinsonian subjects by recording motor symptoms of this disease like FoG and falling [41]. Four accelerometers and one accelerometer/gyroscope are respectively positioned at the patient's extremities and at the waist. The entropy of the acceleration signals for each axis is extracted obtaining a feature vector used to discriminate between FoG or not. The processed and elaborated biomedical data are sent to the point of care in which clinicians can monitor the disease progression and adapt the medical therapy on the basis of the symptoms. Despite the high accuracy (79%) in capturing FoG events using long-term recordings for its

evaluation, the problem was that clinicians received information about the patient's status at previous days and not in real time.

2.2.2 FALL RISK, FALL DETECTION AND FALL PREVENTION

As previously described, falls are sporadic, fast, and unintentional events that can cause severe injuries but also mortality [5], [42]. Falls are mainly experienced by elderly people or people affected by pathologies that cause balance disorders, like PD. Indeed, studies conducted in adults aged 65 revealed a fall frequency between 28% and 45% each year. Falls lead to huge requirements in terms of attendance of emergency departments (from 18% to 40% of emergency attendances are associated with falls consequences), and hospitalization (above 80% of all hospital admissions are due to fall-related injuries). Some of the most frequent injuries due to falls are fractures of the femur, fractures of the lower and upper limbs, and brain injuries which are responsible for 46% of fatal falls. All these factors introduce the problem of very high costs due to falls for the individuals, the families, the healthcare system (in Europe it is estimated to be 25 billion euros each year, only in United Kingdom 2.3 billion of pounds per year), and the society. Fall risk depends on age and gender functional decline, chronic disease, impaired mobility, and medication use. At the same time, risk factors for falls can be grouped in two main categories: intrinsic and extrinsic factors. Intrinsic factors are related to the person's characteristics and include biological aspects like poor muscular strength, poor flexibility, compromised ability in maintaining balance, reduced physical and cognitive functions, and bad medical conditions. They also include demographic aspects such as old age, gender (women are at higher fall risk than men) and falls-history that causes changes in mobility. Finally, behavioural factors like inadequate diet, alcohol abuse, improper medications' use, and patient's sedentary lifestyle. Extrinsic factors are related to environmental aspects like insufficient lighting, slippery surfaces, uneven pavements, and inadequate housing. In fact, most fall incidents (56%) occur when aged people move around their homes, especially in the living room. The before-mentioned concepts are represented in figure 7.

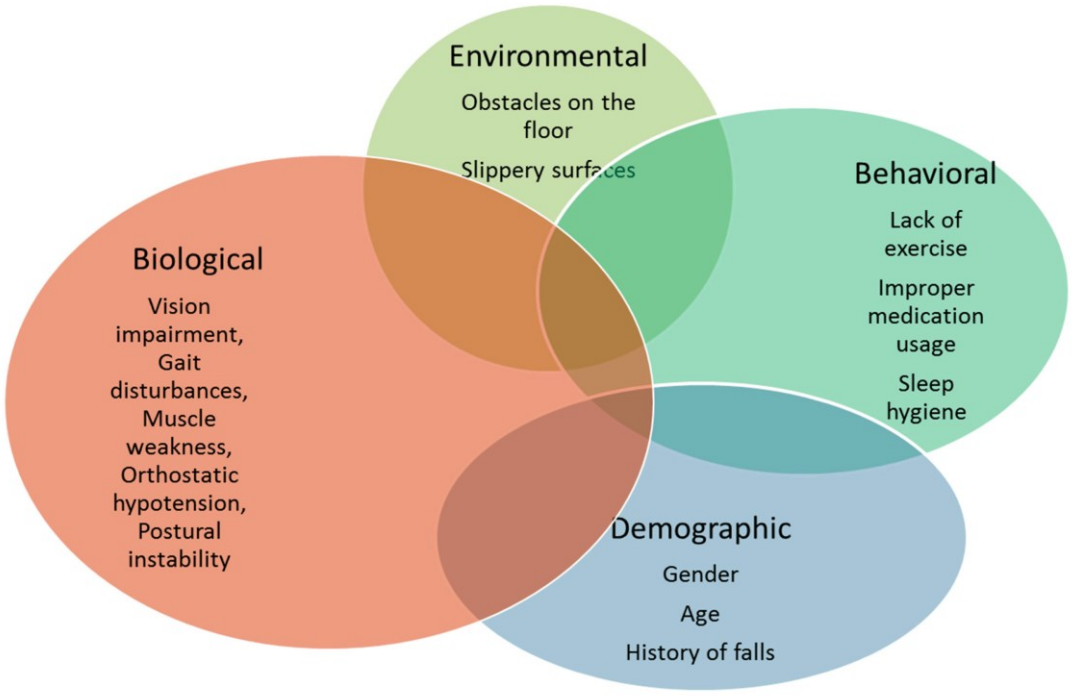

Figure 7: this image shows the main categories in which risk factors associated with falls can be grouped [43].

The development of research and technologies to study the mechanisms of balance and so to assess the fall risk, to detect and predict falls is increasing in the last years. Several techniques are adopted to quantify the postural control in elderly people or in subjects affected by pathological conditions like PD. Both static and dynamic posturographic tests are performed but particular interest is focused on walking or other motor tasks like gait initiation, turning, and avoiding obstacles since it is during these movements that human balance control system is mostly challenged. Indeed, experimental evidence revealed that the greatest incidence of falls occurs during some forms of locomotion. In literature, there are now a lot of studies conducted in laboratories while the subjects were asked to perform a specific physical test and to compile questionnaires in collaboration with the doctor that are useful for the identification of the fall risk, the balance properties of an individual, and the severity of the disease in case of pathological conditions. More recently, in order to generate systems able to assess the fall risk and to detect and/or prevent falls in real-time, methods based on wearable inertial sensors are frequently used. They are attached to specific body's parts while subjects perform simple tasks, ADLs, and falls, and then features related to static and

dynamic stability are extracted from the data acquired through the sensors. Further, machine learning or threshold-based approaches, which are embedded in these devices, are used to provide falls-related information in real-time. These sensors-based systems can be developed in supervised environments (or directly in homes with video recordings) and then tested in patients' homes to verify their accuracy and reliability. Home setting assessment through wearable sensors can help in reducing the above-discussed problems due to falls and considerably increase the quality of life of patients. However, as in the case of FoG, there are still argues about the type of sensors, the sensor's locations, and the best set of features to be used.

Regarding the fall risk assessment and fall detection, several studies (from 2014 to 2020) performed in home-like environments about PD subjects are reported. The work of Stack et al. aimed to investigate the role of home-sensors against the human observation in the detection of fall risk in PD people [44]. Each participants performed common daily activities like walking between rooms, ascending or descending stairs, crossing narrow or larger spaces while wearing five IMU devices (tri-axial accelerometer and tri-axial gyroscope) secured around wrists and ankles, and being video-recorded for validation. The continuous human observation at a patients' home was deemed intrusive because people felt as they were forced to perform some tasks to give the observer "something to film". On the contrary, a wearable device plus cameras placed in the most frequented rooms could be more accepted by the patients and allowed to deeply focus on the challenges that they had to face habitually, and which could cause falls. Moreover, sensors (tri-axial accelerometers located at the pelvis) were found to surpass the human observations in the identification of small deviations of motor dynamics that indicated the starting of a fall event. So, the usage of sensors was revealed as cheaper, more realistic, and useful in solving the privacy issue of some people. In fact, wearable sensors enabled to verify as PD subjects appeared to have higher risk of falls during turning, avoiding obstacles, crossing narrow spaces, and transferring. Anyway, this study could be improved by including a larger number of subjects and by reporting the results of validation protocol. Ayena et al. proposed a method to evaluate the risk of falling by the computation of a score while healthy or PD subjects were performing OLS test by using a smartphone-based system with an instrumented insole [45]. The

above-mentioned insole was composed by accelerometers, force and bending variable sensors. All of them were used to compute balance, gait evaluations, and consequent risk of falling. The users had to perform the OLS test at home while the software was running as a serious game for training balance. Then a closed-loop model using tether and release test (TRT) and the OLS test software were used to generate two scores that folded together into a single score to describe the risk of falls. To obtain a score from the TRT, the average vertical projection of the COM on the ground that is called Centre of Gravity (COG), the standard deviation of COG and calibration factors were used. While from OLS test, the COP position, the standing time, the standard deviation of COP and the COP velocity were considered. These parameters were found to be greater in PD people than in control subjects, demonstrating the balance dysfunction and the increased risk of falls. Moreover, the type of the ground was found to be responsible for varying the OLS test score too, for example revealing higher fall risk in sandy soil as compared to parquet. This system could be used for daily evaluation of the balance properties and fall risk of patients at home but not for long-term monitoring. The study conducted by Haertner et al. focused on quantitative estimation of turning parameters by inspecting their links with fear of falling (FOF) and fall history in parkinsonian subjects [46]. PD people were asked to wear a IMU (3D accelerometer and 3D gyroscope) at the lower back for twelve days while performing their usual activities at home. Extracted turning features were turn duration, turn angle, average angular velocity, starting, middle, and ending angular velocity. It was demonstrated that FOF strongly influenced these turning parameters in PD people since they showed longer turn duration and lower middle angular velocities with respect to PD people without FOF. These deviations reflected a compromised stability during turning and consequent higher risk of falls, confirming the negative impact of FOF in gait and balance of PD subjects. At the same time, positive fall history did not relevantly contribute to the turning behaviour. The validation of this work was obtained by comparing the accuracy of the home-based method with the results of a supervised lab-based method carried out with the same sensors and algorithm. The importance of turn monitoring in the identification of fall risk was also investigated by El-Gohary et al [47]. The study was conducted on subjects' homes in a seven-days period during which PD and healthy participants wore three wearable devices (triaxial accelerometers, tri-axial gyroscopes, tri-axial and

magnetometers) at the pelvis, at the lumbar vertebral level and on the feet. The turning-related parameters were the hourly frequency of turning, the turn duration, the peak and average rotational turning rate and jerk and their variability during day or week. Parkinsonian people were found to do shorter turns with smaller turn angles and a higher variability in all turn metrics during the day than control group. This behaviour was strongly correlated to fall risk and so the monitoring of turning performance could help to prevent fall episodes. The validity of this work was done in the same way of the previous study. The study of Weiss et al. evaluated fall risk in PD patients that wore a body-fixed device for three days while executing common activities in their home [48]. Participants wore a IMU composed by tri-axial accelerometer and tri-axial gyroscope at the lower back. The followed approach consisted in extracting walking segments and focusing on metrics relative to quality and quantity of gait. Features like the total number of walking bouts, the percentage of time spent walking, and the total number of steps for the quantity of walking while quality-related features like amplitude and width of dominant frequency, and the harmonic ratio were extracted. PD people were divided into fallers and non-fallers according to their fall histories and it was observed that fallers walked with compromised gait quality but maintaining the same gait quantity as non-fallers. This was probably due to the impaired postural control, flexibility, and ability in generating a rhythmic gait of fallers. These parameters were found to be useful also as indicators of fall risk, even for subjects that did not fall until the moment of the examination. In addition, fallers were differentiated from non-fallers for an increased medio-lateral variability during walking. This method could be improved by providing other metrics from the walking signal to clarify the clinical utility of this study. Iluz et al. developed an objective, automatic missteps (loss of balance while walking that can lead to fall if the subject is not able to recover the equilibrium) detection system to identify the walking performances of PD people through three days evaluation in a home-environment [49]. Subjects wore a device which embedded tri-axial accelerometer and tri-axial gyroscope at the lower back while performing ADLs. To detect misstep time domain features like average, range, standard deviation and frequency domain features like amplitude, width of the power spectral density in locomotion part were considered. Also in this case, PD fallers and non-fallers were distinguished. The number of missteps was found to be correlated with the fall risk. In

fact, PD fallers produced more missteps than non-fallers and so they could be used as indicators of fall risk. The good accuracy of this approach in detecting missteps was verified by comparing its results with the video-taped laboratory study which used the same algorithm. However, a larger scale study and a higher number of sensors would be useful to confirm the validity of this approach. Silva de Lima et al. developed the PERS system for long-term monitoring and detection of falls in home-like environments [50]. People with PD and healthy subjects, who were also prone to falling, were asked to wear IMU system (tri-axial accelerometer and barometer) at the level of the neck while executing ADLs. This device was worn through a necklace and enabled to press a button to call help-centre in case of occurrence of emergency situations like falls. Otherwise, when a fall was automatically detected the call was automatically sent so that the response centre could provide support or confirm the fall event. The necklace device captured data with IMU sensors and detected falls from changes in height, orientation, and impact that happened during falls. The differences between parkinsonian and control subjects were pointed out by considering some continuous and some categorical variables analysed by a multimodal model combining self-reported and automatic detected falls. The algorithm automatically identified the fall (without the need of pushing the button) in 70% of the cases. The incidence rate of any fall (falls per person-year) was higher in PD participants than control subjects, underling the importance of fall prevention systems for daily-life monitoring of PD people. Indeed, older PD patients were more subjected to falls than healthy people. Moreover, the severity and the duration of the fall were found to be greater in these kinds of people. The study was validated by an analysis performed on thirty-one healthy volunteers to detect typical falls, revealing an accuracy of 95% in fall detection rate. Thus, limits of this approach were that the validity was evaluated without considering PD subjects (only control ones). Then, some fall events were missed by the detection algorithm, or the button press, and finally also other sensors (magnetometers and gyroscopes) could be included in the falls monitoring system. The study of Sturchio et al. aimed at finding the correlation between the risk of falls, the gait and postural instability and ADLs at home environment in subjects affected by PD with orthostatic hypotension [51]. Specific tests were executed in controlled environments while continuously measuring blood pressure with wearable non-invasive monitor and evaluating balance and gait with

wearable sensor system composed by six IMUs (tri-axis accelerometer, tri-axis gyroscope, and tri-axis magnetometer) located on the feet, wrists, sternum, and lumbar region (APDM setting). For balance analysis, the main extracted features from APDM sensors' configuration were jerkiness ($JERK^{sway}$), RMS of acceleration (RMS^{sway}), and centroidal frequency (CF^{sway}). Additionally, home evaluation was executed while patients were also wearing a sensor at the level of the waist that was used for the gait analysis to estimate the waist postural sway ($WS^{walking}$) during home-like activities (Kinesia setting). Through a clustering process, six sets of features related to gait, balance and ADLs were obtained. Researchers did not find any association between falls and in-clinic tests of gait and balance or home-like activities, while kinematic data showed high performances in the prediction of falls with high sensitivity and specificity (>80%). More specifically, CF^{sway} and $JERK^{sway}$ were demonstrated to be the most discriminating sway kinematic parameters for postural instability and prediction of falls in PD patients with orthostatic hypotension. The WS parameter worked well as an indicator of PD motor symptoms and their severity. Moreover, an orthostatic mean arterial pressure < 75 mmHg was found to increase the fall risk. The importance of evaluating motor capabilities in home-like environments to prevent falls was stressed by the fact that only ADLs showed a trend toward falls, while in-clinic activities did not. Limitations of this work are due to small number of subjects, male prevalence, and limited capacities of wearable sensors to accurately capture signals in homes. Del Din et al. proposed a system for the assessment of free-living gait characteristics associated with fall risk [52], [53]. PD and control subjects were asked to wear an accelerometer at the lower back while performing laboratory and seven days home acquisitions. Gait parameters associated with variability, asymmetry, postural control, pace, and rhythm were extracted from walking trials and used as indicators of gait quality and consequent fall risk. These features were found to be significantly different when computed in home or lab setting. Indeed, both control and PD walked with higher variability and asymmetry, decreased pace, and rhythm in laboratory environment than in home. Moreover, PD people had a walking pattern characterized by a slower and shorter steps, increased rhythm, and asymmetry than healthy subjects. They also studied the impact of activity bout length between groups, observing that longer activity bouts highlighted more the differences in gait metrics between the two groups. Although the good results

in the extrapolation of gait parameters, further examinations with the help of video recordings should be introduced to verify the performance of the system.

About fall prediction and detection, recent studies (from 2018 to 2021) relative to healthy subjects (aged people or young people simulating motor behaviours of elderly people) or data coming from databases of falls and ADLs are reported in the following paragraph. Saadeh et al. developed a fall prediction and detection system for long-term monitoring of elderly patients at elevated risk of falls [54]. The participants were elderly people who wore tri-axial accelerometer at the level of the thigh while performing ADLs but also activities resembling different kinds of falls. The system worked in two modalities: fast mode to predict falls, and slow mode to detect falls. The utilized features (mean acceleration, standard deviation, correlation coefficients) for fall prediction were selected to enhance sensitivity and specificity as much as possible that resulted to be very high, 97,8% and 99,1% respectively. The set of features was passed as input of a nonlinear support vector machine learning classifier to distinguish between pre-fall events or normal ADLs. When a fall event was predicted, an alarm was generated to avoid such situation. Fall episode was divided into three phases (pre-fall, fall impact, post-fall) and was analysed by passing only one feature (the total sum vector square) in a patient-specific threshold-based algorithm. Fall detection system allowed to obtain a sensibility and specificity of 98,6% and 99,3% respectively. In presence of fall, the information was communicated to a healthcare provider. Validation was performed by using MobiFall database. The analysis of more falls and fall-like events could improve the presented system. Yu et al. proposed a hybrid model (ConvLSTM) integrating both convolution neural network (CNN) and long short term memory (LSTM) models to predict the fall in older people [55]. This model was evaluated on SisFall, a public dataset which contains falls and ADLs acquired with a wearable inertial device (two accelerometers and gyroscope) attached to the waist. The features were not manually designed but the entire information enclosed in the raw data of accelerometer and gyroscope was used by ConvLSTM to distinguish between three classes: non-fall, pre-impact fall, and fall. The performance of this model was compared with CNN and LSTM approaches, revealing higher sensitivity (>93%) and specificity (>94%) than other models in detecting all the three classes. Since the latency time of ConvLSTM model is quite low,

the proposed system could be embedded in wearable devices to predict the risk of falls in real-time, although its development was done considering a database in which simulated falls were executed and in some cases the duration of pre-impact fall was too short to be clearly identified. Shi et al. created a CNN with a class activation mapping (CAM) to detect pre-impact falls starting from data coming from MobiAct database [56]. The latter contains falls and ADLs acquired through an IMU (accelerometer and gyroscope) device wore at the level of the waist. This approach allowed to visualize hot maps of the fall data to understand the contribution of each region in the fall detection process. Then, researchers combined the CNN method with a threshold-based method to detect falls in the real world. To identify pre-fall phase and distinguish it from impact and recovery phases, the sum vector magnitude (SVM) of acceleration and angular velocity were extracted from CNN as features. During pre-fall, SVM of acceleration was found to be slightly less than one gravitational acceleration and the angular velocity was lower than in ADLs. The system was also tested on real young subjects that wore one IMU device at the waist while simulating different types of falls or ADLs. Despite few fall data were not correctly recognized, the proposed method revealed high sensitivity and specificity of 94,04% and 97,17% in detecting pre-fall events. The work of Kim et al. developed an impact acceleration magnitude prediction model to detect fall before impact to the ground through a deep learning approach [57]. A LSTM regression was applied to reach the purpose. Healthy young participants wore a wearable IMU at the waist composed by tri-axial accelerometer and tri-axial gyroscope while mimicking realistic falls of elderly people. Several features were extracted from tri-axial accelerometer and angular velocity and specifically the SVM, root mean square of the sum of acceleration along three axes, was the value to be predicted in this model through the application of a bi-directional LSTM algorithm. In this way it was also possible to differentiate between different fall types and to identify the directions of the falls. Moreover, pre-fall phase, critical fall phase, post-fall phase, and recovery phase were distinguished. Therefore, a wearable airbag system could be used with the classification model to reduce the injuries caused by the falls. This deep learning model showed a mean absolute percentage error of 6.69 ± 0.35% when a data augmentation procedure was added. The performances in fall prediction and injuries reduction are promising, nevertheless further experiments are required to improve the validity of this

system. The study of Wu et al. proposed a pre-impact fall detection system during walking through a hierarchical classifier [58]. Young healthy subjects wore two IMUs (tri-axial accelerometer and tri-axial gyroscope) at the waist and at the thigh while simulating activities of aged people. Twelve features like average signal magnitude variations of angular velocity at the waist or at the thigh, absolute averages of them, and correlation coefficients between them, were extracted from angular velocity and angle data and then were selected and used with a hierarchical classifier. The algorithm which identified pre-impact fall was triggered when the thigh angle exceeded one of the set thresholds. Non-fall activities, backward- or forward-fall activities were distinguished and correctly detected with a sensitivity of 95,5% and a specificity of 97,3%. However, only two types of falls were considered (forward, backward), and data were obtained from young volunteers that showed obvious differences between simulated falls and real falls of elderly people. Ribeiro et al. developed two strategies to distinguish different locomotion modes, such as normal gait, pre-fall, and fall conditions [59]. Healthy young participants performed walking activities and simulated falls while wearing five IMUs (three-axis accelerometer and tri-axis gyroscope) plus a temperature sensor fixed to the lower back, both back thighs, and both feet. Roll, pitch, yaw angles, gait events, entropy, signal vector magnitude, and FFT features were extracted from the IMUs-acquired signals through CNN. Subsequently, a Principal Component Analysis (PCA) was applied to reduce the number of considered features. Finally, a statistical classifier and a CNN were used for the classification. The CNN classifier revealed greater performances than a statistical one, but CNN could not be used for real-time detection of normal gait, pre-fall, or fall phase, while statistical classifier could (in the way they were done in this study). So, this work represents an example of off-line computation of locomotion phases and future experiments would test the performances of these classifiers in on-line systems to allow a real-time prediction of fall events. Liang et al. fabricated a pre-impact fall alarm system to prevent falls of elderly people in real time by using comfortable wearable devices [60]. Healthy adults performed ADLs and simulated falls while wearing an inertial measurement system at the waist composed by tri-axial accelerometer and tri-axial gyroscope. Falls and ADLs were differentiated through a Hidden Markov model-based support vector machine, by using features coming from acceleration and angular velocity time series as inputs. The proposed classification

algorithm revealed a sensitivity and specificity of 97,22% and 93,75% in detecting pre-impact falls and so could be used as a safe predictor of falls since it could generate an alarm before the fall. At the same time, once the fall had occurred, this device generated a call for help of people in the vicinity. Anyway, data used for the validation of this system derive from youngsters or dummies and not from aged people leading to a limitation in the device applicability for elderly. Moreover, airbag systems should be implemented to reduce the injuries due to falls. The study of Zhong et al. proposed a pre-impact fall-detection and protection system [61]. Participants were young healthy subjects who performed ADLs and falls. The IMU system was located at the waist and consisted of tri-axial accelerometer and tri-axial gyroscope. Vertical velocity and vertical displacement were used as features for the distinction of different types of human motions and falls. The developed threshold-based algorithm was also tested in real environment during a trial in which two subjects wore the IMU sensor (tri-axial accelerometer, tri-axial gyroscope, and tri-axial magnetometer) at the waist and an inflatable airbag system to provide fall protection for a long time. Results from both kinds of experiments demonstrated the good performances (sensitivity 93,6% and specificity 95,6%) in detecting pre-fall situations and in protecting from falls-related injuries. Also in this case, the problem was that data come from young individuals and so do not perfectly mimic data coming from elderly people. Ajerla et al. proposed an efficient real-time fall detection system trying multiple machine learning models and different sensors' positions and sampling frequencies to identify the best solution [62]. Data were taken from MobiAct database which contains ADLs and four kinds of falls acquired from an IMU (tri-axis accelerometer and tri-axis gyroscope) located at the waist. Subsequently, for validating the method in real life, data were also taken from young subjects that were asked to wear five devices (which contained tri-axial accelerometer, tri-axial gyroscope, tri-axial magnetometer, and barometer) at the waist, calf, wrist, chest, and thigh while realizing ADLs and falls. Among all the developed machine learning models, the LSTM one was selected since it reached an accuracy of 99%. A totality of fifty-eight features, like average acceleration, standard deviation of acceleration along three axes, the square root of the sum of the accelerations along three axes, were extracted to distinguish between falls and non-falls. A laptop was used as edge device to real-time streaming and processing of the data acquired through the

IMU. It was proved that the best sensor's position to detect falls was at the waist since it was the steadiest point of the body with the lowest amount of noise. While sensors at the thigh observed falls prior to the other sensors and could be used for fall prediction and prevention. However, systems with multiple sensors working with a sampling frequency of 50 Hz obtained the highest performance in identification of fall events. The work could be improved by introducing fall prevention algorithms and the distinction between different types of falls. Hussain et al. developed a fall detection and recognition system through wearable sensors [13]. SisFall dataset was used as it contains ADLs and different kinds of falls from young and elderly people. A single IMU made by two accelerometers and gyroscope wore at the waist was used for the extraction of the data. Fall detection was considered as a binary classification problem to distinguish between ADL and falls and both data coming from accelerometer and gyroscope were used for the feature's extraction. Fall recognition was studied as a multiclass classification problem as it was necessary to differentiate between fifteen types of falls and each fall comprised a fall pattern and a related ADL. Also in this case, both data coming from accelerometer and gyroscope were taken in consideration to extract useful features, such as maximum and minimum value, mean, orientation of the trunk, SVM. Indeed, it was observed that the performance of the system in fall recognition using single accelerometer or gyroscope was lower than the one using both. Moreover, gyroscope was found to work better than accelerometer for recognizing falls. These features were passed as inputs to machine learning classifiers and for fall detection the k-nearest neighbours (KNN) classifier showed the highest accuracy (99,80%), while for fall recognition the random forest (RF) classifier obtained the best accuracy (96,82%). This model could be improved incorporating fall prediction systems, adding some camera-based or ambient sensors, or considering higher numbers of fall types. Hauth et al. proposed a method for automated detection of loss-of-balance (LOS) events in older adults at risk of falls during daily activities [11]. These subjects wore three IMUs (tri-axial accelerometer and tri-axial gyroscope) on the feet and on the lower trunk for two weeks plus a wrist-worn voice recorder to indicate and describe the occurrence of a LOB episode. Then kinematic features were extracted and through machine learning techniques, classifiers were built to automatically detect LOB events. Gait, stride length, stride time, trunk angles, and trunk angular velocities were considered from the

acquired data. In general cases, both regularized logistic regression and bi-directional long short-term memory (BiLSTM) were able to correctly distinguish between LOB and non-LOB events from the kinematic features. However, due to the high rate of false positives, the precision of the models was compromised, suggesting that further improvements would be required to use this system for real-time detection or prediction of LOB episodes. Other limitations were the low number of participants and the rare occurrence of LOB events during the day that increases the difficulty in their recognition. The work of Rachakonda et al. aimed at realizing a Good-Eye system with a combination of computer-vision and physiological systems to detect and prevent falls [63]. Indeed, falls were found to be related to physiological parameters which are seat, heart rate, blood pressure, temperature, and vision. Good-Eye system was composed by wearable accelerometer sensor wore at the waist to detect increments of acceleration along the axes that can indicate fall or pre-fall events. A wearable sensor able to capture heart rate variability of the person against the resting heart rate. An on-site camera sensor to analyse changes in the orientation and intensity of falls and an off-site camera mounted on the wall to give continuous information about the subject. When a change in acceleration, orientation, and heart rate values was observed, a threshold-based algorithm was used to verify the occurrence of a fall or pre-fall event. The system revealed high accuracy (95%) in detecting and predicting falls but could be improved by incorporating all the sensor data and the model dataset. Zurbuchen et al. proposed a fall detection and recognition system based on wearable devices with a multi-class approach and proving different sampling frequencies [64]. Data were taken from SisFall database where are collected information about ADLs and simulated falls from young and elderly people wearing a IMU device (composed by two tri-axial accelerometers and one tri-axial gyroscope) at the waist. However, only one accelerometer was used for the analysis. Data were acquired, pre-processed, and linear acceleration and angular velocity (magnitude of acceleration and rotation), temporal (variance, standard deviation, mean), and frequency features (power spectral density or entropy) were considered. Five machine learning algorithms were used for classification, but the best results were obtained through Random Forest or Gradient Boosting (sensitivity and specificity near to 99%). The optimal sampling frequency was found to be 50 Hz, over this value not relevant improvements were appreciated. The system

distinguished between ADL or fall. In case of fall detection, the system differentiated between pre-fall, impact, and post-fall phases. Anyway, this work could be improved introducing data from more realistic conditions (real and not simulated falls) and increasing the dataset. Hsieh et al. developed an identification algorithm for fall detection and recognition using wearable devices [65]. Young adults were recruited to simulate different kinds of falls and ADLs while wearing an IMU device (3D accelerometer, 3D gyroscope, and 3D magnetometer) at the level of the waist. Also a camera was used to collect data. Raw data were windowed and then features were extracted. Mean, standard deviation, variance from each time window plus resultants of linear acceleration and angular velocity along three axes were passed as inputs of multiphase classifier and then fragment modification was applied. Multiple machine learning classifiers with different sampling rates were used but K-Nearest Neighbour (kNN) with a window size of 24 samples enabled to obtain the highest performances in terms of sensibility, sensitivity, and accuracy (83,09%, 86,53%, and 90,56% respectively). In this way, it was possible to differentiate between five fall phases, which were pre-fall, free-fall, impact, resting, and recovery. However, this work would require larger dataset, real fall dynamics, and more types of falls as further improvements. Yu et al. created a new motion dataset plus an algorithm for pre-impact fall detection using wearable inertial sensors [66]. The database and detection system were created while young participants were wearing a IMU device composed by three-axis accelerometer, three-axis gyroscope, and three-axis magnetometer at the lower back. Additionally, a video camera was added to the system to obtain accurate temporal labels for falls time, allowing the utilization of the database also for pre-fall detection and prevention (not only for post-fall detection). Three types of algorithms were compared (threshold-based algorithm, machine learning, and deep learning), but the highest sensitivity and specificity (99.32 and 99.01%) were reached via deep learning approach by using ConvLSTM algorithm. Linear acceleration, angular velocity, and Euler angles were passed as inputs of ConvLSTM classifier that performed the features extraction and enabled the distinction between pre-fall or ADL. Also the lead time (the time in between the fall detection and the fall impact) was considered and was found to be higher in ConvLSTM than in other approaches. The system was also tested considering database of real falls cases of adults showing lower performances than previous case, but

promising results as well (sensitivity was 93.33%, specificity was 73,33%). The proposed model could be improved by including more real-world fall and enlarging the dataset. Seketa et al. proposed a fall detection system based on event-centred data segmentation [67]. Three different datasets were used to obtain the raw data but in this work were considered data coming from accelerometer worn at the waist of young subjects while performing ADLs or simulated falls. After a potential fall detection, data segmentation was done to differentiate specific fall phases (pre-impact, impact, post-impact). Eight features were extracted from acceleration vector magnitude and passed as inputs of SVM classifier to distinguish between ADL or fall. A fall was identified as a sudden increase of acceleration that exceeded a threshold value for a short time. The optimal duration of pre-impact and post-impact (3,5 s or 3,75 s) windows was found to be higher than the one of impact window (0,5 s or 1 s) and the overall precision of the system oscillated among 96,1% to 99,7% according to the considered dataset. Limitations of this system were represented by too short ranges of window sizes and data that were acquired from simulated falls and ADLs of young people while this model was thought to be used for elderly subjects. Jung et al. proposed a system for the detection of pre-impact through wearable sensors [68]. Young subjects wore an IMU composed by tri-axial accelerometer, tri-axial gyroscope, and tri-axial magnetometer while performing ADLs or simulated falls. From the raw data, acceleration, and angular velocity magnitude together with vertical angles (roll, pitch) were collected. Then, four thresholds (relative to linear acceleration, angular velocity, and vertical angles) were identified to differentiate between pre-fall or ADL, obtaining 100% sensitivity, 97.54% specificity. In case of pre-fall detection an airbag was inflated as a protection system to avoid excessive damages on the fallers. The system was validated by taking data from SisFall public dataset revealing good performances as well. It could be improved adding more features or including older participants. Saleh et al. generated a machine learning algorithm to detect different fall phases for elderly people [69]. Data were taken from SisFall dataset containing ADLs and simulated falls of young and elderly people through accelerometer sensor wore at the waist. Acquired data were divided into two segments. From the two segments, statistical features were extracted as mean and standard deviation of acceleration to differentiate between fall and ADL. Then, a machine learning classifier (SVM) was used to distinguish falls and ADLs. Falls were also divided into

prefall, impact phase, adjustments, and postfall phases. The first two phases belonged to the first segment, while the other two to the second one. The whole system obtained sensitivity of 99.78% and specificity of 99.82% and a good accuracy/complexity trade-off. The system could be improved by adding the possibility to work with multiple sampling frequencies. Harari et al. developed a smartphone-based system to detect falls in real life [70]. Participants diagnosed as a risk of falling held or wore at the waist a smartphone embedded with a tri-axial accelerometer and a tri-axial gyroscope while performing ADLs or simulated falls on a lab. Then, the system was validated through 90 days observation of the same kind of subjects (carrying or wearing the smartphone). In case of fall detection, a message to faller's and researcher's phones was generated plus the localization of the faller. In addition, a web portal service could be used to explore the characteristics of the fall related conditions. A threshold-based method was used to reduce the number of possible falls. Then, a set of statistical features (standard deviation, mean) relative to linear acceleration and angular velocity were extracted and passed to a machine learning classifier (logistic regression). The sensitivity was 73%, while precision 37,5%. These not so high values were motivated by the facts that people did not carry the smartphone in some cases or cellular reception was lost in others. Serpen et al. proposed a real-time fall detection system through wearable sensors [71]. Young and adult subjects performed falls and ADLs while wearing two IMUs composed by three-axis accelerometer and three-axis gyroscope at the chest and the thigh. Features like standard deviation and RMS of linear acceleration and angular velocity were considered and given as inputs of SVM or random forest classifiers to differentiate between falls or no falls. Moreover, in case of fall occurrence an airbag was inflated to reduce the injuries due to fall. Missed events and false alarms were evaluated and revealed good performances of both classifiers in detecting falls.

2.3 FINAL CONSIDERATIONS ABOUT THE STATE OF THE ART

By looking at the previously reported works about FoG, risk of falls, falls detection and prediction through systems based on wearable IMUs, several considerations can be made. First, one of the main problems regarding many studies is relative to the number and type of participants. As a matter of fact, many works require to increase the dataset to verify the validity of the proposed method. Generally, papers that inspect balance

properties are devoted to the elderly or to subjects affected by pathological conditions that compromise balance. Studies about fall risk assessment have been conducted on parkinsonian subjects since fall risk is strongly influenced by cognitive and motor characteristics typical of PD [5]. On the other hand, there are fewer studies conducted on PD people to detect or predict falls if compared to the number of works conducted on healthy older or healthy young people simulating falls of the elderly. This introduces a systematic error when these works are considered valid for all patients because age and health status must be taken into account. In fact, there are some differences in the fall dynamics of pathological and healthy subjects, but also in falls characteristics of young and aged people. Most importantly, the imitation of a fall does not truly mimic the characteristics of a real fall. However, since falls are generally rare episodes during daily living, it is necessary to simulate them to develop systems able to capture and predict such events [11].

In some works, the execution of specific motor tasks that include walking, turning, stairs ascending or descending, and simulated falls, is required to train the system for the identification or the prediction of falls or FoG events. Subsequently, these systems are tested during patients' daily life. The problem is that these physical tests are developed to induce loss of balance episodes while in usual ADLs their occurrence is significantly reduced. Therefore, the performances of the developed algorithms cannot be always confirmed in home settings. In other cases, data are taken from datasets that can be public or private and contain simulated ADLs and falls.

Another issue is that several fall monitoring systems can separate between falls and non-falls, but they cannot distinguish between different types of falls. For example, falls can occur in forward, sideward, or backward directions generating different dynamics and only few studies developed systems capable of recognizing them [62].

Some studies relative to falls and FoGs adopted one wearable IMU device which includes three sensors that are tri-axial accelerometer, tri-axial gyroscope, and tri-axial magnetometer. They respectively acquire information about linear acceleration, angular velocity, and magnetic field properties from the movement of subject's body parts. However, the sensors' number and type show a large variability from one system to another. Despite the good performances obtained with this configuration of three

sensors, some studies proposed solutions with only one accelerometer, or with accelerometer and gyroscope, or adding visionary or ambient sensors to the wearable ones, as also confirmed in [13]. Single sensor-based systems largely use accelerometer probably due to its low-cost, market availability, and good results in balance analysis. Nevertheless, some experimental trials highlight that a single gyroscope works better than single accelerometer in recognizing or distinguishing falls events. In any case, it is generally assumed that two (or three) sensors' configurations formed by accelerometer and gyroscope (and magnetometer) behave better than single sensor ones. As already said, wearable sensors can be combined with other kinds of technologies. Visionary and ambient sensors, like video-cameras or audio sensors, can be used alone or added to wearable ones to improve their performances and to verify the correct detection or prediction of a loss of balance event. For example, a camera can be positioned on a room to record all the subject's movements and the video can be used for further verification of the wearable system's correct functioning. While audio sensor can be embedded in the wearable configuration in a way that the user can describe a fall or FoG event or verify its occurrence.

The number of IMUs varies from one to eight in the above-reported papers. It is linked to the parts of the patient's body from which researchers want to extract information related to balance. The great majority of the studies positioned one IMU with two sensors (3D accelerometer and 3D gyroscope) at the level of the trunk (specifically at the waist). Indeed, it is considered the steadiest part of body and it is involved in both static and dynamic postural movements to maintain the equilibrium. Laboratory studies stressed as it is a particularly useful position to assess the dynamics of body's COM during quiet tasks and to acquire information related to postural sway, APA, and PR [12]. At the same time, works created for assessment in home settings underline its usefulness in detecting or predicting falls and FoGs also during dynamic movements. Some experimental trials on FoG show that it is best to locate the sensors on the feet in contrast with the most common practice [33]. Additionally, some studies reported that waist-worn devices can create inconveniences, while thigh-worn devices reduce the disturbance experienced by patients [64]. In fact, the second most adopted sensors' location to identify loss of balance events is on the thighs or feet. They have been found

to be particularly interesting for the extraction of gait parameters. Other falls- and FoGs-related system's configurations locate sensors also on the wrists, neck, chest, and ankles. Similar remarkable results have been obtained by positioning sensors simultaneously at the waist and on the thighs or at the waist and wrists [62]. Studies have shown that sensors at the thigh detect falls before the ones placed on the waist and wrist. So, thigh located sensors could be useful in the prediction of falls. On the contrary, sensors at waist and wrist locations work better for distinguishing fall from other activities.

The raw data can be directly captured from wearable sensors or taken from datasets that contain data previously acquired through the same type of sensors while subjects performed ADLs and different kinds of falls. Then, data are generally filtered, windowed, and processed to extract useful features. They can be categorized in temporal, spatial, frequency, linear acceleration, and angular velocity features, as also observed in [42]. Most of them are the traditional gait parameters usually studied in gait analysis like step time, stride time and so on. These parameters are passed as inputs of machine learning or deep learning classifiers or threshold-based algorithms to assess fall risk, detect, or prevent falls, or FoG events. Threshold-based algorithms are more prone to false alarms since they are based on the manual definition of some threshold values outside of which a fall is detected [64]. Machine learning algorithms are more complex, but they automatically learn from data. Deep learning classifiers can automatically perform the feature extraction process but require a lot of input data.

Most of the presented systems have been differently validated by using diverse approaches. Indeed, some of them evaluate the proposed methodology in terms of accuracy, sensibility, and sensitivity or of mean and standard deviation of the error with respect to gold standards (obtained through video recordings or trials in supervised environments). Some more verify the concurrent clinical validity by looking at the correlation with the scales. Although most of the results are good, this heterogeneity in validation protocols creates difficulties in making comparisons between different systems. Additionally, it is always necessary to find the best trade-off between the performance and the latency time. In this respect, some falls or FoGs detection systems

operate in an offline manner which means that they cannot work in real-time but further improvements are required to use them for continuous monitoring.

In conclusion, there is a lack of a gold standard technique for assessing information relative to gait and loss of balance events through wearable IMUs in terms of sensors' numbers, types, and locations, tasks to be performed, features extraction, and validation procedure. However, most of the described methods use similar configurations and procedures, as illustrated in table 1, in which the most adopted solutions in different studies are reported.

The aim of this thesis is to study and propose a method for the home assessment of gait parameters related to fall risk of parkinsonian subjects using a single wearable sensor. To reach this goal, an IMU device was worn by PD subjects in the lumbar region (trunk) and the walking bouts, extracted from the acceleration signal, were used to find meaningful features related to gait quantity and quality which are associated with fall risk. In this way, doctors could evaluate the walking stability of the PD patients and decide the correct medical therapy to apply, preventing as much as possible unwanted fall-related situations and improving the quality of life of these subjects.

Table 1: this table lists the most adopted solutions in different studies. Legend: APA (anticipatory postural adjustment), PR (postural response), FoG (freezing of gait), FRA (fall risk assessment), FD (fall detection), FP (fall prediction), PD (Parkinson's disease), IMU (inertial measurement unit), Acc (3D accelerometer), Gyr (3D gyroscope), Mag (3D magnetometer), QS (quiet standing), OLS (one leg stance), PRM (push and release maneuver), GI (gait initiation), W (walking), ADL (activity of daily living), T (turning), SF (simulated falls), SD (standard deviation), Sens (sensitivity), Spec (specificity).

STUDIES' CATEGORIES BASED ON GOALS	**PARTICIPANTS**	**MOST ADOPTED SENSORS' NUMBERS**	**MOST ADOPTED SENSORS' TYPES**	**MOST ADOPTED SENSORS' LOCATIONS**	**MAIN EXTRACTED FEATURES**	**MAIN TASKS**	**VALIDATIONS**
Sway *APA* *PR* *(lab)*	Healthy and PD	1 IMU with 2 sensors	1 Acc 1 Gyr	Trunk (sternum, waist, pelvis, neck, chest, lower back)	Linear acceleration Angular velocity	QS OLS PRM GI	Clinical validity (clinical scales)
Gait *(lab)*	Healthy and PD	2 IMUs with 3 sensors	1 Acc 1 Gyr 1 Mag	Feet	Temporal Spatial Frequency	W	Clinical validity (clinical scales)
FoG *(home)*	Healthy and PD	1 IMU with 3 sensors	1 Acc 1 Gyr 1 Mag	Waist	Angular velocity Temporal Frequency Freezing ratio	ADLs W T	Accuracy Sens Spec (video recordings)
FRA *FD (home)*	Healthy and PD	1 IMU with 2 sensors	1 Acc 1 Gyr	Trunk (sternum, waist, pelvis, neck, chest, lower back)	Temporal Spatial Frequency Linear acceleration Angular velocity	ADLs W T SF	Accuracy Sens Spec (video recordings)
FD *FP* *(home or supervised environments)*	Healthy elderly and Healthy young	1 IMU with 2 sensors	1 Acc 1 Gyr	Waist	Temporal Spatial Frequency Linear acceleration Angular velocity	ADLs W SF	Accuracy Sens Spec (trials in supervised environments)

CHAPTER 3: THE NEXT GENERATION INERTIAL MEASUREMENT UNIT DEVICE

3.1 GENERAL DESCRIPTION OF THE DEVICE

The device used for the acquisition of data was the Next Generation IMU (NGIMU) which is a fully featured IMU that can be used for real time or data logging applications [72]. This device includes on-board sensors, processing algorithms, and a huge number of communication interfaces to create a smart and versatile platform well suited for different kinds of applications. As already said, NGIMU contains several on-board sensors: tri-axial accelerometer, tri-axial gyroscope, tri-axial magnetometer, barometric pressure sensor, humidity sensor, and temperature sensor. The presence of many sensors is one of the greatest advantages of this instrument since it allows to perform different kinds of measurements simultaneously, enlarging its application range. NGIMU also includes an on-board Attitude Heading Reference System (AHRS) sensor fusion algorithm that merges magnetic and inertial measurements to describe the orientation relative to the Earth without drift. This peculiarity, together with the possibility to individually calibrate each device with the robotic equipment, increases the accuracy and the level of the performance of the NGIMU. External sensors, like force sensors, can be connected to the analogue input interface. While other external electronics, like GPS, can be connected to the auxiliary serial interface. The NGIMU has also a Guided User Interface (GUI) that can be utilized to change the configuration settings, to explore and plot real-time sensor data, to calibrate sensors, and to export data. The real-time data can be converted from XIO file format to CSV file format to be used with MATLAB or Excel. NGIMU is also compatible with many software and commercial applications (like MATLAB), in fact it contains available libraries for the main programming languages. Moreover, the used communication protocol (OSC) allows the compatibility with many platforms like Arduino or smartphones. This device can be comfortably worn by means of a strap or belt in correspondence of a specific part of the body (like the waist, or the foot). The image 8 depicts the NGIMU and the strap.

Figure 8: this image represents the switched on NGIMU device attached to the strap [73].

3.2 TECHNICAL CHARACTERISTICS OF THE DEVICE

The device has a power button that has to be pressed to turn NGIMU on or off [72]. Each time the device is switched on, a timestamped button message is generated to have a useful indication when data logging will be performed. NGIMU contains five LED indicators with five different colours and five different roles. They contain useful information about Wi-Fi, device, SD card and battery status. The “white” LED indicates the Wi-Fi status that can be not connected (slow flashing), connected but waiting IP address (fast flashing), connected and IP address obtained (solid), or disabled (off). The “green” LED indicates the device status, and it is solid when NGIMU is turned on, off when NGIMU is turned off, or it can blink when the power button is pressed. The “yellow” LED represents the SD card status, and when no card is present it is off, when the card is present but not in use it is flashing, and it is solid when the card is present and in use. The “red” LED shows the battery charging, that is off when the charger is not connected, solid when the charging is in process, slow flashing when charging is complete, fast flashing when battery is less than 20%. Image 9 illustrates the device with the five LEDs switched on.

Figure 9: NGIMU device with all LEDs switched on [72].

The housing of the device is composed by plastic and contains a 1000 mAh battery. It is translucent so that the LEDs' activity can be seen. In the plastic housing there is also the indication of the directions of the three axes (X, Y, and Z), so that the device can be correctly positioned. The battery can be charged through external supply or USB and has a long life (4-12 hours). The NGIMU is very compact and unobtrusive since its size is 55,9 x 38,4 x 18 mm and its weight is 46 g.

Analogue voltage measurements from external sensors (like resistive force sensor that measures force as an analogue voltage) can be measured by the eight channels analogue inputs interface. These measurements are timestamped and sent by the device as inputs messages.

The auxiliary serial interface directly regulates the communication with external electronics (like GPS technology) by means of a serial connection. The connection can be direct or mediated by a microcontroller to add others input or output functionalities.

The sample rates of the internal sensors by which all measurements are acquired are fixed and depend on the sensor. For example, gyroscope and accelerometer have a sample rate of 400 Hz, while magnetometer of 20 Hz. At the same time, the user can decide the send rate of each measurement message type, but this does not modify the sample rates of acquisition. Whenever a sample is acquired, a timestamp is created to be a reliable measurement, without the disturbance of the buffering or latency relative to a given commutation channel.

The real-time communication occurs through USB, Wi-Fi, serial, or written to the SD card. The communication protocol is encoded as OSC and this protocol, together with the communication interfaces, allow the compatibility of this device with a wide range of platforms.

All the technical characteristics of the NGIMU device are collected and illustrated in the following table 2.

Table 2: this table summarizes the technical characteristics of the NGIMU sensor [72]. Legend: ° (degree), s (seconds), Hz (Hertz), g (gravity), µT (microtesla), hPa (hectopascal), mAh (milliAmpere hour), V (Volts), h (hours), kHz (kilohertz), GPS (Global Positioning System), AHRS (Attitude Heading Reference System), GHz (gigahertz), GUI (guided user interface).

ON-BOARD SENSORS	Tri-axial gyroscope: scale = ± 2000°/s, sample rate = 400 Hz, resolution = 16-bit. Tri-axial accelerometer: scale = ± 16 g, sample rate = 400 Hz, resolution = 16-bit. Tri-axial magnetometer: scale = ± 1300 µT, resolution = 0,3 µT. Barometric pressure: scale = 300-1100 hPa, resolution = 24-bit. Humidity: range = 0-100%, sample rate = 25 Hz, resolution = 0,008%. Temperature. Battery: current = 1000 mAh, voltage = 4,5-6 V, charging (USB or external supply), life = 4-12 h. Real time clock.
ON-BOARD DATA ACQUISITION	Analogue inputs: channels = 8, voltage = 0-3.1 V, sample rate = 1 kHz. Auxiliary serial for GPS or custom electronics: RS-232 compatible.
ON-BOARD DATA PROCESSING	All sensors are calibrated. AHRS fusion algorithm provides a measurement of orientation relative to the Earth as a quaternion, rotation matrix, or Euler angles. All measurements are timestamped.
COMMUNICATION INTERFACES	USB. Serial: RS-232 compatible. Wi-Fi: band = 5 GHz, built-in or external antennae. SD card.
SOFTWARE FEATURES	Open-source GUI. Configure device settings. Plot real-time data. Log real-time data to file (CSV file format for use with Excel, MATLAB, etc.).

3.3 ACCELEROMETER

The accelerometer is an inertial measurement instrument that can measure the acceleration of a body, i.e. the variation of the velocity of the body over time. As in the case of the seismograph, accelerometer is an absolute motion transducer because it is mounted in the measurement object, and it does not measure the acceleration of a fixed point in the surrounding environment but directly the acceleration of a mass that is moving with the same frequency of the object in motion. The input of the accelerometer is an acceleration, while the output is a displacement. It is an inertial instrument because its functioning principle is based on mass-spring-damper system, as illustrated in figure 10.

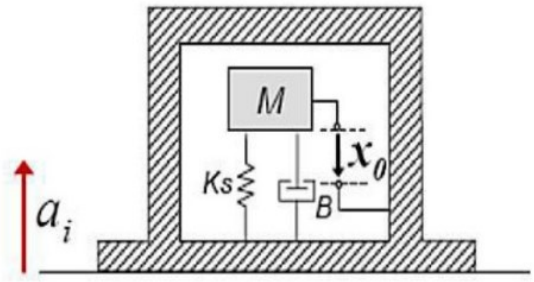

Figure 10: this figure shows the mass-spring-damper system.

According to this principle, a mass (M) is connected to a movable object through a spring (spring constant: Ks) and a damper (damping factor: B). When the object is put in motion and exerts a certain acceleration (a_i), the mass, with a certain inertia, moves from the resting position with a displacement (x_0) that is proportional to the detected acceleration. Then, the sensor transduces the displacement into an electrical signal that can be recorded by the modern measurement instruments. The equation that connects the displacement of the mass to the initial acceleration is eq. (1):

$$a_i = \ddot{x}_0 + \frac{B}{M}\dot{x}_0 + \frac{K_s}{M}x_0 \quad (1)$$

Where a_i is the initial acceleration of the movable object; $\ddot{x}_0$ is the acceleration of the mass; B is the damping factor; M is the inertial mass; $\dot{x}_0$ is the velocity of the mass; K_s is the spring constant; x_0 is the displacement of the mass.

According to the physical principle used to measure the displacement of the mass, there can be different typologies of accelerometers, like strain gauge accelerometers, piezoelectric accelerometers, capacitance accelerometers, and laser accelerometers. The smaller are the dimensions of the accelerometer and the higher will be the resonance frequency. Additionally, small accelerometers do not excessively modify the dynamical characteristics of the structure to be measured. So, accelerometers of IMU devices, like NGIMU, are generally of type MEMS (Micro Electro Mechanical Systems). They allow the integration of compact mechanical and electrical elements in a silicium substrate to reduce the dimensions of conventional sensors and to reduce the cost. So, the tri-axial accelerometer included in the NGIMU can measure the linear acceleration along three different axes (x, y, and z) with respect to the anatomical part to which the sensor has been positioned. Generally, one of the three axes is pointing in AP direction, another axis in ML direction, and the last axis in vertical direction. Before usage, the accelerometer of the NGIMU must be calibrated and this can be done from the GUI of the device with the help of 3D view function, as can be seen in image 11.

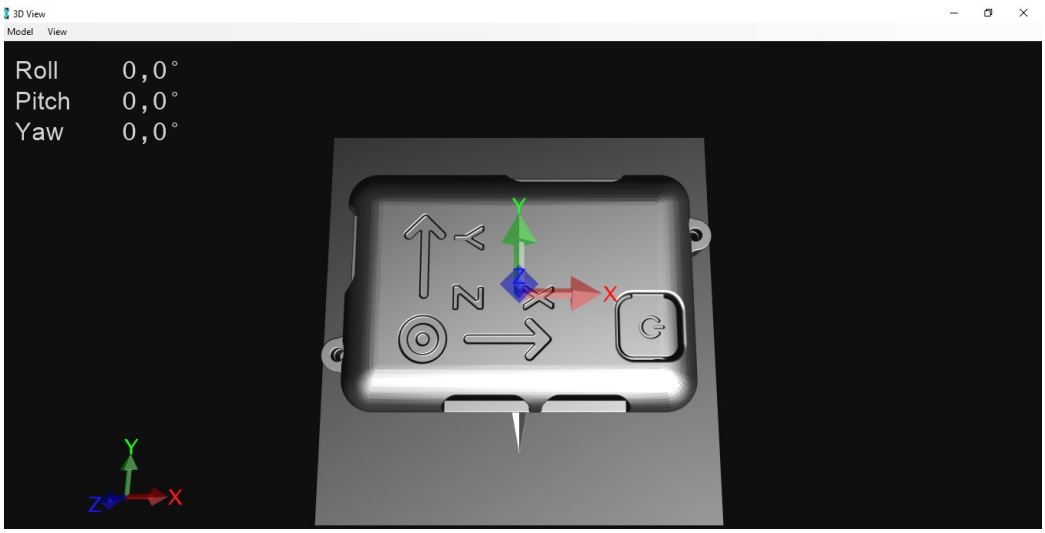

Figure 11: this image shows the 3D View function of the NGIMU software which depicts the three axes of the device's internal sensors (accelerometer, gyroscope, magnetometer etc.) and that can be useful for calibration [72].

3.4 ROTATION MATRICES, EULER ANGLES, AND QUATERNIONS

The kinematics is the branch of mechanics that describes the motion of points, bodies (objects), and system of bodies without consideration of the masses of those objects

nor the forces that may have caused the motion. A material point is an object with negligible size with respect to the space where it can move. A set of material points whose reciprocal distances do not vary during the time can form a rigid body (for example, a sensor attached to the waist is a rigid body).

A reference frame is a set of rules and coordinates (cartesian, cylindrical, spherical, etc.) which is used to describe the position of an object in the space. Generally, to describe the position and the orientation of a rigid body in the space, it is possible to define two different reference frames. One of them is attached to the body itself, it is movable, and it is also known as local reference frame, the other is external to the body, it is fixed, and it is called world reference frame. The position of a rigid body can be defined as the distance between the origin of the local reference frame (centred in one point of the rigid body) and the origin of the world reference frame, defined with respect to the world reference frame. While the orientation of the object is defined as the rotation matrix that describes the rotation of the local reference frame with respect to the world reference frame. These concepts are shown in the following figure 12.

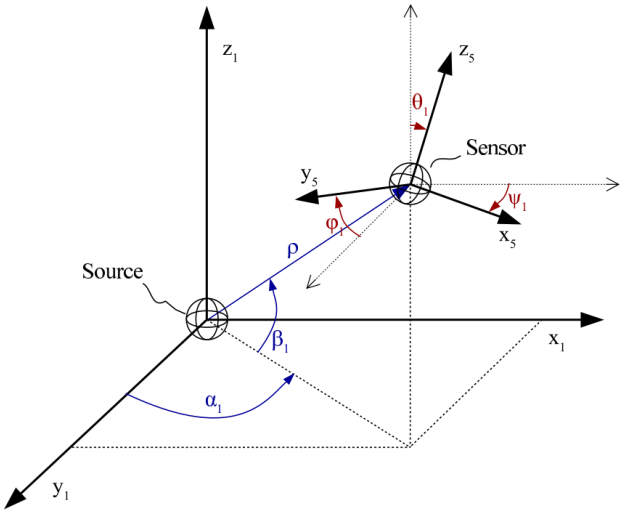

Figure 12: this figure shows the world reference frame (source), and the local reference frame attached to the rigid body (in this case a sensor) with a different position and orientation [74].

The position of the rigid body with respect to the world reference frame is ${}^{source}\rho$.

The orientation of the rigid body is described by the eq. (2):

$$^{source}R_{sensor} = [^{source}x_{sensor}, ^{source}y_{sensor,} ^{source}z_{sensor}] \quad (2)$$

Where $^{source}R_{sensor}$ is the rotation matrix that describes the orientation of the sensor with respect to the source; $^{source}x_{sensor}$, $^{source}y_{sensor}$, $^{source}z_{sensor}$ are the unit vectors which describe the position of the sensor with respect to the source.

Rotation matrices are 3x3 orthonormal matrices composed by nine elements. These elements, in turn, are composed by products of sines and cosines of the angles that describe the different orientation of one body respect to another. Orthonormality introduces six constraints among these nine elements, which are the three degrees of freedom associated with the position and three degrees of freedom associated with the orientation of a rigid body relative to the world frame. The three constraints associated with the orientation are basically three angles which describe the angular displacement of one body with respect to a fixed frame. If there are two reference frames that have the same origin but different orientations, the rotation matrix that describes the orientation of one reference frame with respect to the other, requires three rotations about three independent axes to be computed. If one reference frame experiences more than one rotation with respect to the other frame, the product between the rotation matrices can be used to compute the final rotation matrix (chain rule). This operation depends on the order of the rotations and on the axes about which the rotations have been occurred. Generally, if three rotations have been performed about moving axes with a specific sequence, the Euler angles can be computed and used to describe the final orientation of the rigid body with respect to the fixed frame. So, starting from the situation in which the two frames (movable: xyz and fixed: XYZ) are aligned, Euler angles (figure 13) are defined as: φ angle about which current z axis rotates, θ angle about which current x axis rotates, and Ψ angle about which current z axis rotates. So, knowing these three angles and the order of rotations, the orientation of a rigid body in the space can be defined.

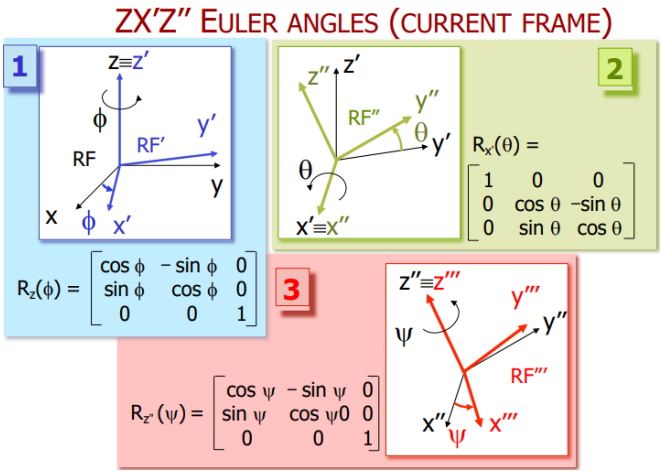

Figure 13: this figure illustrates the Euler angles and elementary rotation matrices obtained after an ordered sequence of rotations about three independent moving axes (z, y, and x).

The NGIMU is a device that measures quantities, like the acceleration, in the sensor reference frame, that is an orthogonal triplet with a particular orientation in the space and it depends on the positioning of the sensor. So, to define the orientation of the NGIMU's sensors with respect to the earth (or world) external fixed reference frame, quaternions are used starting from data of accelerometer and gyroscope.

The unit quaternion is a set of numbers that generalizes in the three-dimensional space the complex numbers and their meaning as rotational operators in the plane. When the axes of two of the three gimbals are driven into a parallel configuration, they "lock" the three-dimensional system in rotation into a degenerate two-dimensional space. This phenomenon is known as gimbal lock, and it is a consequence of the singularity. A singularity corresponds to a loss of one degree of freedom when the inverse problem to find the Euler angles from the rotation matrix cannot be solved. In this case, it is possible to use the unit quaternion representation, eq. (3):

$$Q = \{\eta, \varepsilon\} = \{\cos(\theta/2), \sin(\theta/2)r\} \tag{3}$$

Where Q is the unit quaternion; η is a scalar; ε is a three-dimensional vector; θ is the angle of rotation; r is the rotation matrix.

These terms are constrained by the eq. (4):

$$\eta^2 + \varepsilon_x^2 + \varepsilon_y^2 + \varepsilon_z^2 + = 1 \quad (4)$$

Where ε_x, ε_y, ε_z are the elements of the vector ε.

The absence of rotation is defined by the eq. (5):

$$Q = \{1, 0\} \quad (5)$$

Given the rotation matrix $R = \{r_{ij}\}$, that is shown in the following eq. (6):

$$\begin{aligned} R_x &= [\, 2(\eta^2 + \varepsilon_x^2) - 1 \quad 2(\varepsilon_x\varepsilon_y - \eta\varepsilon_z) \quad 2(\varepsilon_x\varepsilon_z + \eta\varepsilon_y)] \\ R_y &= [\, 2(\varepsilon_x\varepsilon_y - \eta\varepsilon_z) \quad 2(\eta^2 + \varepsilon_y^2) - 1 \quad 2(\varepsilon_y\varepsilon_z + \eta\varepsilon_x)] \\ R_z &= [\, 2(\varepsilon_x\varepsilon_z - \eta\varepsilon_y) \quad 2(\varepsilon_y\varepsilon_z + \eta\varepsilon_x) \quad 2(\eta^2 + \varepsilon_z^2) - 1] \end{aligned} \quad (6)$$

It is always possible to find η and ε, as shown in eq. (7) and eq. (8):

$$\eta = \frac{1}{2}\sqrt{r_{11} + r_{22} + + r_{33} + 1} \quad (7)$$

Where r_{11}, r_{22}, r_{33} are the diagonal elements of the rotation matrix R.

$$\begin{aligned} \varepsilon_x &= \tfrac{1}{2}\,[\,(sgn\,(r_{32} - r_{23})\sqrt{r_{11} - r_{22} - r_{33} + 1}\,] \\ \varepsilon_y &= \tfrac{1}{2}\,[\,(sgn\,(r_{13} - r_{31})\sqrt{r_{22} - r_{33} - r_{11} + 1}\,] \\ \varepsilon_z &= \tfrac{1}{2}\,[\,(sgn\,(r_{21} - r_{12})\sqrt{r_{33} - r_{11} - r_{22} + 1}\,] \end{aligned} \quad (8)$$

Where $sgn(x) = 1$ if x>=0 and $sgn(x) = -1$ if x<0.

Therefore, the real advantage of quaternions is that it is always possible to find a solution of the inverse problem, also in presence of singularities. The drawback is that quaternions do not represent actual angles and so do not allow to obtain an “intuitive” representation of the real rotations around the axes. Instead, Euler angles represent three specific rotations about three axes, and they can be more easily “imagined”. Quaternions are simply four numerical values, but they can be easily found starting from an axis of rotation and an angle of rotation, enabling the description of the orientation of a rigid body with respect to the earth reference frame.

CHAPTER 4: EXPERIMENTAL TRIALS

4.1 LABORATORY TRIALS

In order to test and validate the fall risk identification system proposed in this study, two elderly PD subjects (aged over 70 years) were recruited from the private clinic "Villa dei Pini" (Civitanova Marche, Italy) [75]. Experimental trials were mainly performed in the gym of the clinic and were video recorded through a GoPro to verify the correct functioning of the algorithm. Three NGIMU devices were switched on and positioned on subjects in correspondence of specific body parts by using Velcro straps [72]. One NGIMU device at the level of the lower back, and two NGIMUs one for each foot, as illustrated in figure 14. For the purpose of this study, only the device wore at the level of the lower back was used for the further analysis.

Figure 14: the red circles in this image illustrate the positioning of the three NGIMU devices (one at the lower back, two at the feet).

The three NGIMUs were positioned following specific orientations with the help of the outlined axes in the plastic housing of the NGIMU. Regarding the device at the lower back, the x-axis of the NGIMU was used as ML-axis and points laterally, the y-axis as vertical-axis and points upward, and the z-axis as AP-axis and points forward, as shown in figure 15.

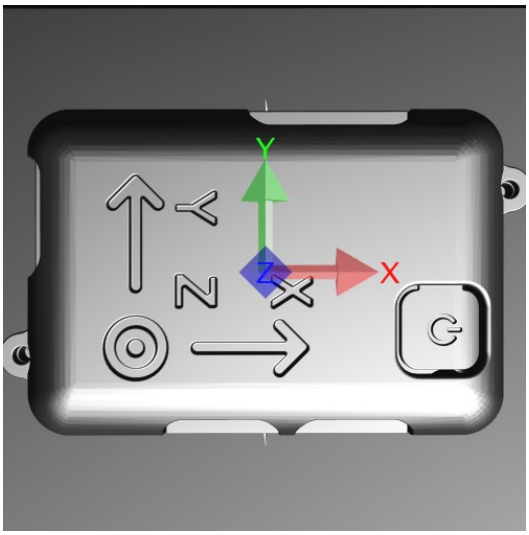

Figure 15: this figure shows the correct orientation of the NGIMU positioned at the lower back. The x-axis of the NGIMU was used as ML-axis and points laterally, the y-axis as vertical-axis and points upward, and the z-axis as AP-axis and points forward [72].

During the experimental trial, one subject (subject 1) was asked to perform these walking paths:

- Timed-up and go test (TUG) in which subject started from sitting on a chair, then walked straight on for some meters, completed a turn of 180° around an obstacle, moved straight on for some meters again, and finally seated again on the chair. This activity was performed twice.
- Trial in which subject started from sitting on a chair, then walked straight on for some meters, ascended and descended from stairs for four times, walked straight on for some meters again, and finally seated again on the chair.
- Trial in which subject walked "freely" inside and outside the clinic for 15 minutes (so experiencing several straight walks, turns, stair ascending and descending activities, and pauses).

The following image 16 illustrates the experimental trials performed by subject 1 during lab study.

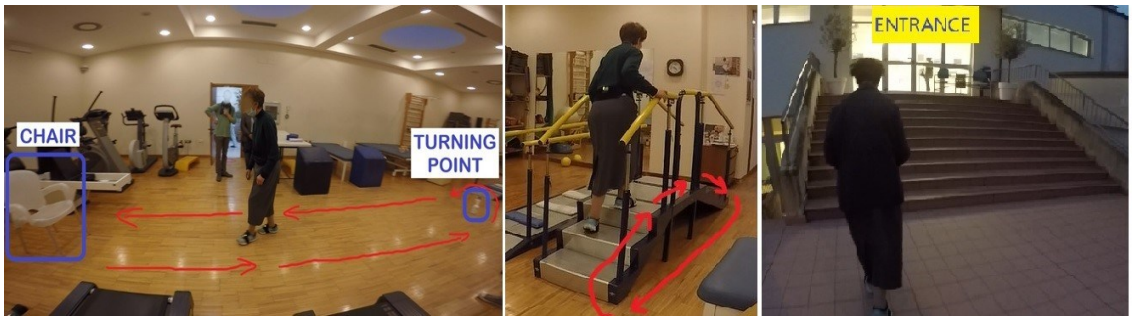

(a) (b) (c)

Figure 16: this figure is formed by three images which illustrate the different tasks performed by subject 1 in laboratory trials. Fig. 16 (a) depicts the TUG task that was repeated twice. Fig. 16 (b) depicts stair ascending and descending task. Fig. 16 (c) depicts the "free" walking task.

Subject 2 was asked to perform only TUG test twice since he was not able to complete the other motor tasks due to severe motor difficulties.

Finally, the three NGIMUs were removed from subjects and switched off.

The algorithm proposed in this thesis considered parameters that had to be extracted from walking activities of a certain "entity", (in terms of walks or activities which included walks with a certain periodicity and duration), to perform the gait analysis and to define the consequent fall risk of each subject. Therefore, the heterogeneity of walking tasks in laboratory trials was adopted to verify that the algorithm correctly identified and worked with these kinds of activities, rejecting the others.

4.2 HOME TRIALS

The aim of this study was to generate an algorithm that could work in home settings during daily activities. Literature findings generally agree that it would be better to define the gait quality and the fall risk while subjects perform common ADLs in their usual daily contexts than during lab examinations. As also described in chapter 2, this kind of analysis allows to obtain a more realistic estimation of the fall risk. In fact, during laboratory trials subjects are just "simulating" specific tasks and these activities are thought to induce loss of balance events, while usual ADLs are less common associated with these kinds of events. Consequently, 8 home trials were performed in this study.

Seven elderly PD people were recruited from the private clinic “Villa dei Pini” (Civitanova Marche, Italy) [75]. They were asked to wear three NGIMU devices (two at feet, one at the lumbar region) with the same orientation as in laboratory trials (figure 15) [72]. Also in this case, only the NGIMU positioned at the lumbar region was considered in this study. The suggested location for the positioning of the NGIMU was at the lower back but some people preferred to position it in a different anatomical part (for example, laterally in correspondence of the hip or frontally at the waist). Since the direction of accelerometer’s axes was of crucial importance in the development of the algorithm, quaternions were used to correct the directions of the three axes in case the device was wrongly oriented, as happened in figure 17 a.

(a) (b)

Figure 17: this figure shows the positioning and the orientation of the NGIMU during one home trial. Fig. 17 (a) illustrates the positioning of the device at the lumbar region (lower back). Fig. 17 (b) depicts the correct orientation of the NGIMU device [72].

During these trials subjects were asked to switch on the device and to wear it while performing their common ADLs during the day. At the same time, they annotated these activities on a diary which can also include additional information about problems with the device (improper positioning or switching off due to the battery discharging) or the description of subject’s health status during the day. These acquisitions were used to train the algorithm and diaries to verify the proper functioning of the proposed system. Indeed, final features that were extracted as indicators of gait quality and fall risk were estimated from these home derived data.

CHAPTER 5: DATA ACQUISITION AND SOFTWARE IMPLEMENTATION

5.1 DATA ACQUISITION

As already said, data were acquired through an NGIMU device located in the lumbar region. Before using the device for the experiments, NGIMU was connected by USB cable to the NGIMU application (software version 1.18) through “Connection” menu of the NGIMU GUI [72]. Then, it was calibrated with the help of “3D View function” from “Graphs” menu of the NGIMU GUI (figure 11) to be sure that the sensors’ axes were correctly oriented. Subsequently, the “Wi-Fi” option was disabled from the “Settings” menu because the device had to record data only through SD card and so Wi-Fi was not used during experimental trials (figure 18). Additionally, the “Send Rates” options of all sensors was manually set at 200 Hz from the same menu (figure 18).

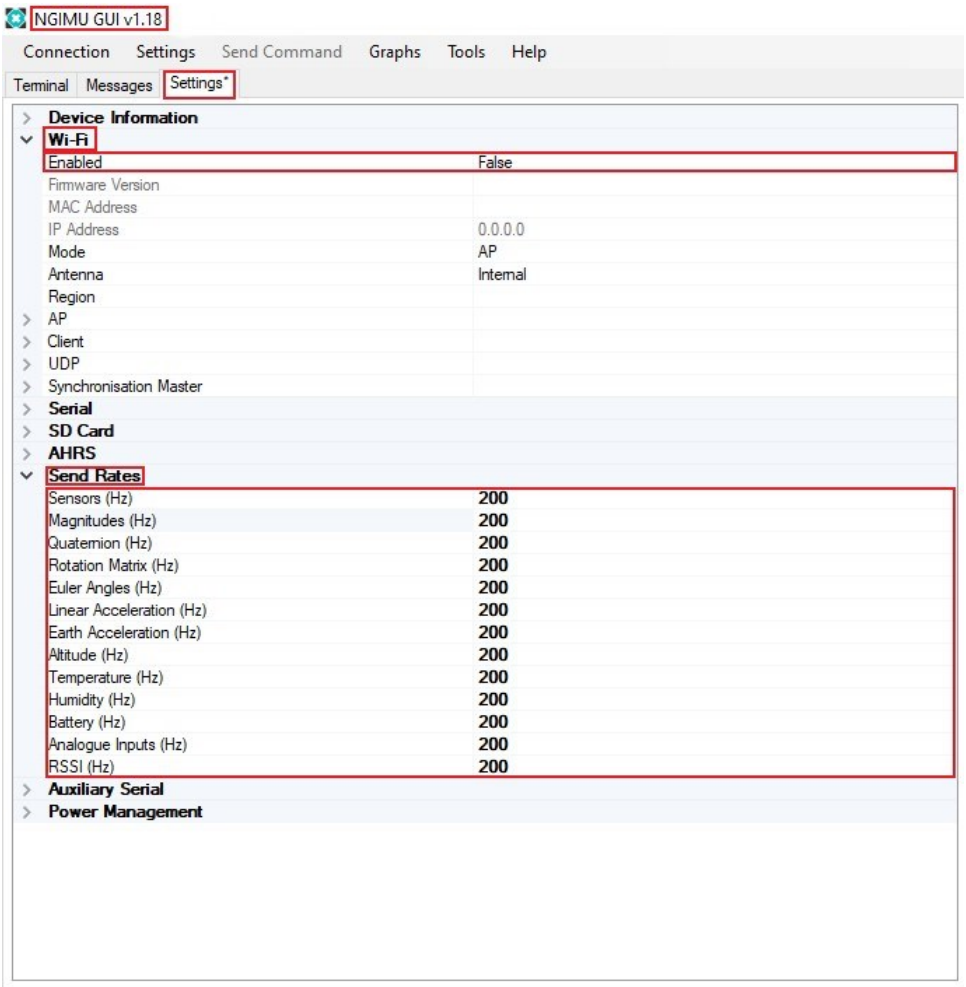

Figure 18: this image depicts the modifications on “Wi-Fi” and “Send Rates” options accessed from “Settings” menu of the NGIMU GUI [72].

After this initial configuration, the device was fully charged, and an empty SD card was inserted in the appropriate location and used for data storage during acquisitions. When the device was switched on, it was verified that green and yellow LEDs' lights were turned on and solid. This indicated the correct functioning of the device and of the SD card. Once an acquisition was completed, data were assessed from the SD card as files in XIO format and were converted in CSV format by means of "SD Card File Converter" from "Tools" menu of NGIMU GUI. To use this functionality, it was needed to simply select the "SD Card File" (the acquisition to convert) and the "Destination Directory" in which store the converted data (figure 19).

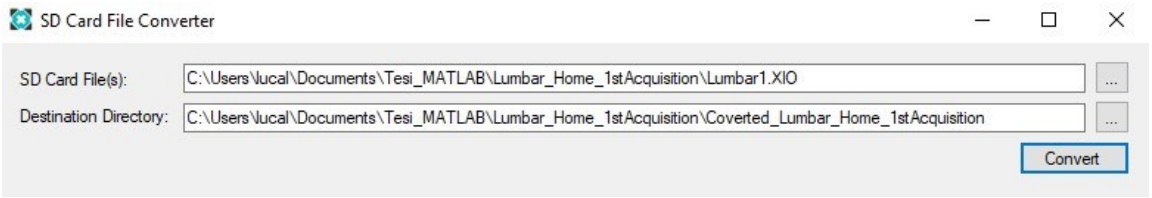

Figure 19: this image shows the "SD Card File Converter" of the NGIMU GUI with an example of "SD Card File" and "Destination Directory" [72].

One of the advantages of the NGIMU is that it is not necessary to repeat the initial configuration procedure since the modified options are stored in the memory of the device and are kept equal for new acquisitions. This fact avoids the consumption of time that is usually spent for these operations. Another advantage is represented by the compact size and low weight of the NGIMU, which make it unobtrusive and convenient. These factors, together with the high accuracy and reliability, the possibility to use quaternions, and the ease of use explain why this device was adopted in this study.

5.2 SOFTWARE IMPLEMENTATION

To recap, two subjects underwent laboratory experiment, while seven people participated to the home experiment. So, totally seven participants were included in this study. All of them were affected by PD, were aged over 70 years old, and were recruited from the private clinic "Villa dei Pini" (Civitanova, Marche, Italy).

As already described, data acquired by NGIMU as XIO files were then converted into CSV files to make them compatible with MATLAB platform (version R2021B). The script elaborated in this study can be approximatively divided into seven main parts (figure

20): pre-processing, extraction of activity segments, extraction of walking segments, re-orientation of sensors' axes with quaternions, extraction of segments which contain "real" steps, computation of parameters, and generation of the final output. The aim of this algorithm was to extract parameters that can describe the gait quantity and the gait quality, that are associated with fall risk in PD individuals. To reach this purpose, the final output controlled the membership of some of the computed parameters with ranges taken from the literature to express considerations about subjects' walking stability and fall risk.

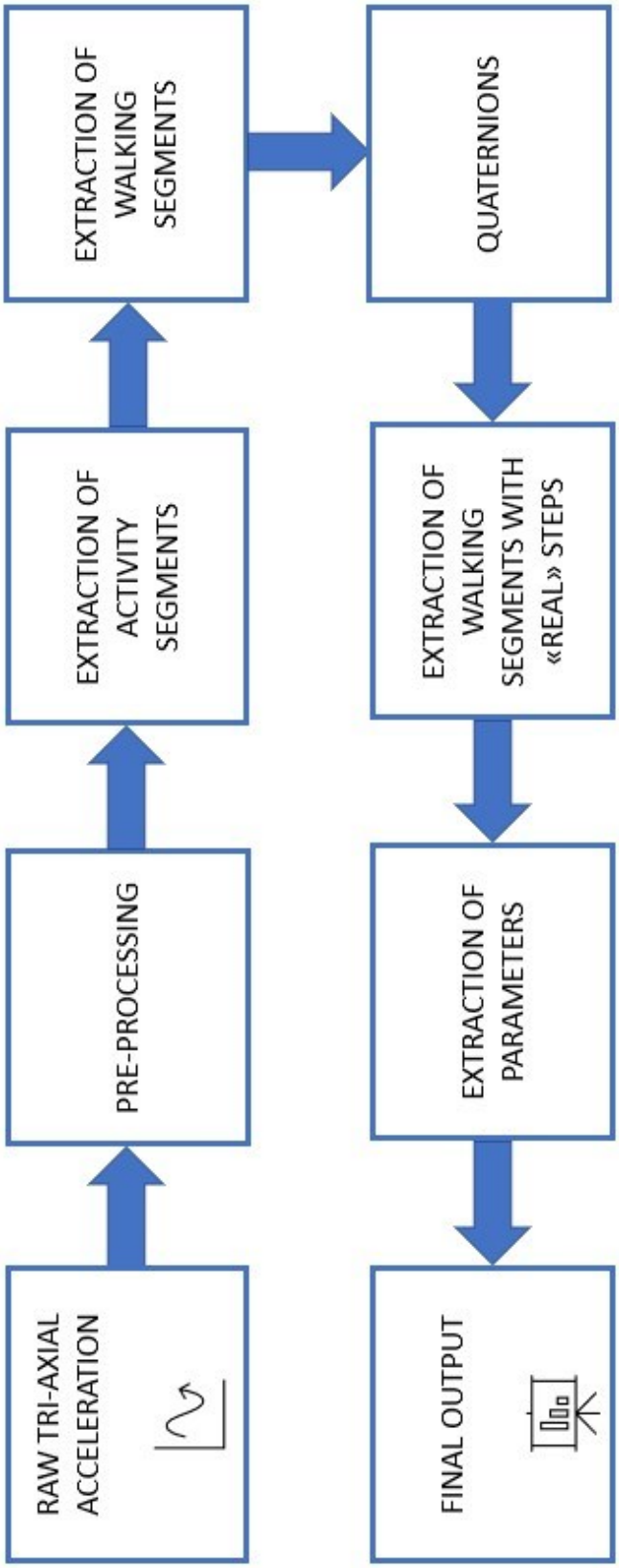

Figure 20: this figure contains the block scheme of the main parts in which the proposed algorithm can be divided.

5.2.1 PRE-PROCESSING

In pre-processing phase, the raw acceleration data along three axes underwent a three steps procedure which consisted of: detrend, mean removal, and filtering (figure 21). First, the best straight-fit line was removed from the three accelerations by means of “detrend” function of MATLAB, as also suggested in [53], [76]. Then, the mean of each signal was removed with the help of “mean” function of MATLAB. Finally, a band pass Butterworth filter was applied by using “butter” and “filtfilt” MATLAB functions. The latter was composed by a second order high pass filter (HPF) with cut-off frequency of 0,5 Hz and a second order low pass filter (LPF) with a cut-off frequency of 5 Hz. The reason behind this choice was that the algorithm had to focus on walking activities which generally occur in the selected range (0,5÷5 Hz) [77].

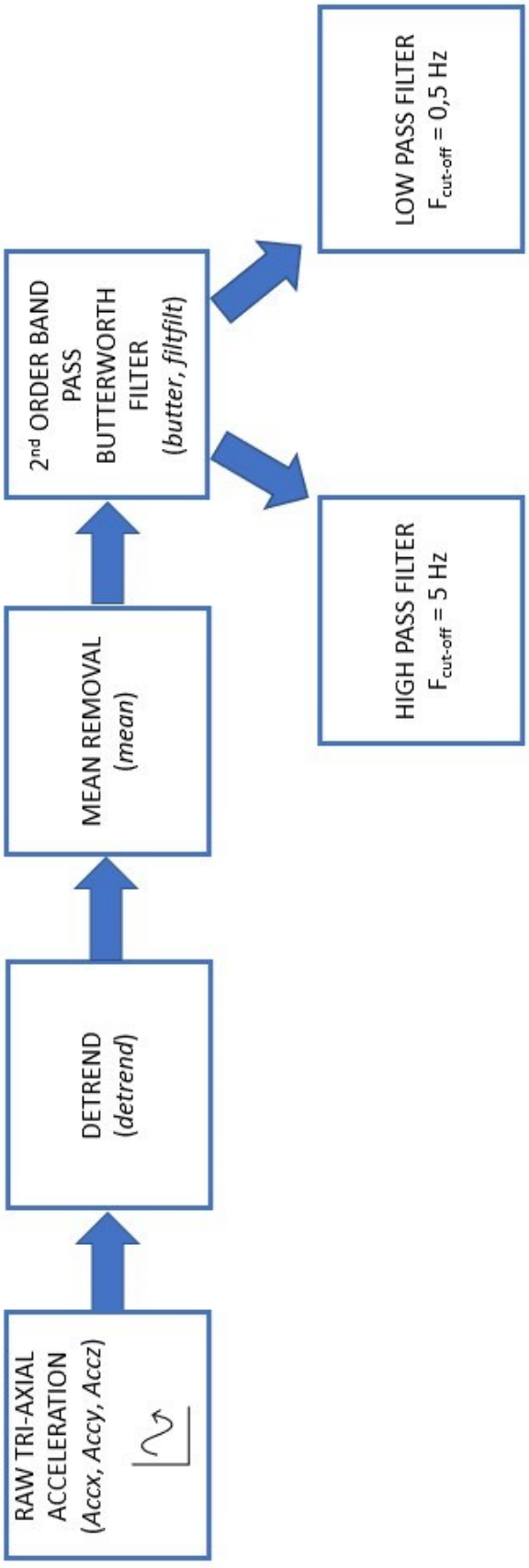

Figure 21: this figure shows the block scheme of the pre-processing. In cursive character there are the names of the used MATLAB functions.

The following figures 22 and 23 show the comparison between the three components of acceleration before and after pre-processing of an acquisition performed in the laboratory.

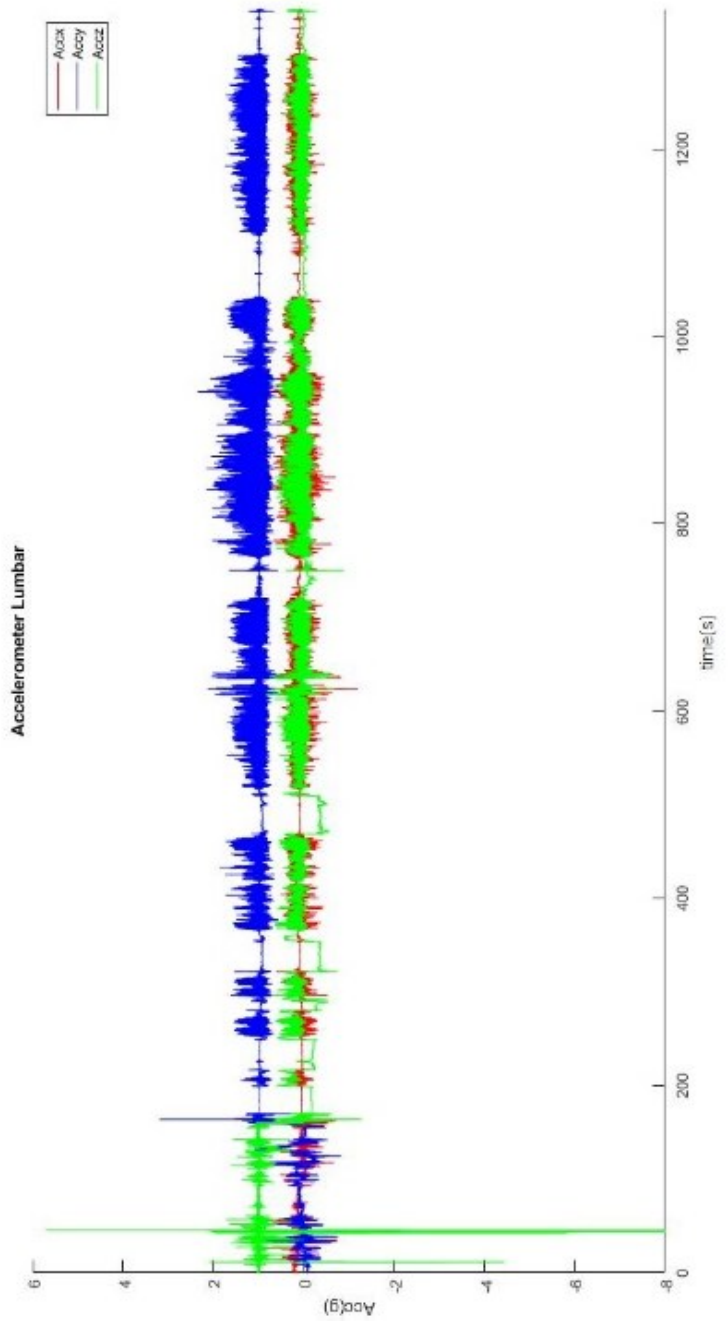

Figure 22: this figure illustrates the three components of acceleration along time before pre-processing of an acquisition performed in the clinic. In the x-axis the time is expressed in seconds (s), in the y-axis the acceleration in gravity (g). “Accx” is the ML acceleration (in red), “Accy” is the vertical acceleration (in blue), “Accz” is the AP acceleration (in green).

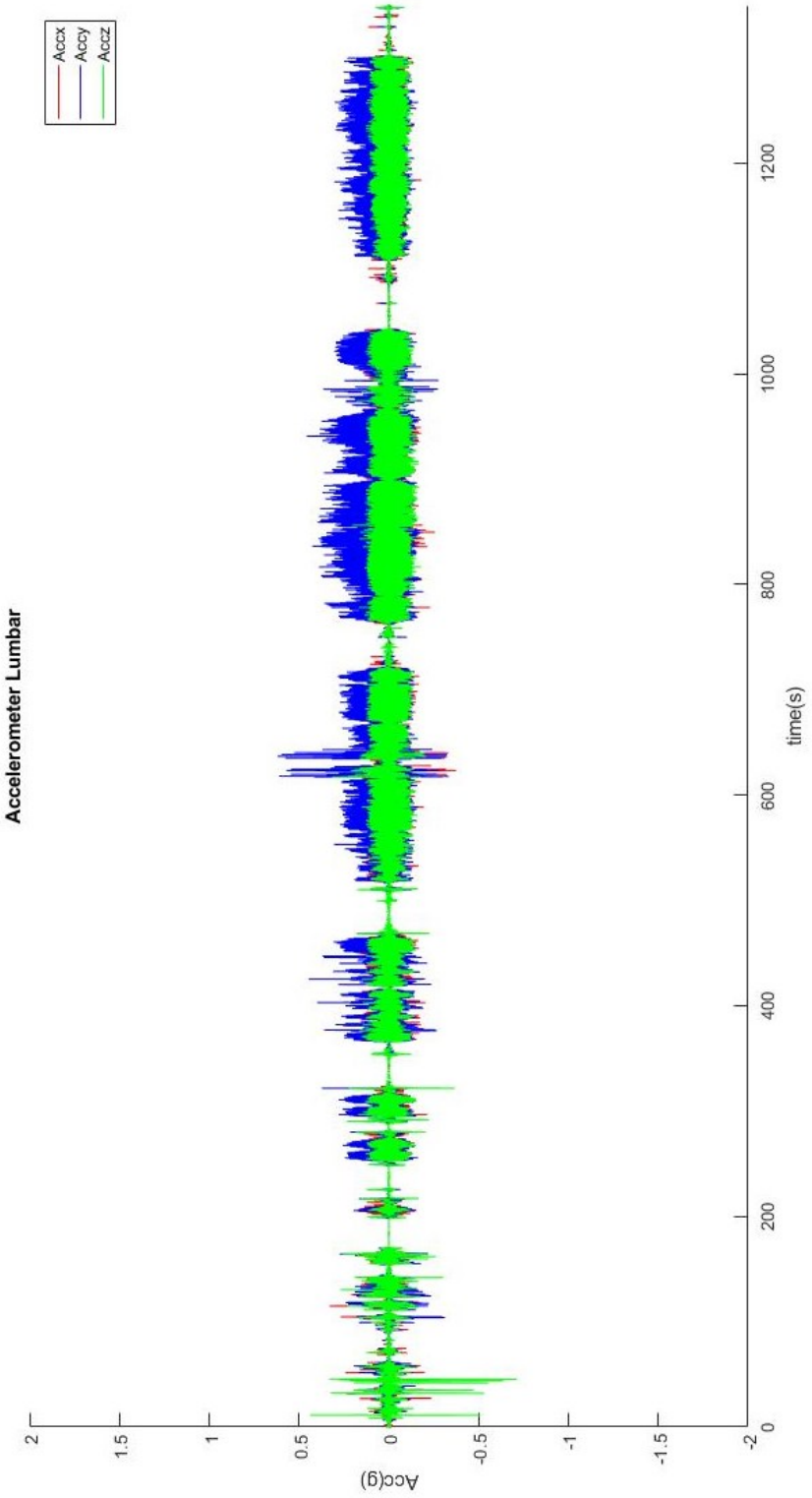

Figure 23: this figure illustrates the three components of acceleration along time after pre-processing of an acquisition performed in the clinic. In the x-axis the time is expressed in seconds (s), in the y-axis the acceleration in gravity (g). “Accx” is the ML acceleration (in red), “Accy” is the vertical acceleration (in blue), “Accz” is the AP acceleration (in green).

5.2.2 EXTRACTION OF ACTIVITY SEGMENTS

The extraction of activity segments from the pre-processed signals occurred through double filtering procedure. An activity was defined as a movement of the device of a certain entity that could be an ADL performed by the subject that was wearing it or simply a strong oscillation of the device due to other causes. First, two-seconds sliding windows with one second of overlapping were extracted from pre-processed accelerations[30]. The length of sliding windows (two-seconds with 50% of overlapping) was set to exclude pauses (also minimal ones) from further steps. Each two-seconds sliding window underwent a signal magnitude area (SMA) threshold-based filter in time domain and an energy (EN) threshold-based filter in frequency domain [77]. The SMA and EN were defined in equations (9-10) as in [54], [78], [77]:

$$SMA = \sum_{i=1}^{N} \sqrt{Accx(t)^2 + Accy(t)^2 + Accz(t)^2} \quad (9)$$

Where *i* is the current two-seconds sliding window, *N* is the total number of two-seconds sliding windows, and *Accx(t)*, *Accy(t)*, *Accz(t)* are the three components of acceleration in time domain.

$$EN = \sum_{i=1}^{N} \sqrt{|fft(Accx(t))|^2 + |fft(Accy(t))|^2 + |fft(Accz(t))|^2} \quad (10)$$

Where fft is the fast Fourier transform.

If the SMA and EN of the current two-seconds sliding window respectively exceeded the 75% of the means of the SMA and EN and this was kept the same for at least three consecutive windows, the two-seconds segment was considered as an activity window, as described in the following expression (ex. (11)):

if *SMA(i, i+1, i+2)>75%(mean(SMA))* ***AND*** *EN(i, i+1, i+2)>75%(mean(EN))* ➔ (11)

➔ *ACT(i) is considered as an ACTIVITY WINDOW*

Subsequently, windows with the same end and the same start were considered as a unique one. Lastly, only activity windows with a duration that was higher than 10 seconds were used for further processing. The length of overlapping windows, the

thresholds based on SMA and EN, and the minimal length of activity segments were empirically selected after performing several trials to obtain the highest precision in the result.

The figure 24 depicts the block scheme of the extraction of activity segments. The figure 25 illustrates the pre-processed acceleration along three axes of an acquisition performed during a laboratory trial, and the step function which highlights the extracted activity segments.

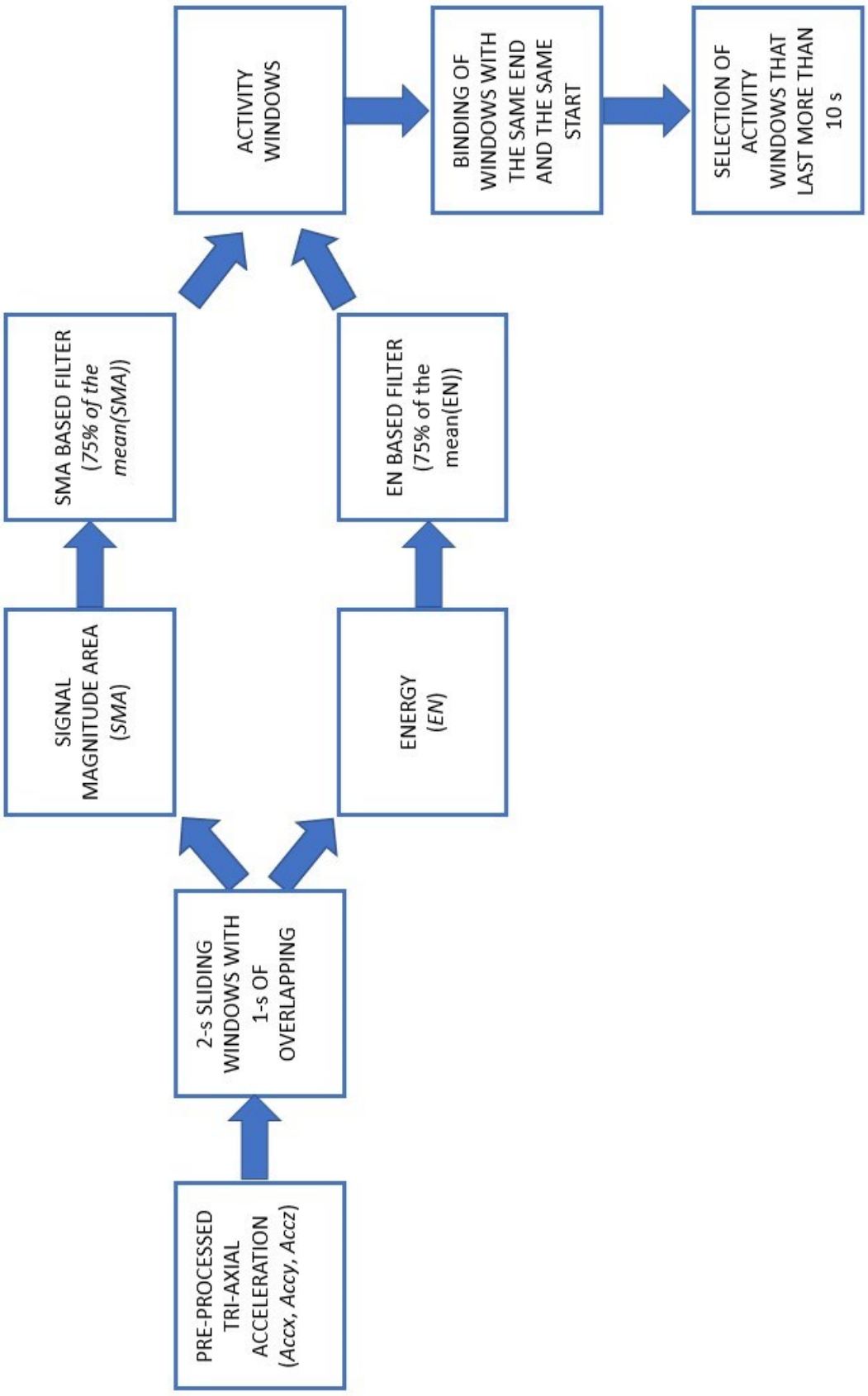

Figure 24: this figure shows the block scheme of the extraction of activity segments.

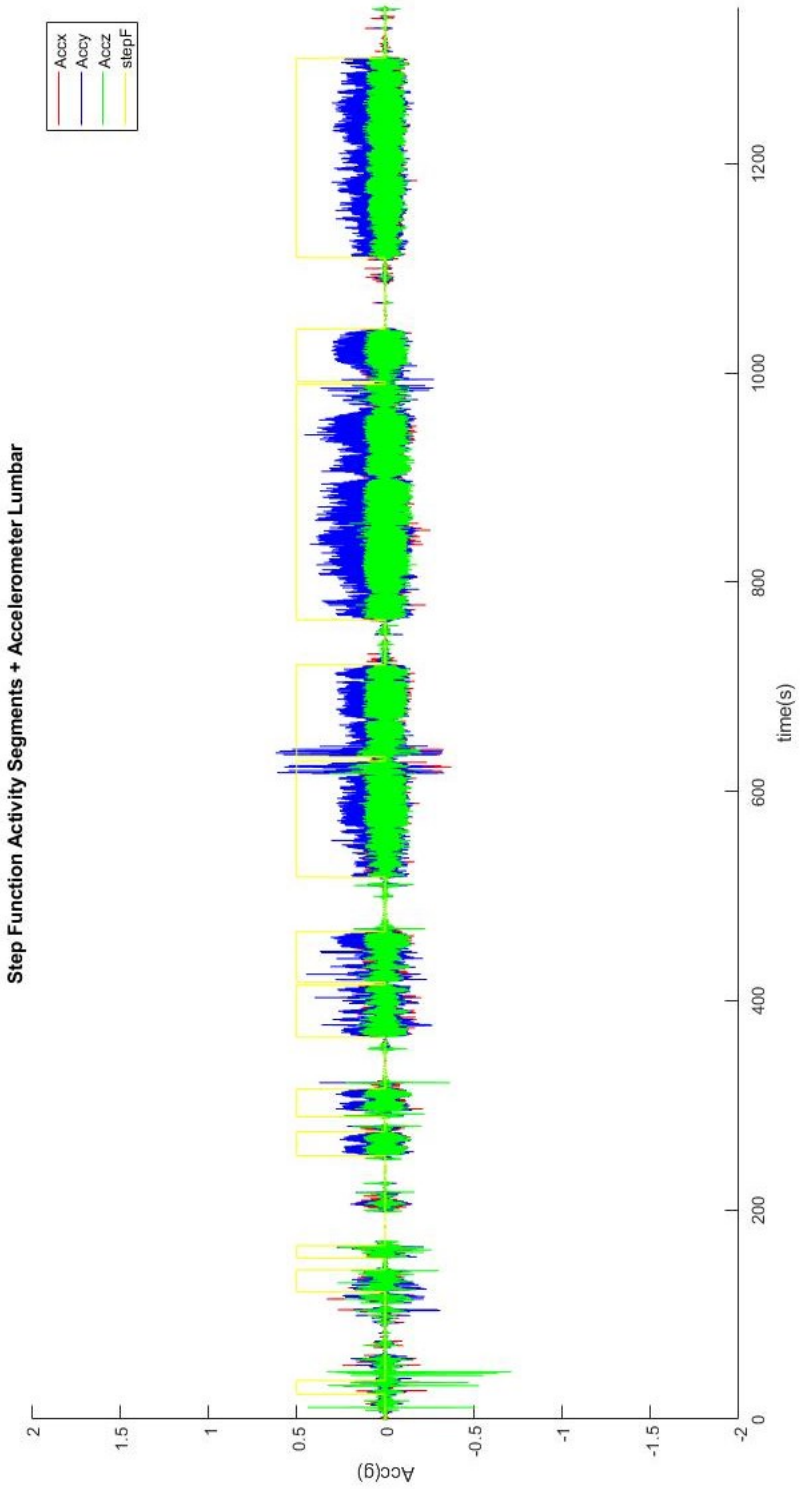

Figure 25: this figure illustrates the three components of acceleration along time of an acquisition performed in the clinic, and the step function (yellow) represents the extracted activity segments longer than 10 s. In the x-axis the time is expressed in seconds (s), in the y-axis the acceleration in gravity (g). “Accx” represents the ML acceleration (in red), “Accy” represents the vertical acceleration (in blue), “Accz” represents the AP acceleration (in green).

5.2.3 EXTRACTION OF WALKING SEGMENTS

To better focus on walking segments and so to remove activity windows that did not include walks, another filter based on periodicity of the signal was performed. For example, rapid movements of the device, sitting and standing up and other kinds of activities were excluded from further process. On the contrary, activities like proper walks, walks while turning, walks while ascending or descending stairs with a certain periodicity were considered. Activity windows computed in the previous step were divided into consecutive five-seconds windows. Since walks are activities characterized by a certain periodicity, the spectrum of AP component of acceleration should have a high dominant component in the (0,75÷3 Hz) range together with lower components at lower or higher frequencies [77]. Therefore, the dominant frequency of each five-seconds window was computed and it was verified its membership to the range associated with locomotion (0,75÷3 Hz). Moreover, the local maxima for each five-seconds sliding window were found. If three or more of these maxima exceeded a threshold (set at 75% of the absolute maxima), the five-seconds window was not considered a walking window. If more than 60% of number of five-seconds windows, (in which the original activity segment was divided), were not recognized as walking bouts, the entire activity segment was discarded (ex. (12)).

$$\textit{If}\ \ 0{,}75\ Hz < DF < 3\ Hz \rightarrow pks = findpeaks(AP5\text{-}secACT(i)) \rightarrow$$
$$\rightarrow \textit{if}\ pks(i, i+1, i+2) < 75\%(MAX\ PK) \rightarrow V(i) = AP5\text{-}secACT(i) \rightarrow C = \Sigma(V(i)) \rightarrow \quad (12)$$
$$\rightarrow \textit{if}\ \ C<60\%(N) \rightarrow W(i) = ACT(i)\ was\ considered\ a\ walking\ segment.$$

Where *N* is the number of the five-seconds sliding windows in which the original activity windows was divided, *AP5-secACT(i)* is the antero-posterior acceleration in the five-seconds sliding window, *i* is the considered window, *DF* is the dominant frequency, *pks* is the amplitude of all the peaks, *MAX PK* is the absolute maximum peak, *V(i)* is the five-seconds window considered as valid, *C* is the sum of all valid five-seconds windows, *W(i)* is the walking segment.

Also in this case, the length of sliding windows and the thresholds based on absolute maximum and on the number of "valid" walking windows were empirically selected after performing several trials to obtain the highest precision in the result.

The figure 26 depicts the block scheme of the extraction of walking segments. The figure 27 illustrates the pre-processed acceleration along three axes of an acquisition performed during a laboratory trial, and the step function highlights the extracted walking segments.

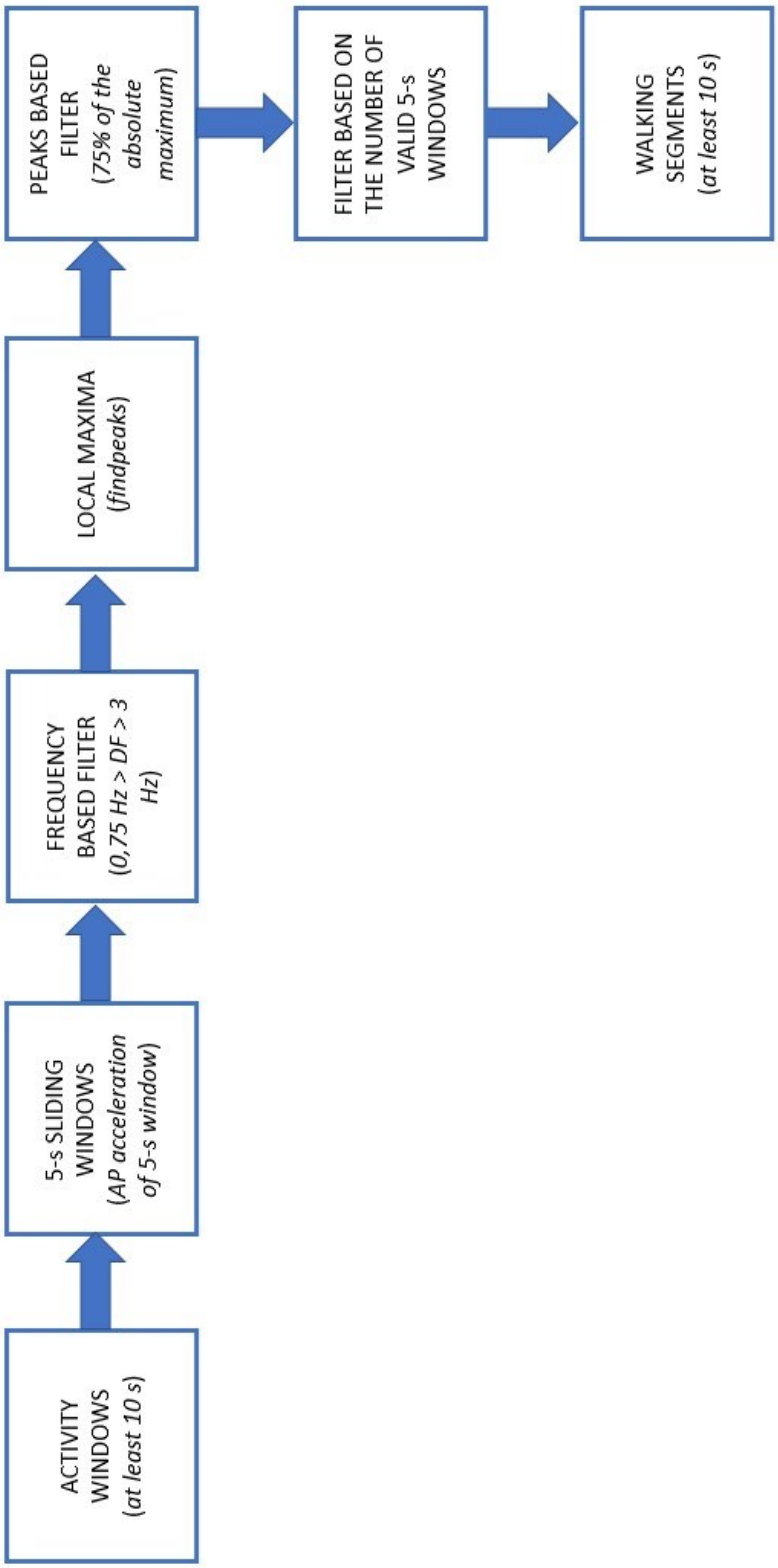

Figure 26: this figure shows the block scheme of the extraction of walking segments.

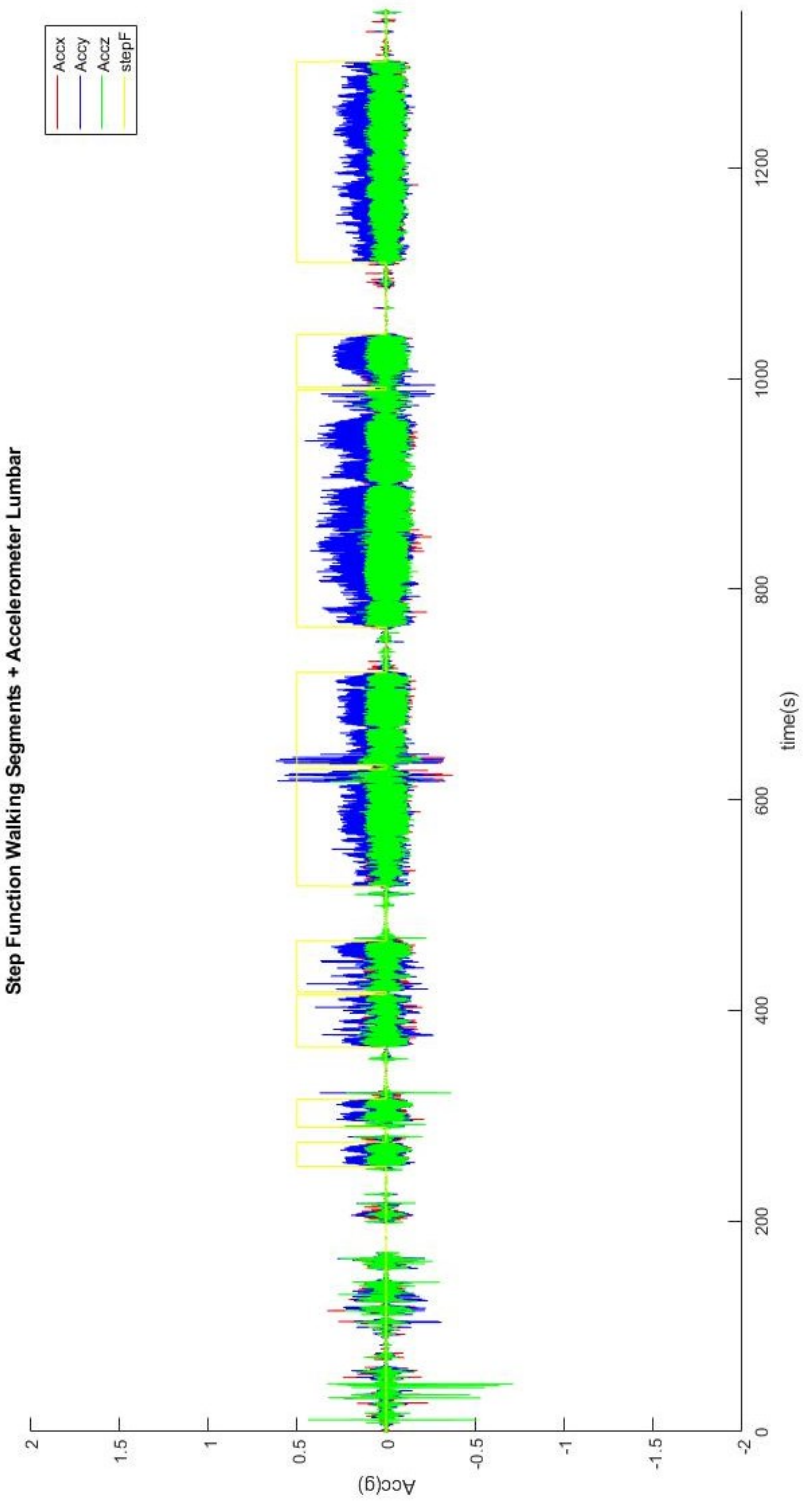

Figure 27: this figure illustrates the three components of acceleration along time of an acquisition performed in the clinic, and the step function (yellow) represents the extracted walking segments longer than 10 s. In the x-axis the time is expressed in seconds (s), in the y-axis the acceleration in gravity (g). “Accx” is the ML acceleration (in red), “Accy” is the vertical acceleration (in blue), “Accz” is the AP acceleration (in green).

5.2.4 QUATERNIONS

Next, the AHRS (Attitude and Heading Reference System) function was used since it played a key role in the computation of quaternions. It utilized data coming from internal sensors of the NGIMU (accelerometer and gyroscope) and data fusion algorithms to provide a univocal measure of the orientation of the body segment on which the device was positioned. Due to the high level of accuracy in the measurements provided by the sensors, the AHRS function was considered as an objective evaluation tool. Then, quaternions were computed through this algorithm. The matrix of quaternions was composed by four column vectors (q_1, q_2, q_3, q_4) that could be used for the computation of Euler angles and for the implementation of "quaternRotate" and "quaternConj" functions of the AHRS algorithm. The latter were used to move from the representation of the accelerometer's orientation in the movable body segment reference frame (x, y, z) to the fixed earth reference frame (X, Y, Z). So, also walking segments were expressed in the fixed earth reference frame. The figure 28 depicts the block scheme relative to the usage of quaternions. The figure 29 illustrates the rotated acceleration along three axes of an acquisition performed during a laboratory trial after the implementation of quaternions, and the step function highlights the extracted walking segments.

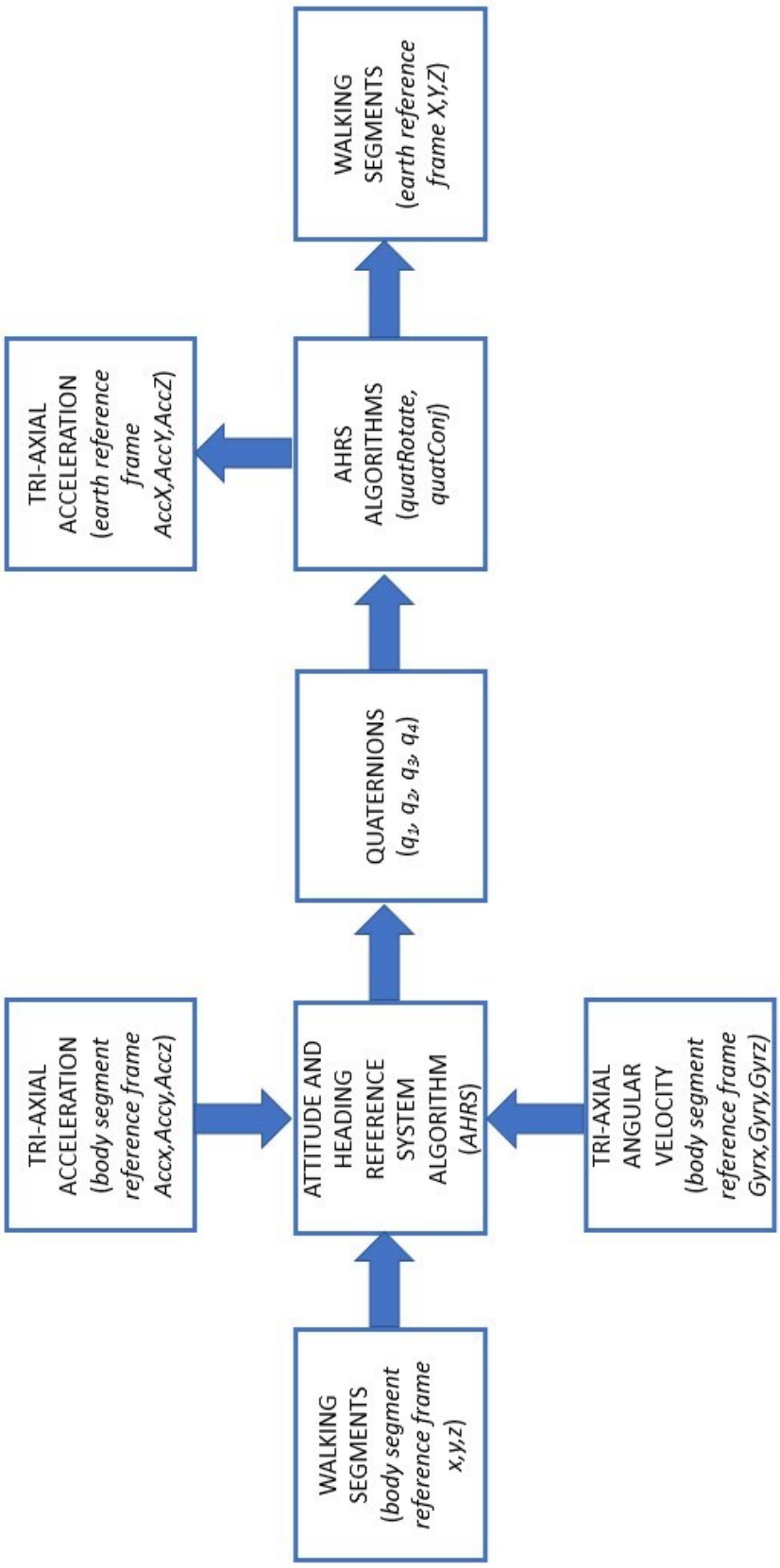

Figure 28: this figure shows the block scheme of the expression of accelerations and walking segments from the body segment reference frame to the earth reference frame through the application of quaternions.

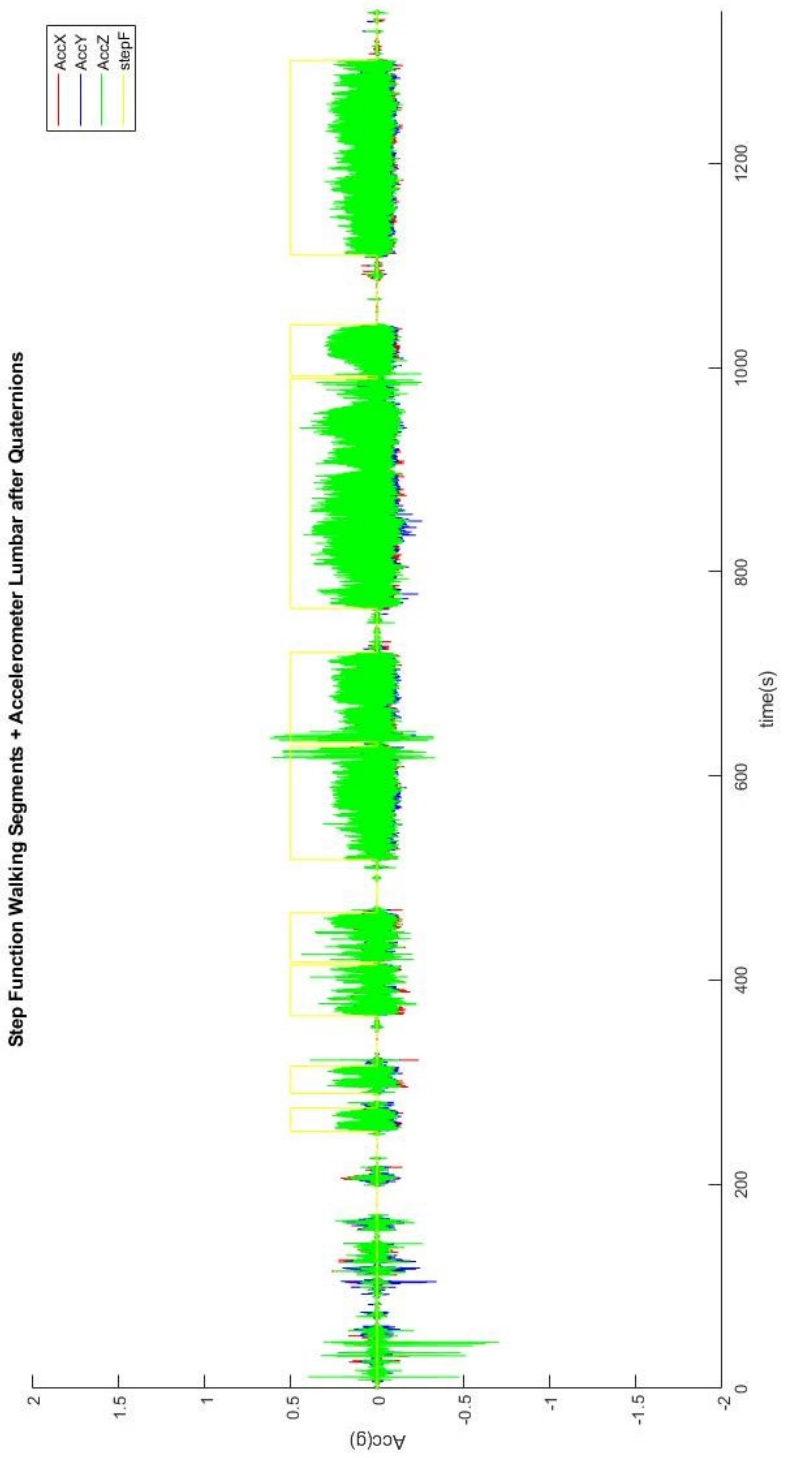

Figure 29: this figure illustrates the three components of the rotated acceleration along time of an acquisition performed in the clinic after the implementation of quaternions, and the step function (yellow) represents the extracted walking segments longer than 10 s. In the x-axis the time is expressed in seconds (s), in the y-axis the acceleration in gravity (g). “AccX” is the ML acceleration (in red), “AccY” is the vertical acceleration (in blue), “AccZ” is the AP acceleration (in green).

5.2.5 EXTRACTION OF WALKING SEGMENTS WITH "REAL" STEPS

After this step, the extraction of walking segments with "real" steps was performed. "Real steps" means that, walking segments characterized by step patterns with a certain duration, and periodicity between steps were considered. Instead, segments with unproper characteristics were excluded. Thus, windows containing activities (like turnings while walking, stair ascending or descending while walking, and so on) with very small and fast steps were not considered. This procedure was implemented to be sure that parameters, later used as fall risk indicators, were computed from "real" walking segments with proper steps. To reach this purpose, the AP component of acceleration (AccZ) was first integrated through "cumtrapz" function of MATLAB [76]. Then, the integrated AP acceleration (INT) was differentiated through continuous wavelet transform (cwt_1) and the best straight-fit line was removed from cwt_1 by using "cwt" and "detrend" MATLAB functions. As also suggested in [76], an estimated wavelet scale and Daubechies first-order wavelet (db_1) were used for the cwt. The estimated scale parameter (a_1) was computed as eq. (13):

$$a_1 = \frac{CEN_1}{\frac{DF}{Ts}} \tag{13}$$

Where CEN_1 was the centroidal frequency of the db_1 wavelet, *DF* was the most dominant frequency of the spectrum of the AP acceleration (AccZ), *Ts* was the sampling period.

Subsequently, the local minima of the cwt_1 were found by using the "findpeaks" MATLAB function and they were considered the heel strike (HS) events. Then, the first order differentiated signal (cwt_1) was differentiated again (cwt_2) by using "cwt" with a new estimated wavelet scale and Daubechies second order (db_2) wavelet. The estimated scale parameter (a_2) was computed as eq. (14):

$$a_2 = \frac{CEN_2}{\frac{DF}{Ts}} \tag{14}$$

Where CEN_2 was the centroidal frequency of the db_2 wavelet, *DF* was the most dominant frequency of the spectrum of the AP acceleration (AccZ), *Ts* was the sampling period.

In this case, the local maxima of this second order differentiated signal (cwt_2) were detected as toe off (TO) events. The condition to consider HSs and TOs as "real" events of the gait cycle, was that their magnitudes had to be higher than 10% of the mean of all peaks found with "findpeaks" MATLAB function. The figure 30 illustrates an example of step detection (identification of HSs and TOs) from a walking segment obtained from the AP acceleration after finding cwt_1 and cwt_2. The subject was performing the TUG test during the laboratory trial. The thresholds based on the mean of all peaks were observed from [76] but then empirically adjusted after performing several trials to obtain the highest precision in the result.

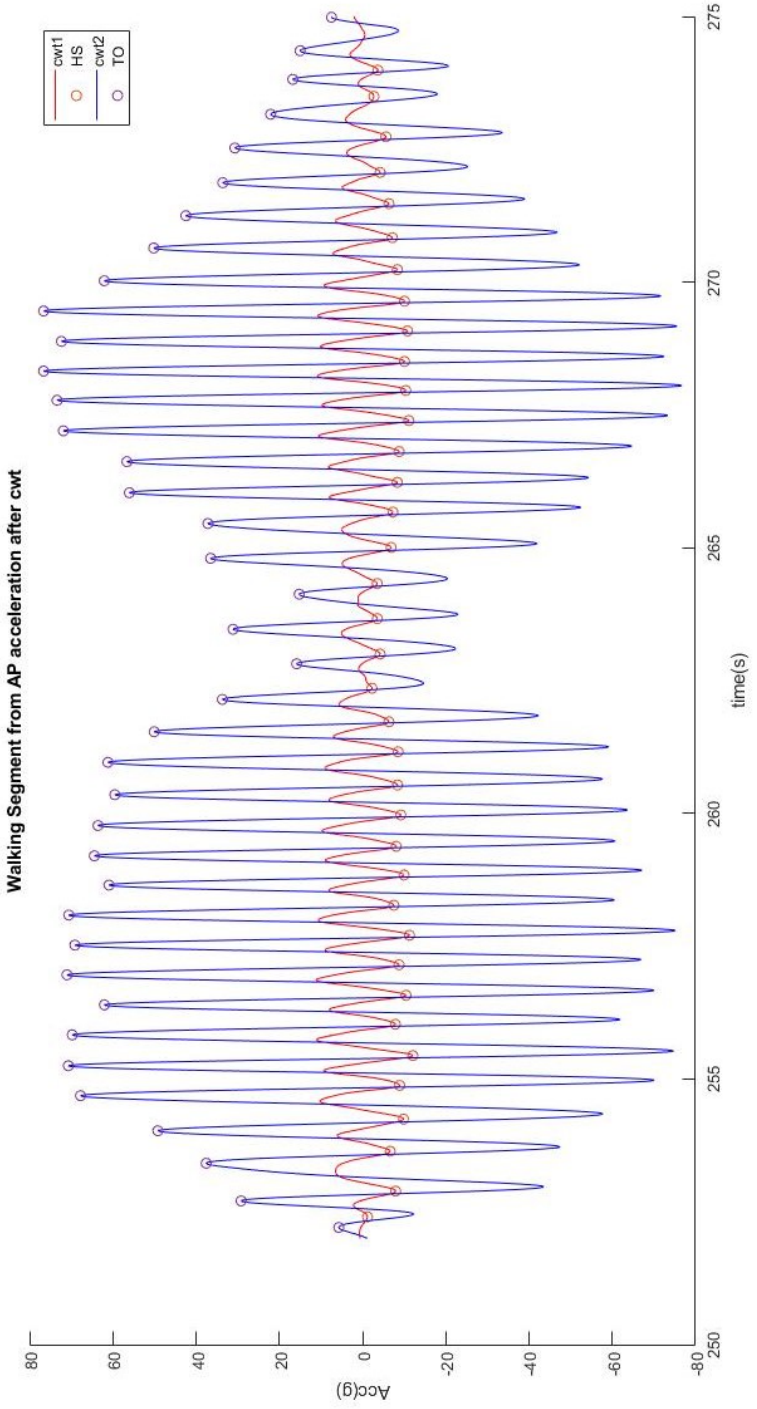

Figure 30: this image depicts a walking segment from AP acceleration after finding cwt_1 and cwt_2. This walking bout represents the TUG test performed during laboratory experiment; indeed, it is possible to appreciate a regular walking followed by turning while walking and a regular walking again. The blue line represents the cwt_1 and the blue circles the HS events, while the red line represents the cwt_2 and the red circle the TO events. In the x-axis the time is expressed in seconds (s), in the y-axis the acceleration in gravity (g).

In some cases, there was a constant alternance between maxima and minima for the entire window. In other cases, this did not occur. For example, in figure 31 which represents another TUG test performed during a laboratory trial, the correct alternance was not guaranteed in two parts, indicated by black squares and black crosses. These irregularities were due to two main factors. First, the extraction of walking segments from previous steps could have included some activities that were not proper walks probably due to thresholds issues. In the first black square of figure 31, there is a short pause that was wrongly included in the walking segment. Second, very small and fast steps were not detected by the algorithm (they did not exceed 10% of the mean of all peaks) as they were not considered “real” steps to be used in the further extraction of gait parameters. In the second black square of figure 31, there is a missed minimum in between two maxima due to very short steps during turning.

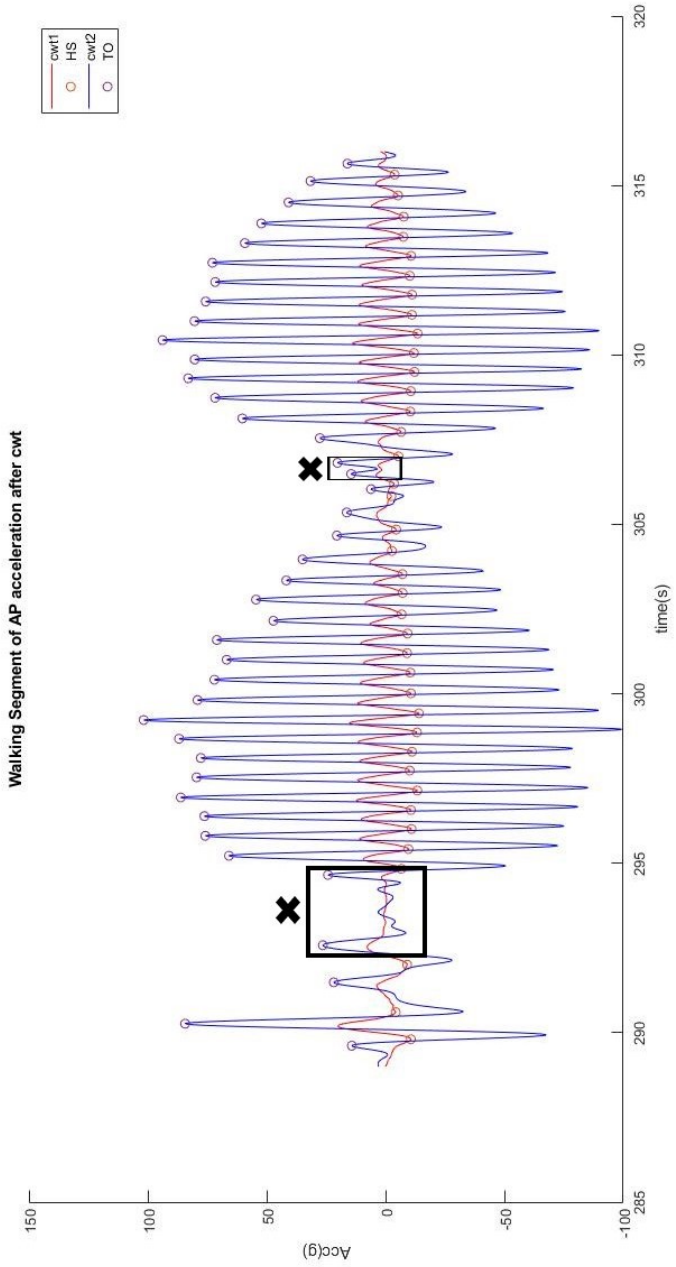

Figure 31: this figure illustrates a walking segment from AP acceleration after finding cwt_1 and cwt_2. This walking bout represents the TUG test performed during laboratory experiment; indeed, it is possible to appreciate a regular walking followed by turning while walking and a regular walking again. The blue line represents the cwt_1 and the blue circles the HS events, while the red line represents the cwt_2 and the red circle the TO events. The two black squares with the two black crosses highlight the lack of alternance between HSs and TOs. In the first case, it was due to a pause wrongly included in the walking segment. In the second case, it was due to a very short step that was not considered a "real" step during turning (missed HS). In the x-axis the time is expressed in seconds (s), in the y-axis the acceleration in gravity (g).

So, the alternance of maxima and minima in walking windows coming from previous steps was controlled through a specific procedure. Starting from the first minimum, all maxima and minima of the walking window were inspected up to the last “valid” minimum. When an irregularity (lack of perfect alternance) was detected, the original walking segment was divided into sub-segments defined from the first “valid” minimum to the last “valid” minimum. These sub-segments included regions with perfect alternance and had to be longer than ten seconds. At the end of this process, windows with a perfect alternance of maxima and minima, which started and ended with two “valid” minima, were considered “valid” walking segments, and were used for the computation of gait parameters related to fall risk. The figure 32 depicts the block scheme relative to the extraction of walking segments with “real” steps. The figure 33 illustrates the result of the filter based on alternance of maxima and minima on walking segment represented in figure 31. The step function highlights the “valid” walking segment (longer than ten seconds and with perfect alternance) that will be used in the next step of the program.

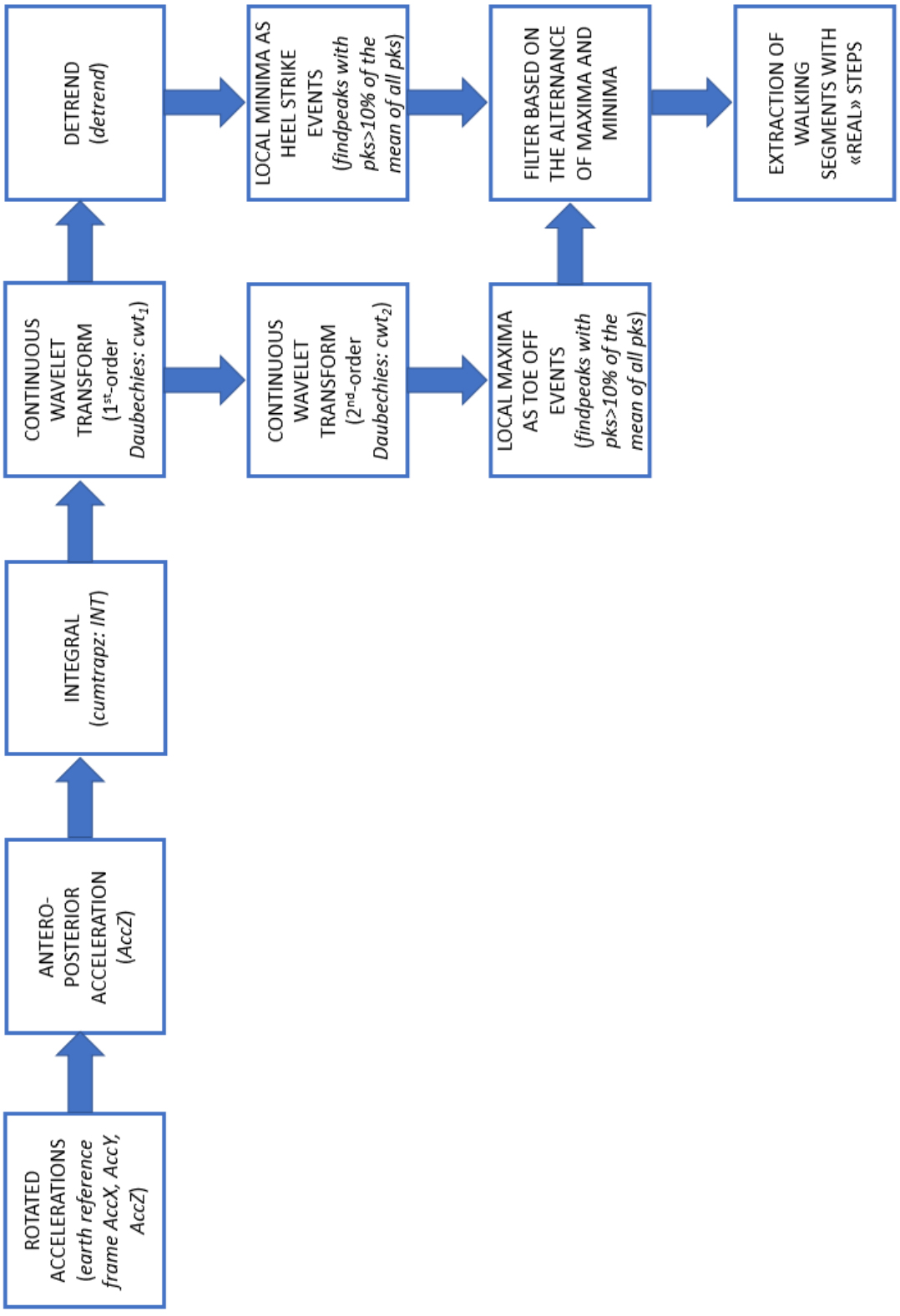

Figure 32: this figure shows the block scheme of the extraction of walking segments with “valid” steps.

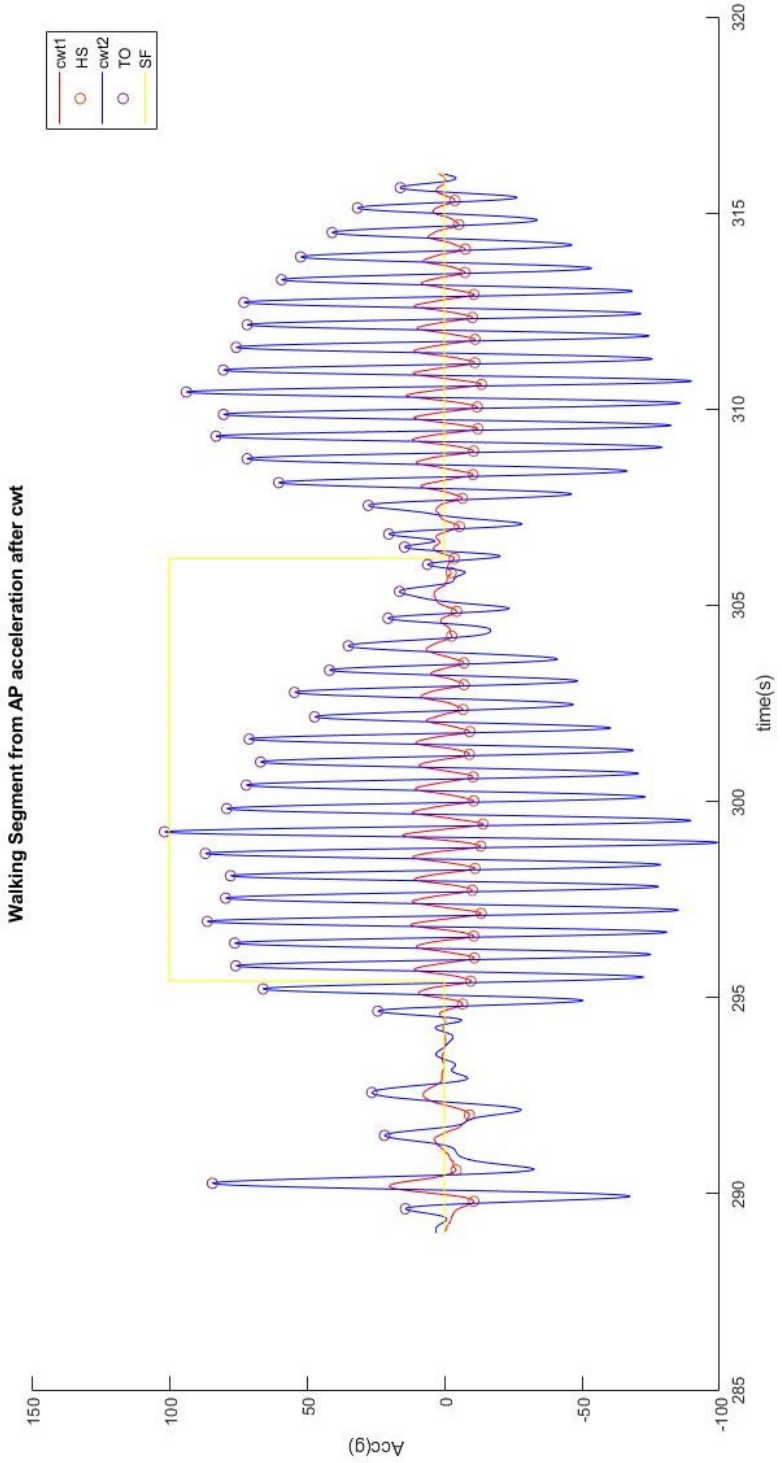

Figure 33: this figure illustrates the walking segment extracted from walking window of figure 31. The blue line represents the cwt_1 and the blue circles the HS events, while the red line represents the cwt_2 and the red circle the TO events. The yellow box represents the step function which contains the "valid" walking bout, characterized by perfect alternance of maxima and minima and that is longer than 10 s. In the x-axis the time is expressed in seconds (s), in the y-axis the acceleration in gravity (g).

5.2.6 EXTRACTION OF PARAMETERS

Walking windows detected from previous step were used for the extraction of gait parameters related to fall risk. All parameters were taken from the literature and were found to be correlated with fall risk, some more some less. These metrics can be divided into three main groups: metrics related to the quantity of walking, frequency derived metrics related to the quality of walking, and temporal derived metrics related to the quality of walking.

The first group included: the total number of walking bouts (*bouts*), the total walking duration expressed as a percentage (*%*), the total number of steps (*steps*), the median walking bout duration (*s*), the median number of steps per bouts (*steps/bout*), and the cadence (*steps/min*). These parameters were used as indicators of the amount of walking during the entire recording and they were taken from [48], [77], [79]. The latter found that this group of metrics showed similar results when recordings between PD fallers and PD non-fallers were compared. Thus, these features cannot be used as fall risk indicators alone since they are not strictly related to fall risk.

The second group was composed by: the dominant frequency (*Hz*), the amplitude (*psd=power/rad/s*), the width (*Hz*), the slope (*psd/Hz*) of the dominant harmony of the power spectral density in the walking band (0,5÷3 Hz) of the AP component of acceleration (after pre-processing and quaternions), and the harmonic ratio (*unitless*). This cluster of metrics was taken from [48], [77], [79], but also from [80]. These features were found to be strongly related to fall risk since they showed significant differences between PD fallers and PD non-fallers. The amplitude was used as indicator of the strength of the frequency in the signal. The width provided a measure of the frequency dispersion and variability. The slope, that was computed as the ratio between amplitude and width, reflected both the periodicity and the frequency dispersion. According to these definitions, lower amplitude, lower slope, and larger width reflect larger stride-to-stride variability and a reduced gait pattern. In detail, the power spectral density was computed by using the “periodogram” function of MATLAB. Then, only the locomotor band (0,5÷3 Hz) was considered. An example of power spectral density computed from AP acceleration of a walking window and relative metrics is reported in figure 34.

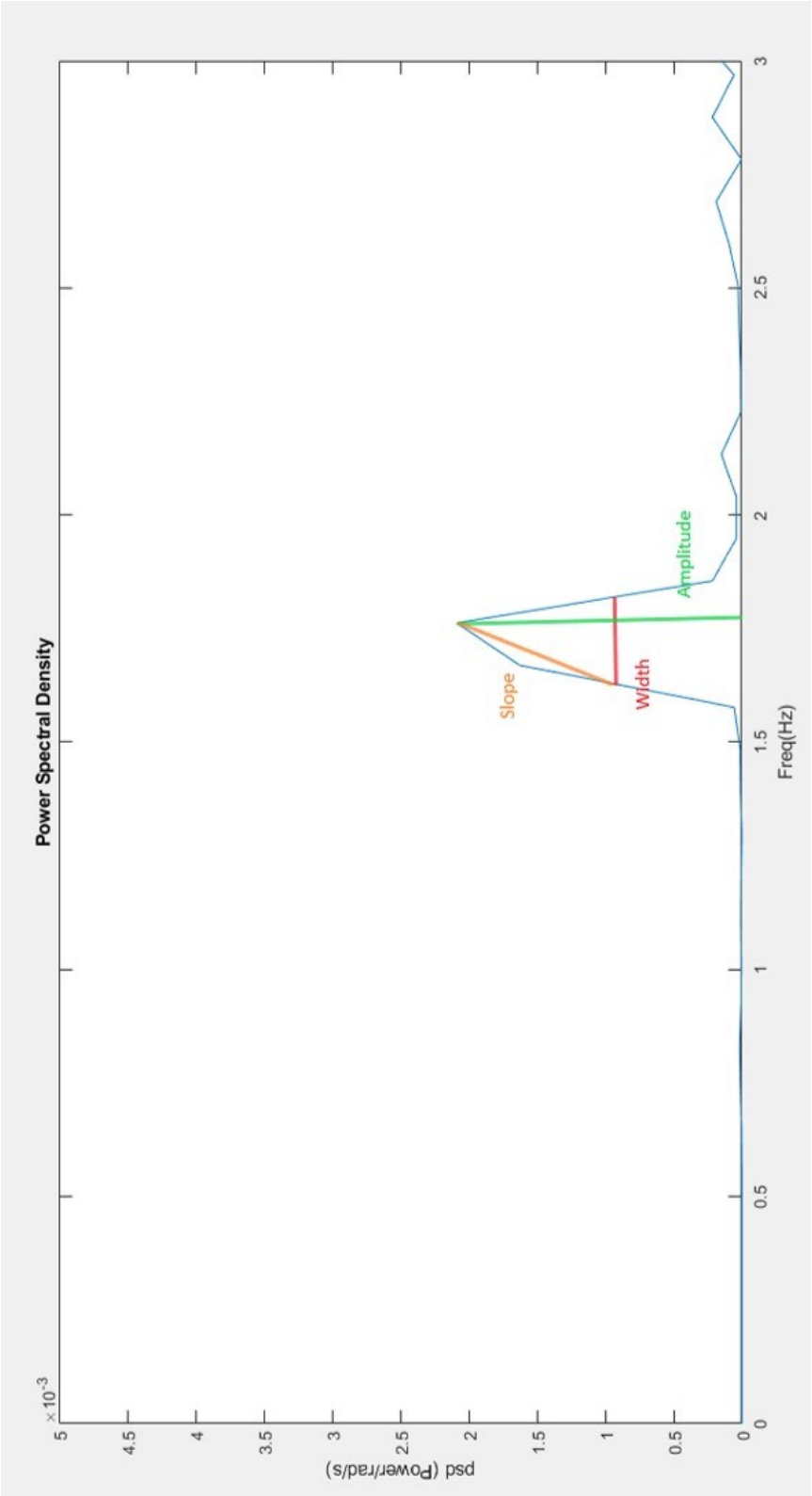

Figure 34: this picture shows the power spectral density extracted from AP acceleration of a walking window and the relative frequency derived metrices. The amplitude is the vertical green line, the width is the horizontal red line, and the slope is the oblique orange line. In the x-axis there is the frequency (Hz), in the y-axis there is the power spectral density (psd=power/rad/s).

The harmonic ratio is generally described as a measure of walking smoothness, rhythmicity, or stability [80]. More precisely, it is used as a measure of stride-to-stride symmetry since it provides a measure of the harmonic composition of AP, ML, and vertical accelerations for a given stride. Additionally, the harmonic ratio computed from lumbar AP acceleration can be considered an indicator of the whole-body movement. The higher is its value, the higher is the gait smoothness. It is defined from the discrete Fourier transform as the ratio between the sum of the amplitudes of the odd harmonics (1,3,5,…19) and the sum of the amplitudes of the even harmonics (2,4,6,…20). Only the first twenty harmonics are considered because most of the powers occurs below 10 Hz for normal cadences, with normal stride frequencies in the range (0,8÷1,1 Hz).

The third group included: the step time (*s*), the stride time (*s*), the stance time (*s*), the swing time (*s*), the double support time (*s*), the single support time (*s*), the step time variability (*s*), the stride time variability (*s*), the stance time variability (*s*), the double support time variability (*s*), the step regularity (*unitless*), the stride regularity (*unitless*), the step time asymmetry (*unitless*), the stride time asymmetry (*unitless*), the stance time asymmetry (*unitless*), the double support time asymmetry (*unitless*). Some of them are the traditional measures of gait and were described in the chapter 1.4. The other metrics are relevant indicators of rhythmicity, asymmetry, and variability. All of them reflect the gait quality and in some works were also associated with fall risk [30]. The variability was computed as the standard deviation of all steps (left and right) within walking bouts from AP acceleration [53]. It was determined by using the “std” MATLAB function. The step regularity was calculated as the correlation coefficient between the AP acceleration signal and the same signal shifted to the average step time [81]. Instead, the stride regularity was determined as the correlation coefficient between the AP acceleration signal and the same signal shifted to the average stride time. In this way, it was observed the correlation between left and right steps. Regularities were computed by using “corrcoef” function of MATLAB. The asymmetry was defined as the absolute value of the difference between means of left and right steps for each walking window [53]. The asymmetry was not influenced by the recognition of true right and left steps since it represents the absolute difference between the means of left and right steps. So, the first step of each walking bout was hypothesized to be the left step, while the second

step the right one. The closer variability and asymmetry are to zero, the better is the gait pattern. On the other hand, the larger the regularity is, the higher is the gait quality. Consequently, also the fall risk is supposed to increase in this case.

All parameters were first extracted from each walking window. Features from the first group were directly put in the final table and left as they were. Instead, all frequency and temporal features included in the second and third group were computed as weighted means before inserting in the final table. They were extracted from each walking window and then were averaged assigning weights proportional to the duration of the walking bout to which they belonged. Therefore, a longer bout was more significant than a shorter one and influenced more the final values of parameters computed in that window. At the end of this operation, all metrics were collected in the final table that represents a sort of summary of the subjects' gait characteristics (in terms of quantity and quality of walking) related to fall risk for the entire recording. Some frequency and temporal parameters were used for the final graph, formed by histograms arranged in rows (on each row there is a parameter). They were compared with values found in literature to determine their membership to normal or abnormal ranges [48], [52], [80]. All these literature studies were conducted on elderly PD subjects to extract walking features from acceleration signal acquired through wearable sensor. In addition, some temporal parameters were expressed as a percentage and compared with values found in [22]. Final tables and final graphs are reported in the following chapter. The figure 35 shows the block scheme relative to the extraction of parameters.

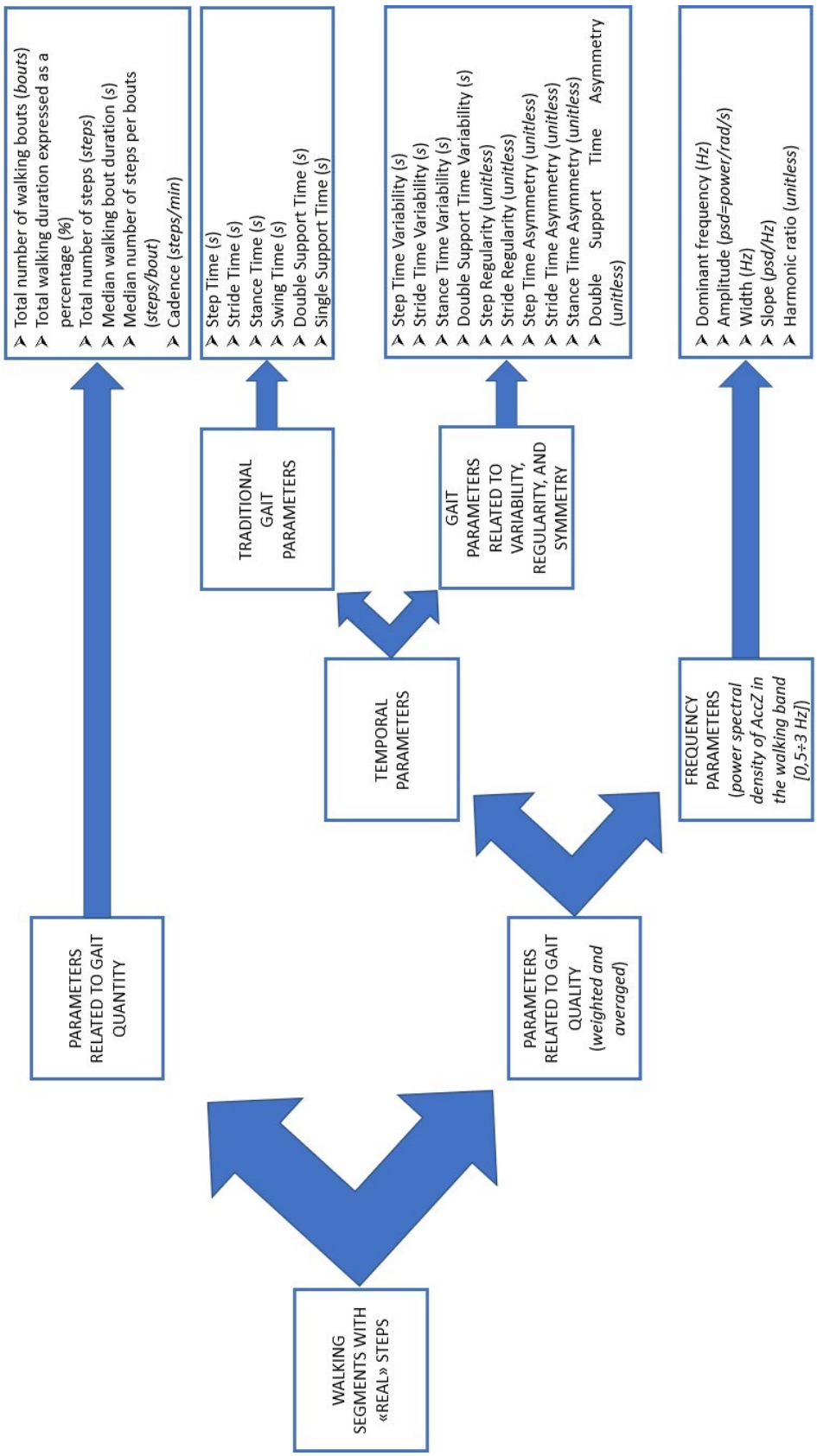

Figure 35: this image depicts the block scheme relative to the extraction of parameters.

5.2.7 GRAPHICAL USER INTERFACE

A graphical user interface (GUI) was developed to allow the direct visualization of final graphs and gait parameters in a synoptic view. In the top left of the GUI, there is the “LOAD FILE & START” panel that enables to load an excel file (“csv” format) and to start the execution of the program. The file is the acquisition performed by the subject during a lab or home trial. Then, results of the program execution are plotted in the top right of the GUI. The “SELECT PLOT” panel is used to select the graph to be shown. It can be the graph related to step time or the graph related to stride time. At the bottom of the GUI, “GAIT PARAMETERS” panel illustrates the averaged and weighted values of the gait parameters related to fall risk computed from the entire acquisition. An example of the GUI after the running of the lab trial of subject 1 is reported in figure 36.

Figure 36: this figure depicts the GUI extracted from the lab trial of subject 1.

CHAPTER 6: RESULTS

6.1 EXPLANATION OF THE FINAL OUTPUTS

As already described in the previous chapter, four outputs were obtained from each recording: two tables and two graphs. The first table was composed by all the parameters extracted from the entire recording. Except for parameters related to the quantity of walking, the other metrics were computed as weighted averages with respect to the duration of walking windows from which they were calculated. The second table was composed by stance time, swing time, double support time, and single support time, all expressed in time and as a percentage of the gait cycle duration (stride time). The table also included the "normal" values of these metrics according to the [22]. For "normal" values it was intended values that were valid for healthy non-fallers subjects that underwent the gait analysis in [22]. The first graph was composed by six histograms arranged in rows. Each histogram was in turn composed by several rectangles or blocks, each of them indicated the value of a specific parameter computed in a specific walking window. Dominant frequency, harmonic ratio, step time, step time variability, step time regularity, and step time asymmetry were reported in the first graph since they were related to step time. The second graph was created with the same methodology of the first graph, but most of the reported parameters were different and more related to stride time. Dominant frequency, harmonic ratio, stride time, stride time variability, stride time regularity, and stride time asymmetry were included in the second graph. Moreover, each rectangle of the histograms was coloured in red, yellow, or green according to its membership to fallers ("abnormal"), near threshold, or non-fallers ("normal") range respectively. These ranges were defined from values observed in [48], [52], [80] and were listed in table 3. These studies considered the same kind of subjects and a very similar methodology (accelerometer on lumbar region while performing ADLs at home) with respect to the present thesis. Moreover, for "normal" range it was intended the range extracted from PD non-fallers, while for "abnormal" range it was intended the range extracted from PD fallers.

Table 3: this table listed the six parameters reported in the first graph and the ranges defined from values taken from the literature. Legend: DF (Dominant Frequency), HR (Harmonic Ratio), StepT (Step Time), StepV (Step Time Variability), StepR (Step Time Regularity), StepA (Step Time Asymmetry), Hz (Hertz), s (seconds).

PARAMETERS	**MEASUREMENT UNIT**	**ABNORMAL or FALLERS RANGE *("red")***	**RANGE NEAR THE THRESHOLD ("*yellow*")**	**NORMAL or NON-FALLERS RANGE ("*green*")**	**LITERATURE**
Dominant Frequency (DF)	Hz	DF < 1,00 DF > 2,30	1,00 ≤ DF < 1,60 2,20 ≤ DF < 2,30	1,60 ≤ DF < 2,20	J.L. Roche et al. [80]
Harmonic Ratio (HR)	Unitless	HR < 1,61	1,61 ≤ HR < 2,09	HR ≤ 2,09	A. Weiss et al. [48]
Step Time (StepT)	s	StepT < 0,43 StepT > 1,00	0,43 ≤ StepT < 0,45 0,63 ≤ StepT < 1,00	0,45 ≤ StepT < 0,63	J.L. Roche et al. [80]
Step Time Variability (StepV)	s	StepV > 1,18	0,18 ≤ StepV < 0,21	StepV ≤ 0,21	S. Del Din et al. [52]
Step Time Regularity (StepR)	s	StepR < 0,25	0,25 ≤ StepR < 0,40	StepR ≥ 0,40	A. Weiss et al. [48]
Step Time Asymmetry (StepA)	s	StepA < 0,06	0,06 ≤ StepA < 0,16	StepR ≥ 0,16	S. Del Din et al. [52]

Table 4: this table listed the six parameters reported in the second graph and the ranges defined from values taken from the literature. Legend: DF (Dominant Frequency), HR (Harmonic Ratio), StrideT (Stride Time), StrideV (Stride Time Variability), StrideR (Stride Time Regularity), StrideA (Stride Time Asymmetry), Hz (Hertz), s (seconds).

PARAMETERS	**MEASUREMENT UNIT**	**ABNORMAL or FALLERS RANGE *("red")***	**RANGE NEAR THE THRESHOLD ("*yellow*")**	**NORMAL or NON-FALLERS RANGE ("*green*")**	**LITERATURE**
Dominant Frequency (DF)	Hz	DF < 1,00 DF > 2,30	1,00 ≤ DF < 1,60 2,20 ≤ DF < 2,30	1,60 ≤ DF < 2,20	J.L. Roche et al. [80]
Harmonic Ratio (HR)	Unitless	HR < 1,61	1,61 ≤ HR < 2,09	HR ≤ 2,09	A. Weiss et al. [48]
Stride Time (StrideT)	s	StrideT < 0,86 StrideT > 2,00	0,86 ≤ StrideT < 0,90 1,25 ≤ StrideT < 2,00	0,90 ≤ StrideT < 1,25	J.L. Roche et al. [80]
Stride Time Variability (StrideV)	s	StrideV > 1,18	0,18 ≤ StrideV < 0,21	StrideV ≤ 0,21	S. Del Din et al. [52]
Stride Time Regularity (StrideR)	s	StrideR < 0,25	0,25 ≤ StrideR < 0,40	StrideR ≥ 0,40	A. Weiss et al. [48]
Stride Time Asymmetry (StrideA)	s	StrideA < 0,06	0,06 ≤ StrideA < 0,16	StrideA ≥ 0,16	S. Del Din et al. [52]

6.2 RESULTS FROM LABORATORY RECORDINGS

Results from the experiments carried out in the clinic ("Villa dei Pini") are reported in this paragraph.

SUBJECT 1

Tables 5 and 6 and figures 37 and 38 illustrates the experimental results from subject 1 during the laboratory trial.

Table 5: this table lists the values of the gait parameters related to fall risk for the subject 1 during the laboratory trial. Legend: s (seconds), min (minutes), Hz (Hertz), psd (power spectral density), rad/s (radians per seconds).

SUBJECT 1 (*lab*)	
PARAMETERS	**VALUES**
PARAMETERS RELATED TO THE QUANTITY OF WALKING	
Total Number of Walking Bouts (TWB)	9 *bouts*
Total Walking Duration as a Percentage (TWDp)	48,3774 *%*
Total Number of Steps (TNS)	1123 *steps*
Median Walking Bout Duration (MWBD)	72,5406 *s*
Median Number of Steps per Bouts (MNSB)	124,7778 *steps/bout*
Cadence (Cad)	103,2066 *steps/min*
PARAMETERS RELATED TO THE QUALITY OF WALKING (averaged and weighted)	
Frequency measures	
Dominant Frequency	1,7348 *Hz*
Amplitude	0,0012 *psd (power/rad/s)*
Width	0,0773 *Hz*
Slope	0,0523 p*sd/Hz*
Harmonic Ratio	2,0638 *(unitless)*
Temporal measures	
Step Time	0,5902 *s*
Stride Time	1,1792 *s*
Stance Time	0,8234 *s*
Swing Time	0,3559 *s*
Double Support Time	0,2347 *s*
Single Support Time	0,9446 *s*
Step Time Variability	0,0743 *s*
Stride Time Variability	0,1078 *s*
Stance Time Variability	0,1097 *s*
Double Support Time Variability	0,0785 *s*
Step Regularity	0,3568 *(unitless)*
Stride Regularity	0,1769 *(unitless)*
Asymmetry Step Time	0,0187 *(unitless)*
Asymmetry Stride Time	0,0105 *(unitless)*
Asymmetry Stance Time	0,0306 *(unitless)*
Asymmetry Double Support Time	0,0125 *(unitless)*

Table 6: this table lists the values of some gait parameters expressed in time and as a percentage of the gait cycle for the subject 1 during the laboratory trial. These values are compared with percentages found in literature. Legend: s (seconds).

SUBJECT 1 (*lab*)				
GAIT PARAMETERS	**EXPERIMENTAL PARAMETERS AS A PERCENTAGE OF GAIT CYCLE**	**LITERATURE PARAMETERS AS A PERCENTAGE OF GAIT CYCLE [22]**	**EXPERIMENTAL PARAMETERS IN SECONDS (s)**	**GAIT CYCLE DURATION IN SECONDS (s)**
Stance Time	69,8233 *%*	60 *%*	0,8234 *s*	1,1792 s
Swinge Time	30,1767 *%*	40 *%*	0,3559 *s*	
Double Support Time	19,8997 *%*	20 *%*	0,2347 *s*	
Single Support Time	80,1003 *%*	80 *%*	0,9446 *s*	

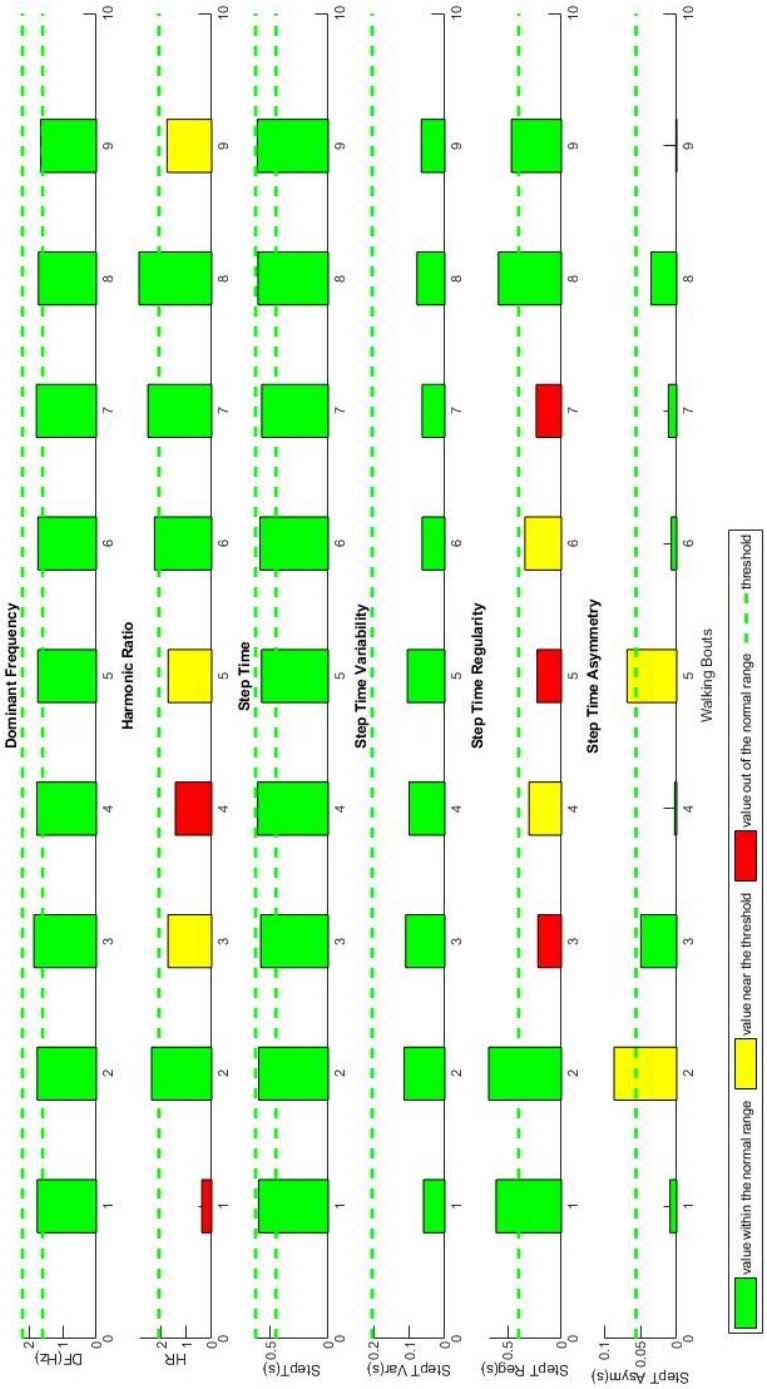

Figure 37: this figure illustrates the first graph composed by six histograms with parameters related to step time extracted from the subject 1 (lab recording). Each rectangle represents the value of the parameter computed in a specific walking bout. Green colour means that the value of the parameter is within the normal or non-fallers range; yellow that it is near the threshold; red that it is out of the normal range; the dotted green line is the threshold. In the x-axis there is the number of walking bout, in the y-axis there are the magnitudes of the parameters.

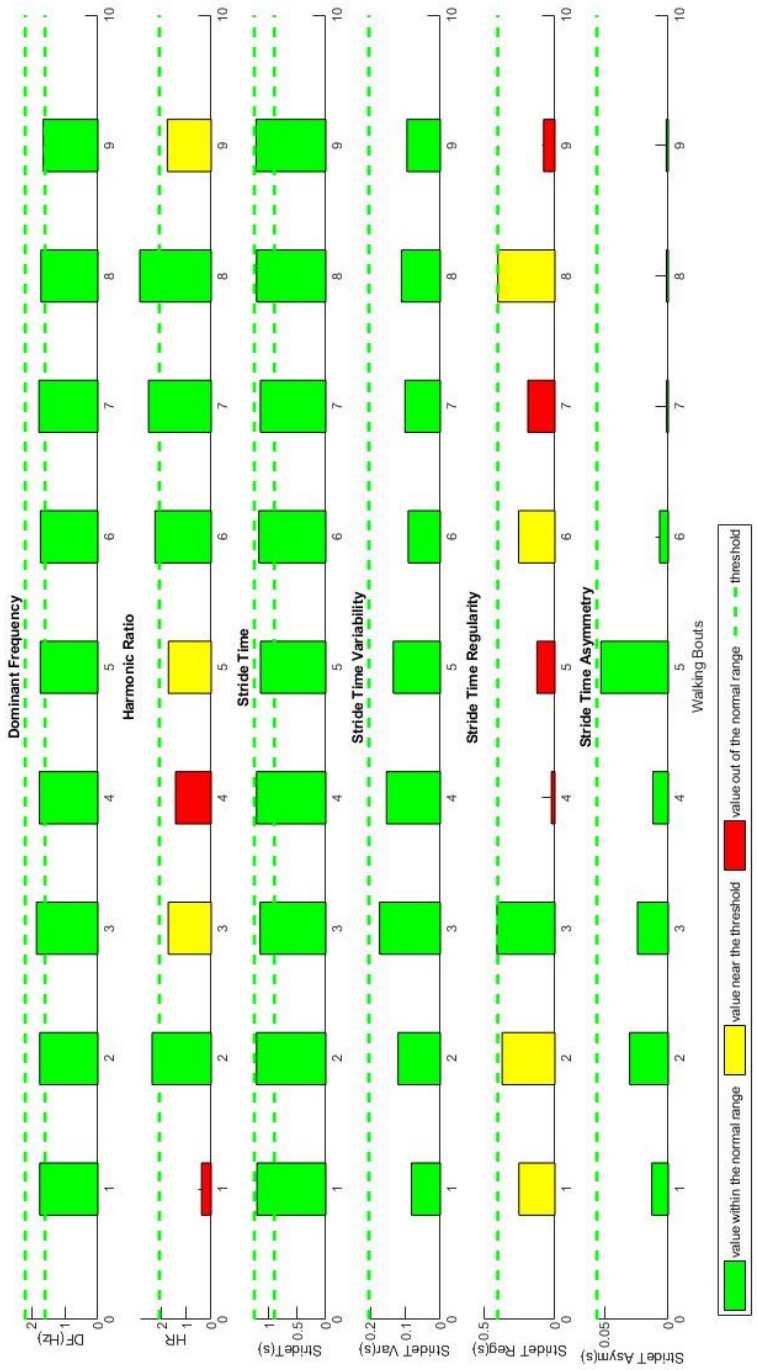

Figure 38: this figure illustrates the second graph composed by six histograms with parameters related to stride time extracted from the subject 1 (lab recording). Each rectangle represents the value of the parameter computed in a specific walking bout. Green colour means that value of the parameter is within the normal or non-fallers range; yellow that it is near the threshold; red that it is out of the normal range; the dotted green line is the threshold. In the x-axis there is the number of walking bout, in the y-axis there are the magnitudes of the parameters.

SUBJECT 2

Tables 7 and 8 and figures 39 and 40 illustrates the experimental results from subject 2 during the laboratory trial.

Table 7: this table lists the values of the gait parameters related to fall risk for the subject 2 during the laboratory trial. Legend: s (seconds), min (minutes), Hz (Hertz), psd (power spectral density), rad/s (radians per seconds).

SUBJECT 2 (*lab*)	
PARAMETERS	**VALUES**
PARAMETERS RELATED TO THE QUANTITY OF WALKING	
Total Number of Walking Bouts (TWB)	2 *bouts*
Total Walking Duration as a Percentage (TWDp)	9,3250 *%*
Total Number of Steps (TNS)	82 *steps*
Median Walking Bout Duration (MWBD)	32,3400 *s*
Median Number of Steps per Bouts (MNSB)	41,0000 *steps/bout*
Cadence (Cad)	76,0668 *steps/min*
PARAMETERS RELATED TO THE QUALITY OF WALKING (averaged and weighted)	
Frequency measures	
Dominant Frequency	1,2420 *Hz*
Amplitude	0,000068518 *psd (power/rad/s)*
Width	0,0985 *Hz*
Slope	0,00082541 p*sd/Hz*
Harmonic Ratio	1,9892 *(unitless)*
Temporal measures	
Step Time	1,1575 *s*
Stride Time	1,9698 *s*
Stance Time	0,8885 *s*
Swing Time	1,0813 *s*
Double Support Time	0,0924 *s*
Single Support Time	1,8773 *s*
Step Time Variability	2,9368 *s*
Stride Time Variability	2,9995 *s*
Stance Time Variability	0,2949 *s*
Double Support Time Variability	0,3383 *s*
Step Regularity	0,0853 *(unitless)*
Stride Regularity	0,0597 *(unitless)*
Asymmetry Step Time	0,9512 *(unitless)*
Asymmetry Stride Time	0,9851 *(unitless)*
Asymmetry Stance Time	0,0735 *(unitless)*
Asymmetry Double Support Time	0,0221 *(unitless)*

Table 8: this table lists the values of some gait parameters expressed in time and as a percentage of the gait cycle for the subject 2 during the laboratory trial. These values are compared with percentages found in literature. Legend: s (seconds).

SUBJECT 2 (*lab*)				
GAIT PARAMETERS	**EXPERIMENTAL PARAMETERS AS A PERCENTAGE OF GAIT CYCLE**	**LITERATURE PARAMETERS AS A PERCENTAGE OF GAIT CYCLE [22]**	**EXPERIMENTAL PARAMETERS IN SECONDS (s)**	**GAIT CYCLE DURATION IN SECONDS (s)**
Stance Time	45,1065 *%*	60 *%*	0,8885 *s*	1,9698 s
Swinge Time	54,8935 *%*	40 *%*	1,0813 *s*	
Double Support Time	4,6933 *%*	20 *%*	0,0924 *s*	
Single Support Time	95,3067 *%*	80 *%*	1,8773 *s*	

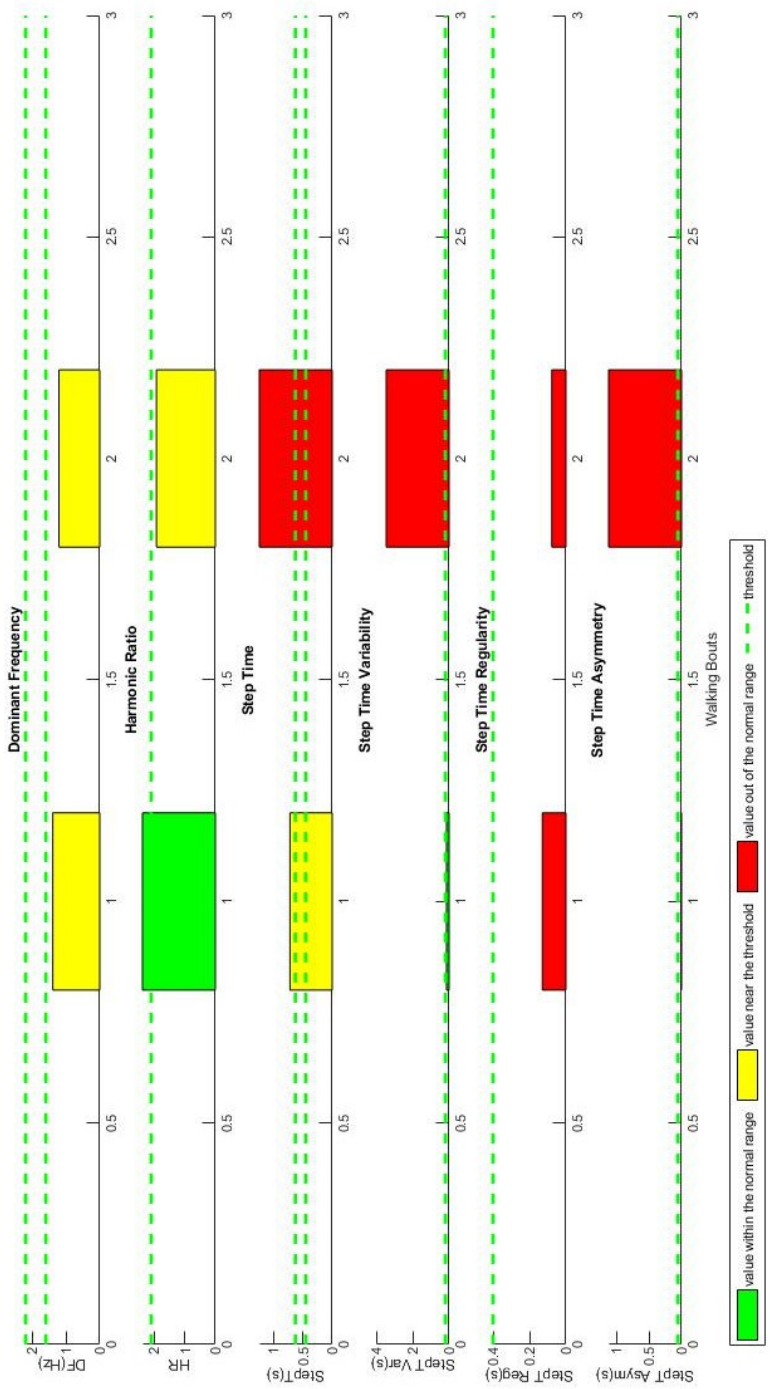

Figure 39: this figure illustrates the first graph composed by six histograms with parameters related to step time extracted from the subject 2 (lab recording). Each rectangle represents the value of the parameter computed in a specific walking bout. Green colour means that the value of the parameter is within the normal or non-fallers range; yellow that it is near the threshold; red that it is out of the normal range; the dotted green line is the threshold. In the x-axis there is the number of walking bout, in the y-axis there are the magnitudes of the parameters.

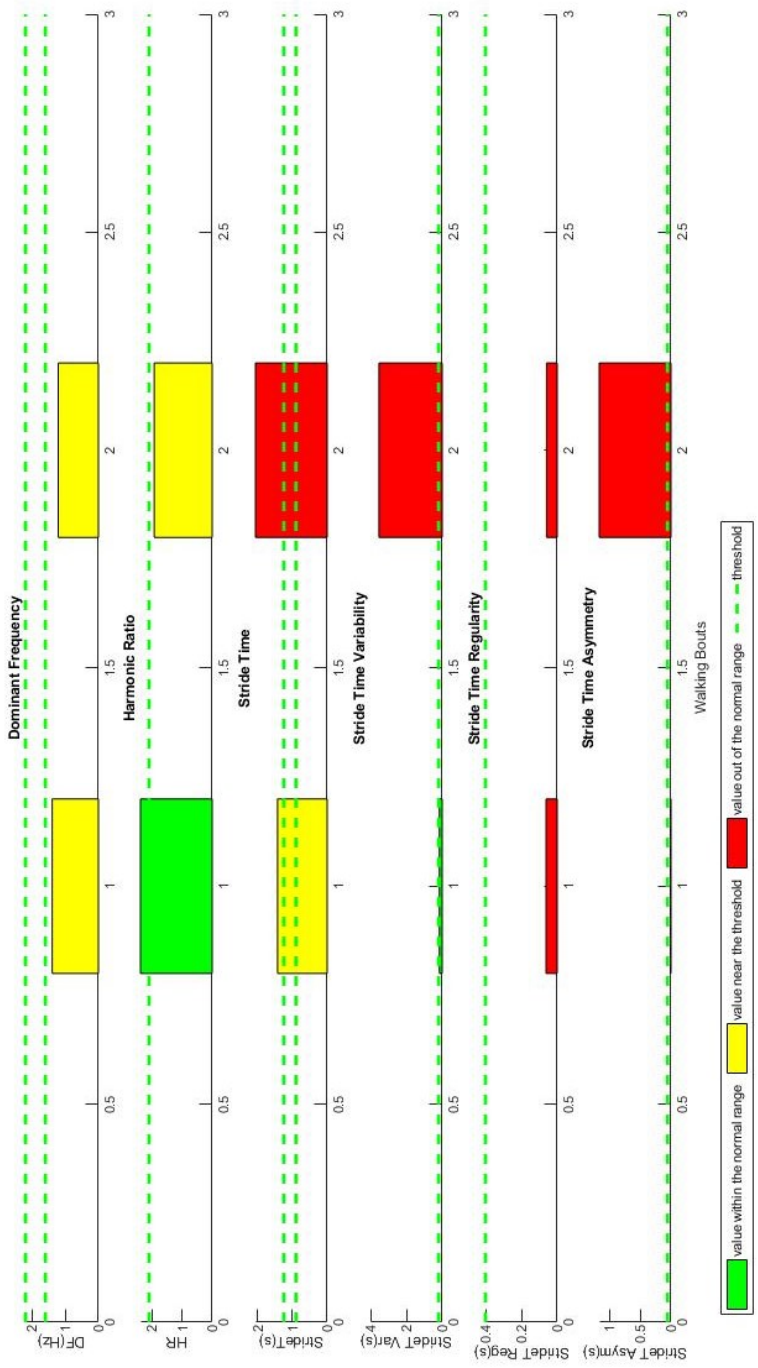

Figure 40: this figure illustrates the second graph composed by six histograms with parameters related to stride time extracted from the subject 2 (lab recording). Each rectangle represents the value of the parameter computed in a specific walking bout. Green colour means that value of the parameter is within the normal or non-fallers range; yellow that it is near the threshold; red that it is out of the normal range; the dotted green line is the threshold. In the x-axis there is the number of walking bout, in the y-axis there are the magnitudes of the parameters.

6.3 RESULTS FROM HOME RECORDINGS

Results from the long-term recordings carried out in the patients' homes are reported in this paragraph.

SUBJECT 1 FIRST RECORDING

Tables 9 and 10 and figures 41 and 42 illustrates the experimental results from the subject 1 during the first home recording.

Table 9: this table lists the values of the gait parameters related to fall risk for the subject 1 during the first acquisition performed at home. Legend: s (seconds), min (minutes), Hz (Hertz), psd (power spectral density), rad/s (radians per seconds).

SUBJECT 1 first recording (*home*)	
PARAMETERS	**VALUES**
PARAMETERS RELATED TO THE QUANTITY OF WALKING	
Total Number of Walking Bouts (TWB)	37 *bouts*
Total Walking Duration as a Percentage (TWDp)	4,0230 *%*
Total Number of Steps (TNS)	2923 *steps*
Median Walking Bout Duration (MWBD)	39,0826 *s*
Median Number of Steps per Bouts (MNSB)	79,0000 *steps/bout*
Cadence (Cad)	121,2817 *steps/min*
PARAMETERS RELATED TO THE QUALITY OF WALKING (averaged and weighted)	
Frequency measures	
Dominant Frequency	2,0031 *Hz*
Amplitude	0,0015 *psd (power/rad/s)*
Width	0,0755 *Hz*
Slope	0,0637 p*sd/Hz*
Harmonic Ratio	2,7901 *(unitless)*
Temporal measures	
Step Time	0,5058 *s*
Stride Time	1,0099 *s*
Stance Time	0,8222 *s*
Swing Time	0,1877 *s*
Double Support Time	0,3166 *s*
Single Support Time	0,6933 *s*
Step Time Variability	0,0746 *s*
Stride Time Variability	0,1042 *s*
Stance Time Variability	0,0966 *s*
Double Support Time Variability	0,0599 *s*
Step Regularity	0,2733 *(unitless)*
Stride Regularity	0,2409 *(unitless)*
Asymmetry Step Time	0,0337 *(unitless)*
Asymmetry Stride Time	0,0073 *(unitless)*
Asymmetry Stance Time	0,0234 *(unitless)*
Asymmetry Double Support Time	0,0285 *(unitless)*

Table 10: this table lists the values of some gait parameters expressed in time and as a percentage of the gait cycle for the subject 1 during the first home recording. These values are compared with percentages found in literature. Legend: s (seconds).

SUBJECT 1 first recording (*home*)				
GAIT PARAMETERS	**EXPERIMENTAL PARAMETERS AS A PERCENTAGE OF GAIT CYCLE**	**LITERATURE PARAMETERS AS A PERCENTAGE OF GAIT CYCLE [22]**	**EXPERIMENTAL PARAMETERS IN SECONDS (s)**	**GAIT CYCLE DURATION IN SECONDS (s)**
Stance Time	81,4155 *%*	60 *%*	0,8222 *s*	1,0099 s
Swinge Time	18,5845 *%*	40 *%*	0,1877 *s*	
Double Support Time	31,3493 *%*	20 *%*	0,3166 *s*	
Single Support Time	68,6507 *%*	80 *%*	0,6933 *s*	

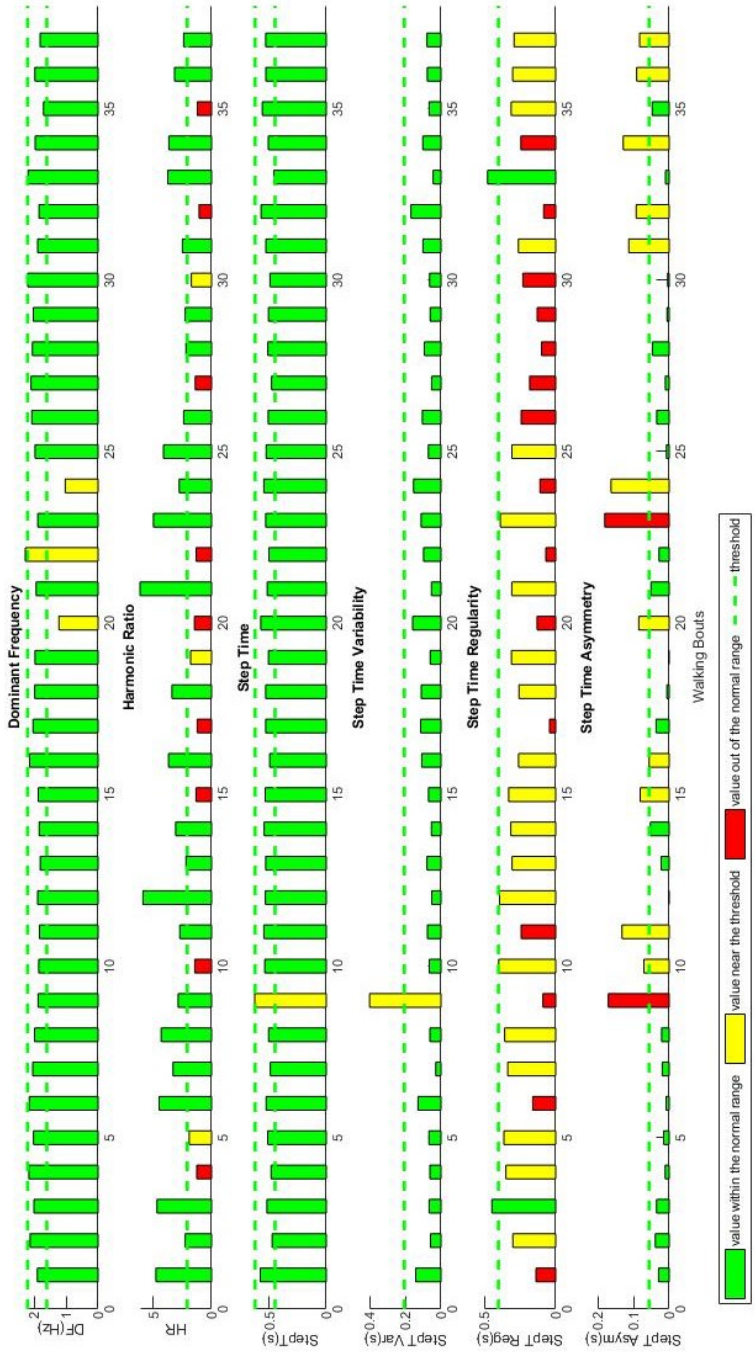

Figure 41: this figure illustrates the first graph composed by six histograms with parameters related to step time extracted from the subject 1 (first home recording). Each rectangle represents the value of the parameter computed in a specific walking bout. Green colour means that the value of the parameter is within the normal or non-fallers range; yellow that it is near the threshold; red that it is out of the normal range; the dotted green line is the threshold. In the x-axis there is the number of walking bout, in the y-axis there are the magnitudes of the parameters.

Figure 42: this figure illustrates the second graph composed by six histograms with parameters related to stride time extracted from the subject 1 (first home recording). Each rectangle represents the value of the parameter computed in a specific walking bout. Green colour means that value of the parameter is within the normal or non-fallers range; yellow that it is near the threshold; red that it is out of the normal range; the dotted green line is the threshold. In the x-axis there is the number of walking bout, in the y-axis there are the magnitudes of the parameters.

SUBJECT 1 SECOND RECORDING

Tables 11 and 12 and figures 43 and 44 illustrates the experimental results from the subject 1 during the second home recording.

Table 11: this table lists the values of the gait parameters related to fall risk for the subject 1 during the second acquisition performed at home. Legend: s (seconds), min (minutes), Hz (Hertz), psd (power spectral density), rad/s (radians per seconds).

SUBJECT 1 second recording (*home*)	
PARAMETERS	**VALUES**
PARAMETERS RELATED TO THE QUANTITY OF WALKING	
Total Number of Walking Bouts (TWB)	65 *bouts*
Total Walking Duration as a Percentage (TWDp)	6,0198 *%*
Total Number of Steps (TNS)	4781 *steps*
Median Walking Bout Duration (MWBD)	36,4108 *s*
Median Number of Steps per Bouts (MNSB)	73,5538 *steps/bout*
Cadence (Cad)	121,2067 *steps/min*
PARAMETERS RELATED TO THE QUALITY OF WALKING (averaged and weighted)	
Frequency measures	
Dominant Frequency	2,0566 *Hz*
Amplitude	0,0019 *psd (power/rad/s)*
Width	0,0897 *Hz*
Slope	0,0650 p*sd/Hz*
Harmonic Ratio	2,3453 *(unitless)*
Temporal measures	
Step Time	0,5115 *s*
Stride Time	1,0154 *s*
Stance Time	0,8298 *s*
Swing Time	0,1857 *s*
Double Support Time	0,3235 *s*
Single Support Time	0,6919 *s*
Step Time Variability	0,1419 *s*
Stride Time Variability	0,1810 *s*
Stance Time Variability	0,1135 *s*
Double Support Time Variability	0,0652 *s*
Step Regularity	0,4001 *(unitless)*
Stride Regularity	0,2888 *(unitless)*
Asymmetry Step Time	0,0416 *(unitless)*
Asymmetry Stride Time	0,0212 *(unitless)*
Asymmetry Stance Time	0,0293 *(unitless)*
Asymmetry Double Support Time	0,0187 *(unitless)*

Table 12: this table lists the values of some gait parameters expressed in time and as a percentage of the gait cycle for the subject 1 during the second home recording. These values are compared with percentages found in literature. Legend: s (seconds).

SUBJECT 1 second recording (*home*)				
GAIT PARAMETERS	**EXPERIMENTAL PARAMETERS AS A PERCENTAGE OF GAIT CYCLE**	**LITERATURE PARAMETERS AS A PERCENTAGE OF GAIT CYCLE [22]**	**EXPERIMENTAL PARAMETERS IN SECONDS (s)**	**GAIT CYCLE DURATION IN SECONDS (s)**
Stance Time	81,7143 *%*	60 *%*	0,8298 *s*	1,0154 s
Swinge Time	18,2857 *%*	40 *%*	0,1857 *s*	
Double Support Time	31,8617 *%*	20 *%*	0,3535 *s*	
Single Support Time	68,1383 *%*	80 *%*	0,6919 *s*	

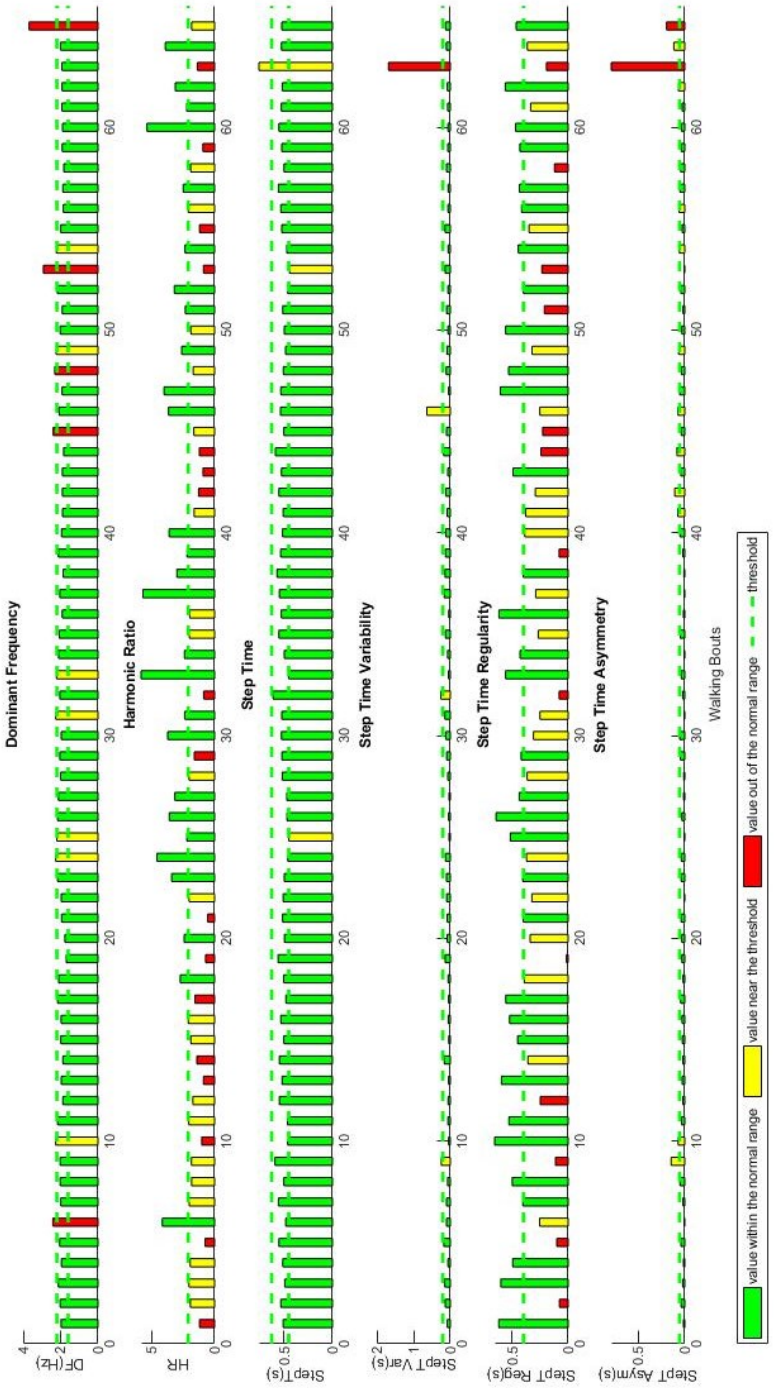

Figure 43: this figure illustrates the first graph composed by six histograms with parameters related to step time extracted from the subject 1 (second home recording). Each rectangle represents the value of the parameter computed in a specific walking bout. Green colour means that the value of the parameter is within the normal or non-fallers range; yellow that it is near the threshold; red that it is out of the normal range; the dotted green line is the threshold. In the x-axis there is the number of walking bout, in the y-axis there are the magnitudes of the parameters.

Figure 44: this figure illustrates the second graph composed by six histograms with parameters related to stride time extracted from the subject 1 (second home recording). Each rectangle represents the value of the parameter computed in a specific walking bout. Green colour means that value of the parameter is within the normal or non-fallers range; yellow that it is near the threshold; red that it is out of the normal range; the dotted green line is the threshold. In the x-axis there is the number of walking bout, in the y-axis there are the magnitudes of the parameters.

SUBJECT 2

Tables 13 and 14 and figures 45 and 46 illustrates the experimental results from subject 2 during the home recording.

Table 13: this table lists the values of the gait parameters related to fall risk for the subject 2 during the acquisition performed at home. Legend: s (seconds), min (minutes), Hz (Hertz), psd (power spectral density), rad/s (radians per seconds).

SUBJECT 2 (*home*)	
PARAMETERS	**VALUES**
PARAMETERS RELATED TO THE QUANTITY OF WALKING	
Total Number of Walking Bouts (TWB)	19 *bouts*
Total Walking Duration as a Percentage (TWDp)	2,6685 *%*
Total Number of Steps (TNS)	688 *steps*
Median Walking Bout Duration (MWBD)	20,0826 *s*
Median Number of Steps per Bouts (MNSB)	36,2105 *steps/bout*
Cadence (Cad)	108,1846 *steps/min*
PARAMETERS RELATED TO THE QUALITY OF WALKING (averaged and weighted)	
Frequency measures	
Dominant Frequency	1,8235 *Hz*
Amplitude	0,000079139 *psd (power/rad/s)*
Width	0,1231 *Hz*
Slope	0,00085379 p*sd/Hz*
Harmonic Ratio	1,6770 *(unitless)*
Temporal measures	
Step Time	0,5799 *s*
Stride Time	1,1584 *s*
Stance Time	0,9260 *s*
Swing Time	0,2324 *s*
Double Support Time	0,3498 *s*
Single Support Time	0,8087 *s*
Step Time Variability	0,1337 *s*
Stride Time Variability	0,1785 *s*
Stance Time Variability	0,1592 *s*
Double Support Time Variability	0,0899 *s*
Step Regularity	0,1809 *(unitless)*
Stride Regularity	0,1510 *(unitless)*
Asymmetry Step Time	0,0496 *(unitless)*
Asymmetry Stride Time	0,0119 *(unitless)*
Asymmetry Stance Time	0,0786 *(unitless)*
Asymmetry Double Support Time	0,0347 *(unitless)*

Table 14: this table lists the values of some gait parameters expressed in time and as a percentage of the gait cycle for the subject 2 during the home recording. These values are compared with percentages found in literature. Legend: s (seconds).

SUBJECT 2 (*home*)				
GAIT PARAMETERS	**EXPERIMENTAL PARAMETERS AS A PERCENTAGE OF GAIT CYCLE**	**LITERATURE PARAMETERS AS A PERCENTAGE OF GAIT CYCLE [22]**	**EXPERIMENTAL PARAMETERS IN SECONDS (s)**	**GAIT CYCLE DURATION IN SECONDS (s)**
Stance Time	79,9360 *%*	60 *%*	0,9260 *s*	1,1584 s
Swinge Time	20,0640 *%*	40 *%*	0,2324 *s*	
Double Support Time	30,1950 *%*	20 *%*	0,3498 *s*	
Single Support Time	69,8050 *%*	80 *%*	0,8087 *s*	

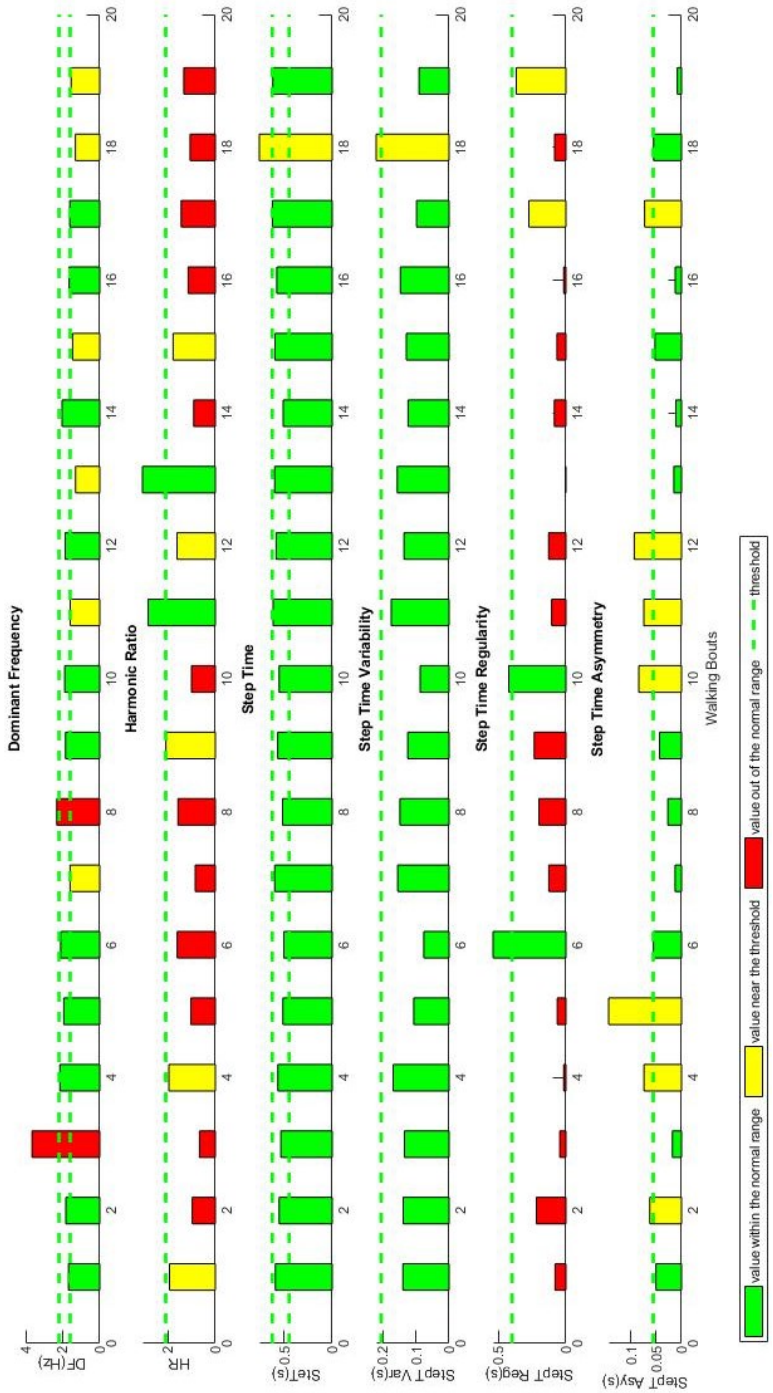

Figure 45: this figure illustrates the first graph composed by six histograms with parameters related to step time extracted from the subject 2 (home recording). Each rectangle represents the value of the parameter computed in a specific walking bout. Green colour means that the value of the parameter is within the normal or non-fallers range; yellow that it is near the threshold; red that it is out of the normal range; the dotted green line is the threshold. In the x-axis there is the number of walking bout, in the y-axis there are the magnitudes of the parameters.

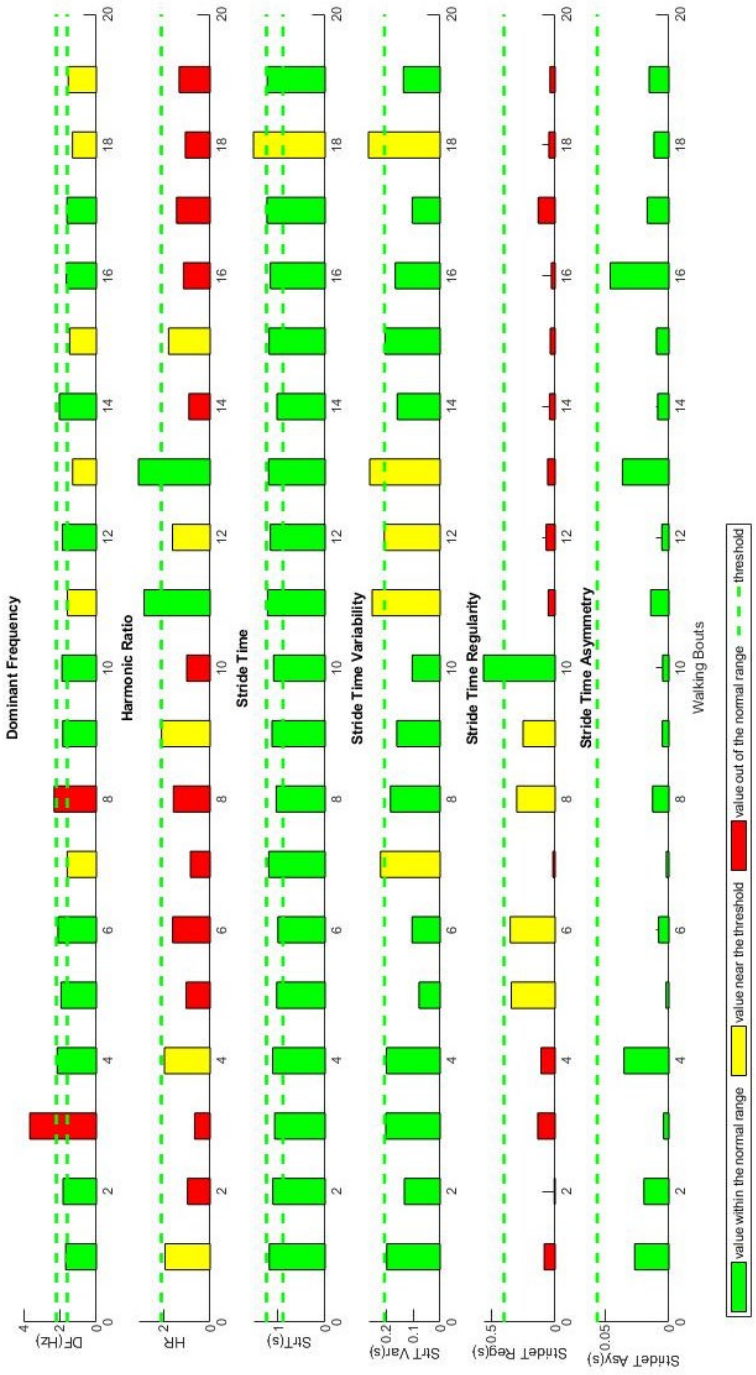

Figure 46: this figure illustrates the first graph composed by six histograms with parameters related to stride time extracted from the subject 2 (home recording). Each rectangle represents the value of the parameter computed in a specific walking bout. Green colour means that the value of the parameter is within the normal or non-fallers range; yellow that it is near the threshold; red that it is out of the normal range; the dotted green line is the threshold. In the x-axis there is the number of walking bout, in the y-axis there are the magnitudes of the parameters.

SUBJECT 3

Tables 15 and 16 and figures 47 and 48 illustrates the experimental results from the subject 3 during the home recording.

Table 15: this table lists the values of the gait parameters related to fall risk for the subject 3 during the acquisition performed at home. Legend: s (seconds), min (minutes), Hz (Hertz), psd (power spectral density), rad/s (radians per seconds).

SUBJECT 3 (*home*)	
PARAMETERS	**VALUES**
PARAMETERS RELATED TO THE QUANTITY OF WALKING	
Total Number of Walking Bouts (TWB)	26 *bouts*
Total Walking Duration as a Percentage (TWDp)	4,7552 *%*
Total Number of Steps (TNS)	3370 *steps*
Median Walking Bout Duration (MWBD)	71,5763 *s*
Median Number of Steps per Bouts (MNSB)	129,6154 *steps/bout*
Cadence (Cad)	108,6522 *steps/min*
PARAMETERS RELATED TO THE QUALITY OF WALKING (averaged and weighted)	
Frequency measures	
Dominant Frequency	1,8283 *Hz*
Amplitude	0,0738 *psd (power/rad/s)*
Width	0,0307 *Hz*
Slope	32,9471 p*sd/Hz*
Harmonic Ratio	2,5327 *(unitless)*
Temporal measures	
Step Time	0,5650 *s*
Stride Time	1,1284 *s*
Stance Time	0,9208 *s*
Swing Time	0,2076 *s*
Double Support Time	0,3649 *s*
Single Support Time	0,7634 *s*
Step Time Variability	0,0585 *s*
Stride Time Variability	0,0887 *s*
Stance Time Variability	0,0780 *s*
Double Support Time Variability	0,0410 *s*
Step Regularity	0,7180 *(unitless)*
Stride Regularity	0,6942 *(unitless)*
Asymmetry Step Time	0,0380 *(unitless)*
Asymmetry Stride Time	0,0046 *(unitless)*
Asymmetry Stance Time	0,0178 *(unitless)*
Asymmetry Double Support Time	0,0183 *(unitless)*

Table 16: this table lists the values of some gait parameters expressed in time and as a percentage of the gait cycle for the subject 3 during the home recording. These values are compared with percentages found in literature. Legend: s (seconds).

SUBJECT 3 (*home*)				
GAIT PARAMETERS	**EXPERIMENTAL PARAMETERS AS A PERCENTAGE OF GAIT CYCLE**	**LITERATURE PARAMETERS AS A PERCENTAGE OF GAIT CYCLE [22]**	**EXPERIMENTAL PARAMETERS IN SECONDS (s)**	**GAIT CYCLE DURATION IN SECONDS (s)**
Stance Time	81,6030 *%*	60 *%*	0,9208 *s*	1,1284 *s*
Swinge Time	18,3970 *%*	40 *%*	0,2076 *s*	
Double Support Time	32,3413 *%*	20 *%*	0,3649 *s*	
Single Support Time	67,6587 *%*	80 *%*	0,7634 *s*	

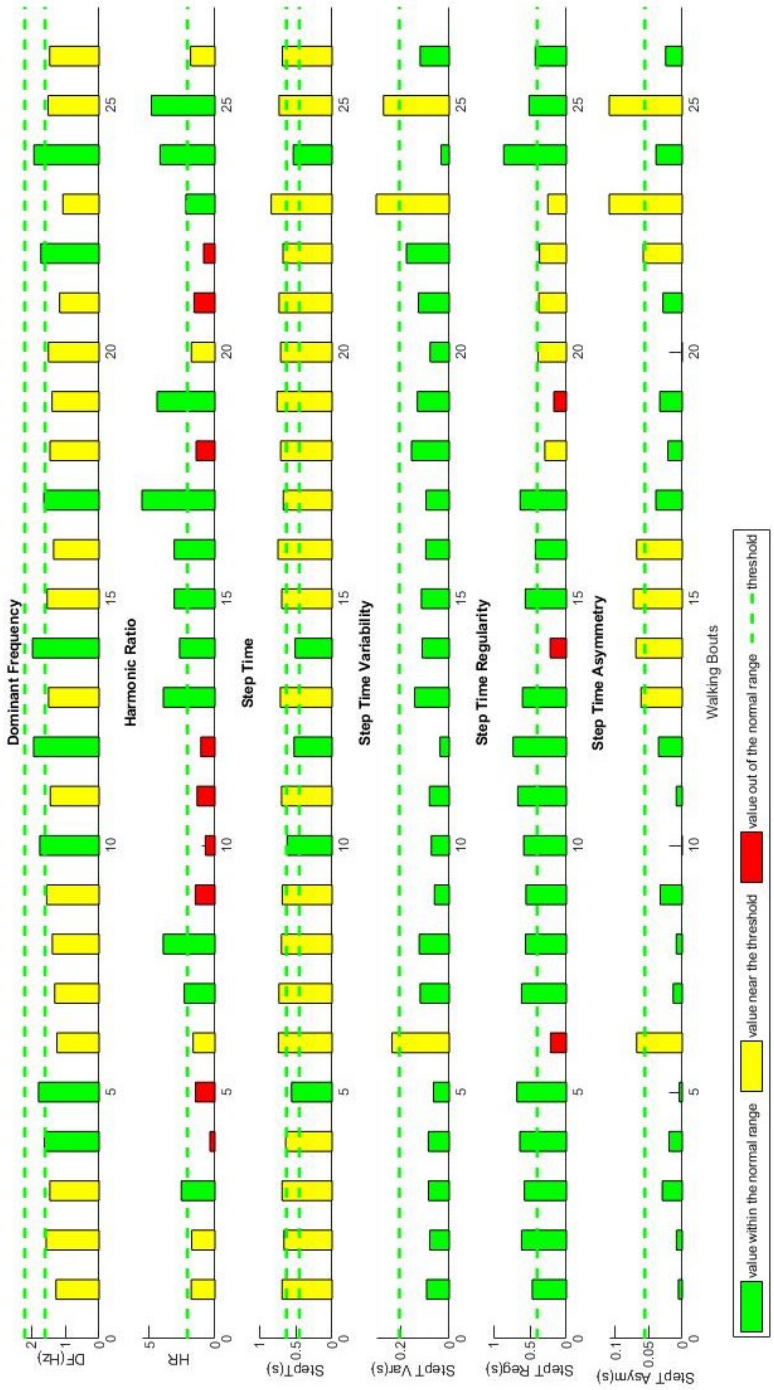

Figure 47: this figure illustrates the first graph composed by six histograms with parameters related to step time extracted from the subject 3 (home recording). Each rectangle represents the value of the parameter computed in a specific walking bout. Green colour means that the value of the parameter is within the normal or non-fallers range; yellow that it is near the threshold; red that it is out of the normal range; the dotted green line is the threshold. In the x-axis there is the number of walking bout, in the y-axis there are the magnitudes of the parameters.

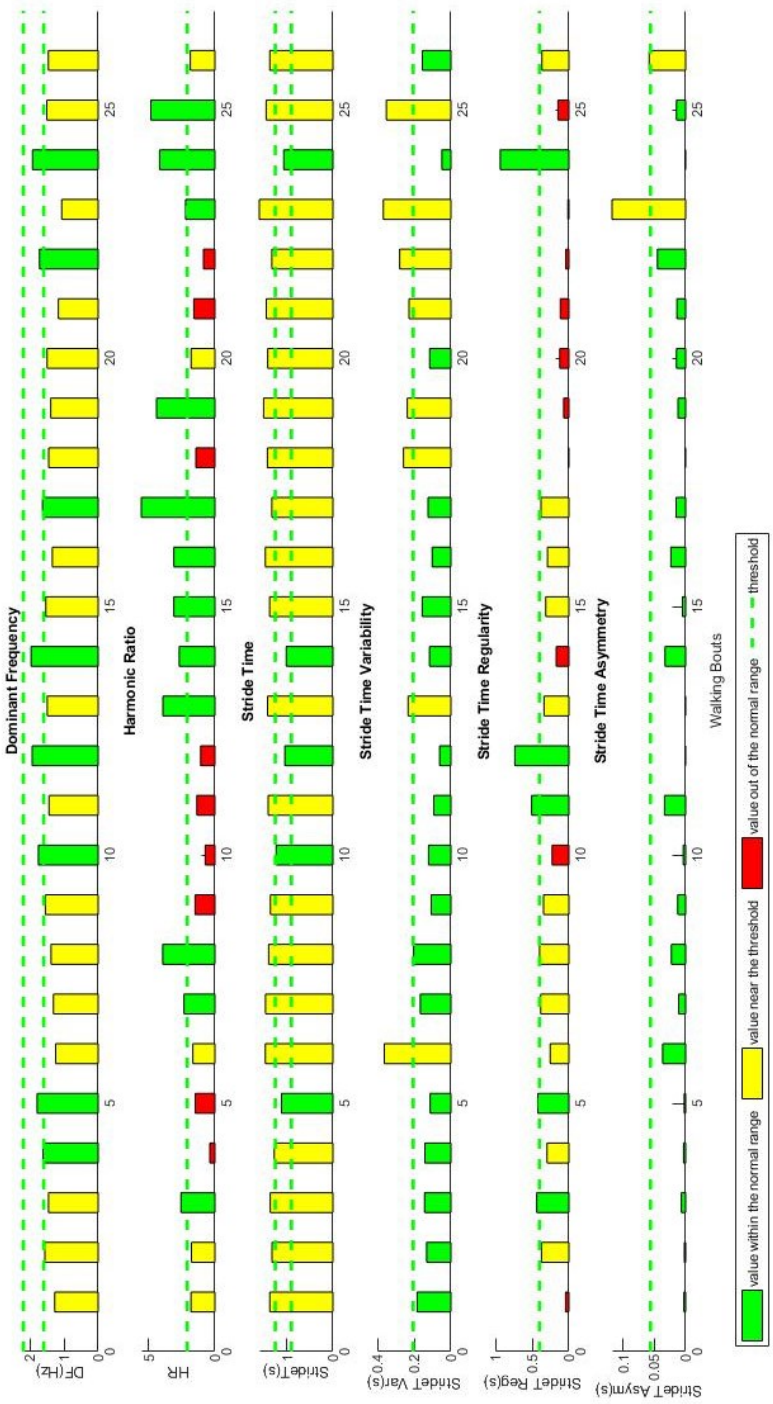

Figure 48: this figure illustrates the second graph composed by six histograms with parameters related to stride time extracted from the subject 3 (home recording). Each rectangle represents the value of the parameter computed in a specific walking bout. Green colour means that value of the parameter is within the normal or non-fallers range; yellow that it is near the threshold; red that it is out of the normal range; the dotted green line is the threshold. In the x-axis there is the number of walking bout, in the y-axis there are the magnitudes of the parameters.

SUBJECT 4

Tables 17 and 18 and figures 49 and 50 illustrates the experimental results from the subject 4 during the home recording.

Table 17: this table lists the values of the gait parameters related to fall risk for the subject 4 during the acquisition performed at home. Legend: s (seconds), min (minutes), Hz (Hertz), psd (power spectral density), rad/s (radians per seconds).

SUBJECT 4 (*home*)	
PARAMETERS	**VALUES**
PARAMETERS RELATED TO THE QUANTITY OF WALKING	
Total Number of Walking Bouts (TWB)	49 *bouts*
Total Walking Duration as a Percentage (TWDp)	4,8632 *%*
Total Number of Steps (TNS)	1743 *steps*
Median Walking Bout Duration (MWBD)	25,9034 *s*
Median Number of Steps per Bouts (MNSB)	35,5714 *steps/bout*
Cadence (Cad)	82,3941 *steps/min*
PARAMETERS RELATED TO THE QUALITY OF WALKING (averaged and weighted)	
Frequency measures	
Dominant Frequency	1,4318 *Hz*
Amplitude	0,0006186 *psd (power/rad/s)*
Width	0,1039 *Hz*
Slope	0,0128 p*sd/Hz*
Harmonic Ratio	2,5911 *(unitless)*
Temporal measures	
Step Time	0,7622 *s*
Stride Time	1,5203 *s*
Stance Time	1,2567 *s*
Swing Time	0,2637 *s*
Double Support Time	0,4996 *s*
Single Support Time	1,0207 *s*
Step Time Variability	0,1457 *s*
Stride Time Variability	0,1969 *s*
Stance Time Variability	0,1771 *s*
Double Support Time Variability	0,1051 *s*
Step Regularity	0,2773 *(unitless)*
Stride Regularity	0,2167 *(unitless)*
Asymmetry Step Time	0,0557 *(unitless)*
Asymmetry Stride Time	0,0227 *(unitless)*
Asymmetry Stance Time	0,0714 *(unitless)*
Asymmetry Double Support Time	0,0397 *(unitless)*

Table 18: this table lists the values of some gait parameters expressed in time and as a percentage of the gait cycle for the subject 4 during the home recording. These values are compared with percentages found in literature. Legend: s (seconds).

SUBJECT 4 (*home*)				
GAIT PARAMETERS	**EXPERIMENTAL PARAMETERS AS A PERCENTAGE OF GAIT CYCLE**	**LITERATURE PARAMETERS AS A PERCENTAGE OF GAIT CYCLE [22]**	**EXPERIMENTAL PARAMETERS IN SECONDS (s)**	**GAIT CYCLE DURATION IN SECONDS (s)**
Stance Time	82,6574 *%*	60 *%*	1,2567 *s*	1,5203 s
Swinge Time	17,3426 *%*	40 *%*	0,2637 *s*	
Double Support Time	32,8639 *%*	20 *%*	0,4996 *s*	
Single Support Time	67,1361 *%*	80 *%*	1,0207 *s*	

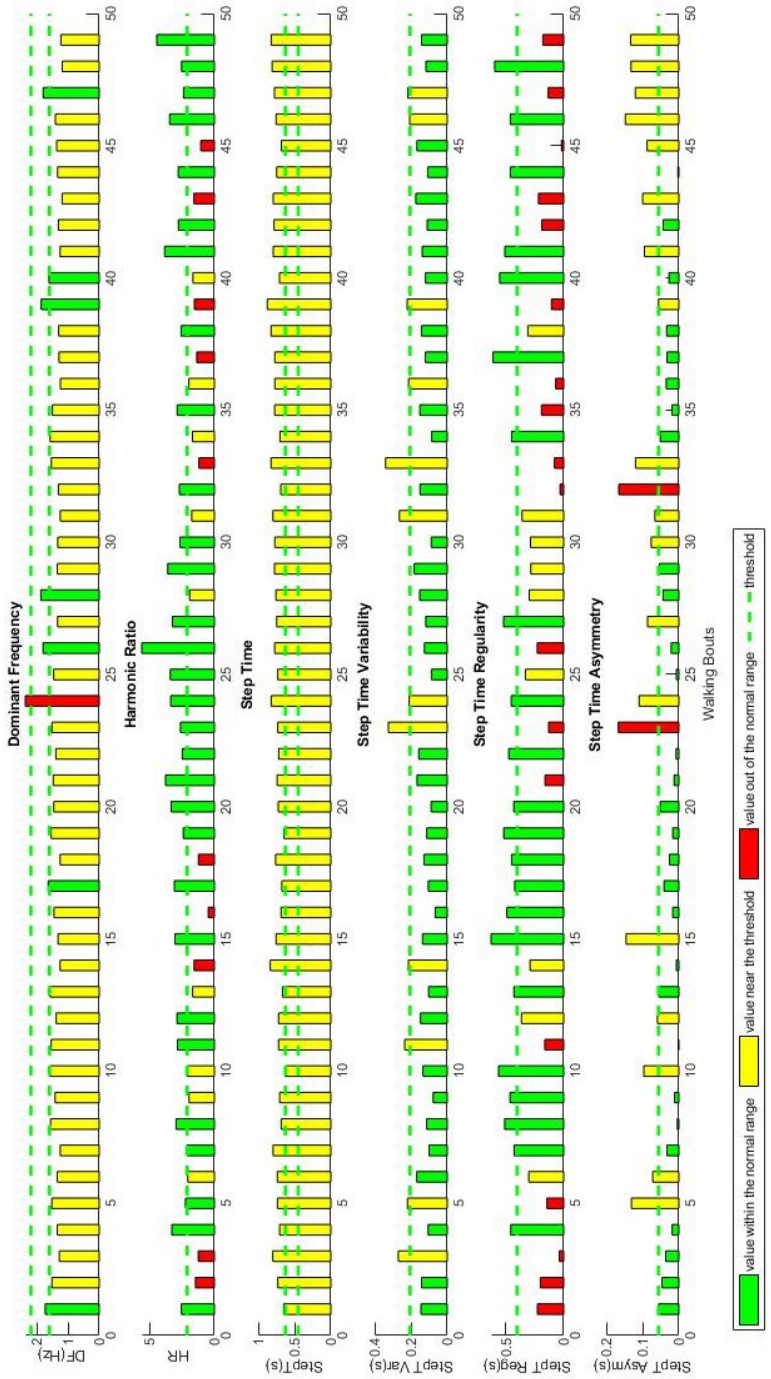

Figure 49: this figure illustrates the first graph composed by six histograms with parameters related to step time extracted from the subject 4 (home recording). Each rectangle represents the value of the parameter computed in a specific walking bout. Green colour means that the value of the parameter is within the normal or non-fallers range; yellow that it is near the threshold; red that it is out of the normal range; the dotted green line is the threshold. In the x-axis there is the number of walking bout, in the y-axis there are the magnitudes of the parameters.

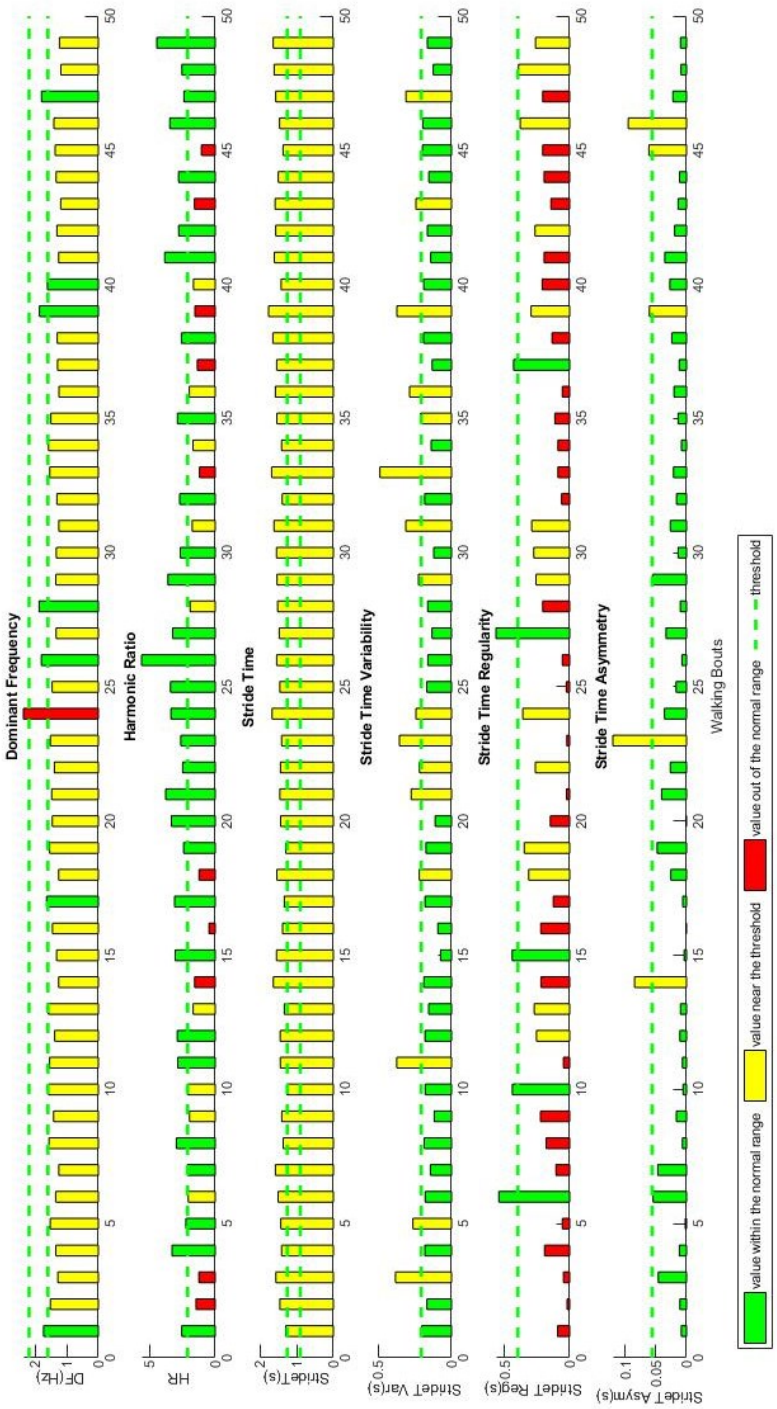

Figure 50: this figure illustrates the second graph composed by six histograms with parameters related to stride time extracted from the subject 4 (home recording). Each rectangle represents the value of the parameter computed in a specific walking bout. Green colour means that value of the parameter is within the normal or non-fallers range; yellow that it is near the threshold; red that it is out of the normal range; the dotted green line is the threshold. In the x-axis there is the number of walking bout, in the y-axis there are the magnitudes of the parameters.

SUBJECT 5

Tables 19 and 20 and figures 51 and 52 illustrates the experimental results from the subject 5 during the home recording.

Table 19: this table lists the values of the gait parameters related to fall risk for the subject 5 during the acquisition performed at home. Legend: s (seconds), min (minutes), Hz (Hertz), psd (power spectral density), rad/s (radians per seconds).

SUBJECT 5 (*home*)	
PARAMETERS	**VALUES**
PARAMETERS RELATED TO THE QUANTITY OF WALKING	
Total Number of Walking Bouts (TWB)	143 *bouts*
Total Walking Duration as a Percentage (TWDp)	9,9333 *%*
Total Number of Steps (TNS)	8023 *steps*
Median Walking Bout Duration (MWBD)	32,2338 *s*
Median Number of Steps per Bouts (MNSB)	56,1049 *steps/bout*
Cadence (Cad)	104,4337 *steps/min*
PARAMETERS RELATED TO THE QUALITY OF WALKING (averaged and weighted)	
Frequency measures	
Dominant Frequency	1,7589 *Hz*
Amplitude	0,00057512 *psd (power/rad/s)*
Width	0,0951 *Hz*
Slope	0,0113 p*sd/Hz*
Harmonic Ratio	2,2009 *(unitless)*
Temporal measures	
Step Time	0,5944 *s*
Stride Time	1,1843 *s*
Stance Time	0,9787 *s*
Swing Time	0,2057 *s*
Double Support Time	0,3853 *s*
Single Support Time	0,7990 *s*
Step Time Variability	0,1278 *s*
Stride Time Variability	0,1803 *s*
Stance Time Variability	0,1621 *s*
Double Support Time Variability	0,0934 *s*
Step Regularity	0,3151 *(unitless)*
Stride Regularity	0,2542 *(unitless)*
Asymmetry Step Time	0,0425 *(unitless)*
Asymmetry Stride Time	0,0130 *(unitless)*
Asymmetry Stance Time	0,0582 *(unitless)*
Asymmetry Double Support Time	0,0343 *(unitless)*

Table 20: this table lists the values of some gait parameters expressed in time and as a percentage of the gait cycle for the subject 5 during the home recording. These values are compared with percentages found in literature. Legend: s (seconds).

SUBJECT 5 (*home*)				
GAIT PARAMETERS	**EXPERIMENTAL PARAMETERS AS A PERCENTAGE OF GAIT CYCLE**	**LITERATURE PARAMETERS AS A PERCENTAGE OF GAIT CYCLE [22]**	**EXPERIMENTAL PARAMETERS IN SECONDS (s)**	**GAIT CYCLE DURATION IN SECONDS (s)**
Stance Time	82,6342 *%*	60 *%*	0,9787 *s*	1,1843 s
Swinge Time	17,3658 *%*	40 *%*	0,2057 *s*	
Double Support Time	32,5326 *%*	20 *%*	0,3853 *s*	
Single Support Time	67,4674 *%*	80 *%*	0,7990 *s*	

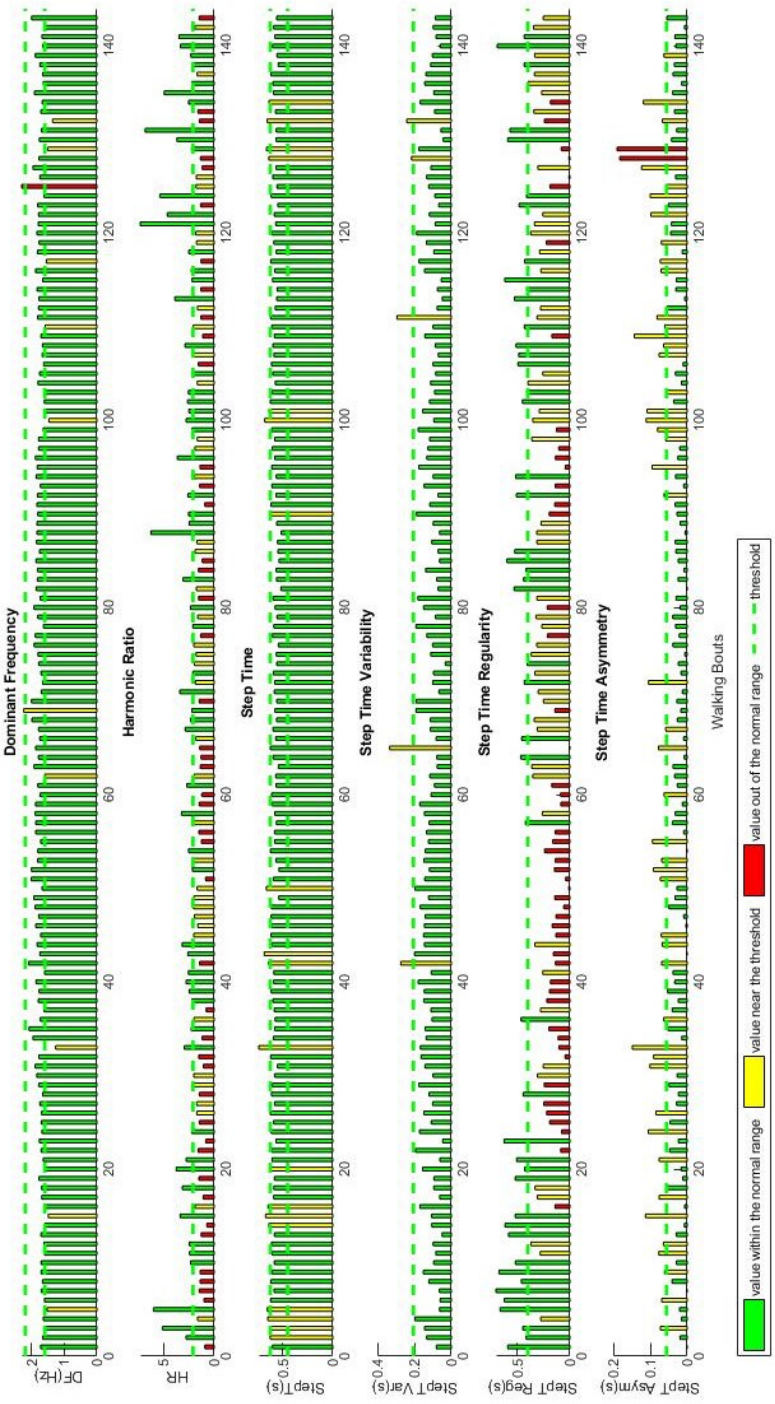

Figure 51: this figure illustrates the first graph composed by six histograms with parameters related to step time extracted from the subject 5 (home recording). Each rectangle represents the value of the parameter computed in a specific walking bout. Green colour means that the value of the parameter is within the normal or non-fallers range; yellow that it is near the threshold; red that it is out of the normal range; the dotted green line is the threshold. In the x-axis there is the number of walking bout, in the y-axis there are the magnitudes of the parameters.

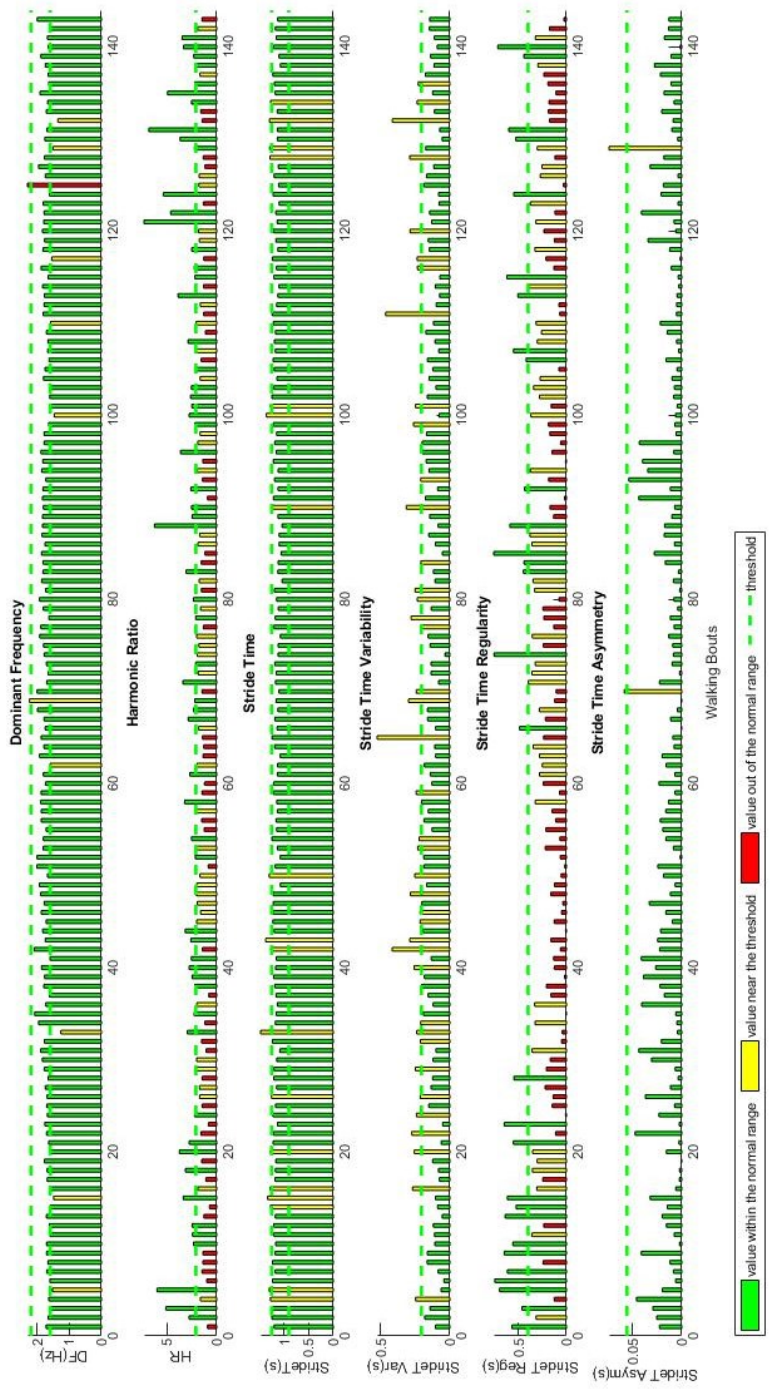

Figure 52: this figure illustrates the second graph composed by six histograms with parameters related to stride time extracted from the subject 5 (home recording). Each rectangle represents the value of the parameter computed in a specific walking bout. Green colour means that value of the parameter is within the normal or non-fallers range; yellow that it is near the threshold; red that it is out of the normal range; the dotted green line is the threshold. In the x-axis there is the number of walking bout, in the y-axis there are the magnitudes of the parameters.

SUBJECT 6

Tables 21 and 22 and figures 53 and 54 illustrates the experimental results from the subject 6 during the home recording.

Table 21: this table lists the values of the gait parameters related to fall risk for the subject 6 during the acquisition performed at home. Legend: s (seconds), min (minutes), Hz (Hertz), psd (power spectral density), rad/s (radians per seconds).

SUBJECT 6 (*home*)	
PARAMETERS	**VALUES**
PARAMETERS RELATED TO THE QUANTITY OF WALKING	
Total Number of Walking Bouts (TWB)	94 *bouts*
Total Walking Duration as a Percentage (TWDp)	11,7944 *%*
Total Number of Steps (TNS)	5345 *steps*
Median Walking Bout Duration (MWBD)	37,2521 *s*
Median Number of Steps per Bouts (MNSB)	56,8617 *steps/bout*
Cadence (Cad)	91,5842 *steps/min*
PARAMETERS RELATED TO THE QUALITY OF WALKING (averaged and weighted)	
Frequency measures	
Dominant Frequency	1,5368 *Hz*
Amplitude	0,0118 *psd (power/rad/s)*
Width	0,0752 *Hz*
Slope	0,4695 p*sd/Hz*
Harmonic Ratio	2,6363 *(unitless)*
Temporal measures	
Step Time	0,6779 *s*
Stride Time	1,3525 *s*
Stance Time	1,1190 *s*
Swing Time	0,2335 *s*
Double Support Time	0,4423 *s*
Single Support Time	0,9102 *s*
Step Time Variability	0,1331 *s*
Stride Time Variability	0,1891 *s*
Stance Time Variability	0,1665 *s*
Double Support Time Variability	0,1007 *s*
Step Regularity	0,5199 *(unitless)*
Stride Regularity	0,4359 *(unitless)*
Asymmetry Step Time	0,0427 *(unitless)*
Asymmetry Stride Time	0,0155 *(unitless)*
Asymmetry Stance Time	0,0464 *(unitless)*
Asymmetry Double Support Time	0,0292 *(unitless)*

Table 22: this table lists the values of some gait parameters expressed in time and as a percentage of the gait cycle for the subject 6 during the home recording. These values are compared with percentages found in literature. Legend: s (seconds).

SUBJECT 6 (*home*)				
GAIT PARAMETERS	**EXPERIMENTAL PARAMETERS AS A PERCENTAGE OF GAIT CYCLE**	**LITERATURE PARAMETERS AS A PERCENTAGE OF GAIT CYCLE [22]**	**EXPERIMENTAL PARAMETERS IN SECONDS (s)**	**GAIT CYCLE DURATION IN SECONDS (s)**
Stance Time	82,7388 *%*	60 *%*	1,1190 *s*	1,3525 s
Swinge Time	17,2612 *%*	40 *%*	0,2335 *s*	
Double Support Time	32,7011 *%*	20 *%*	0,4423 *s*	
Single Support Time	67,2989 *%*	80 *%*	0,9102 *s*	

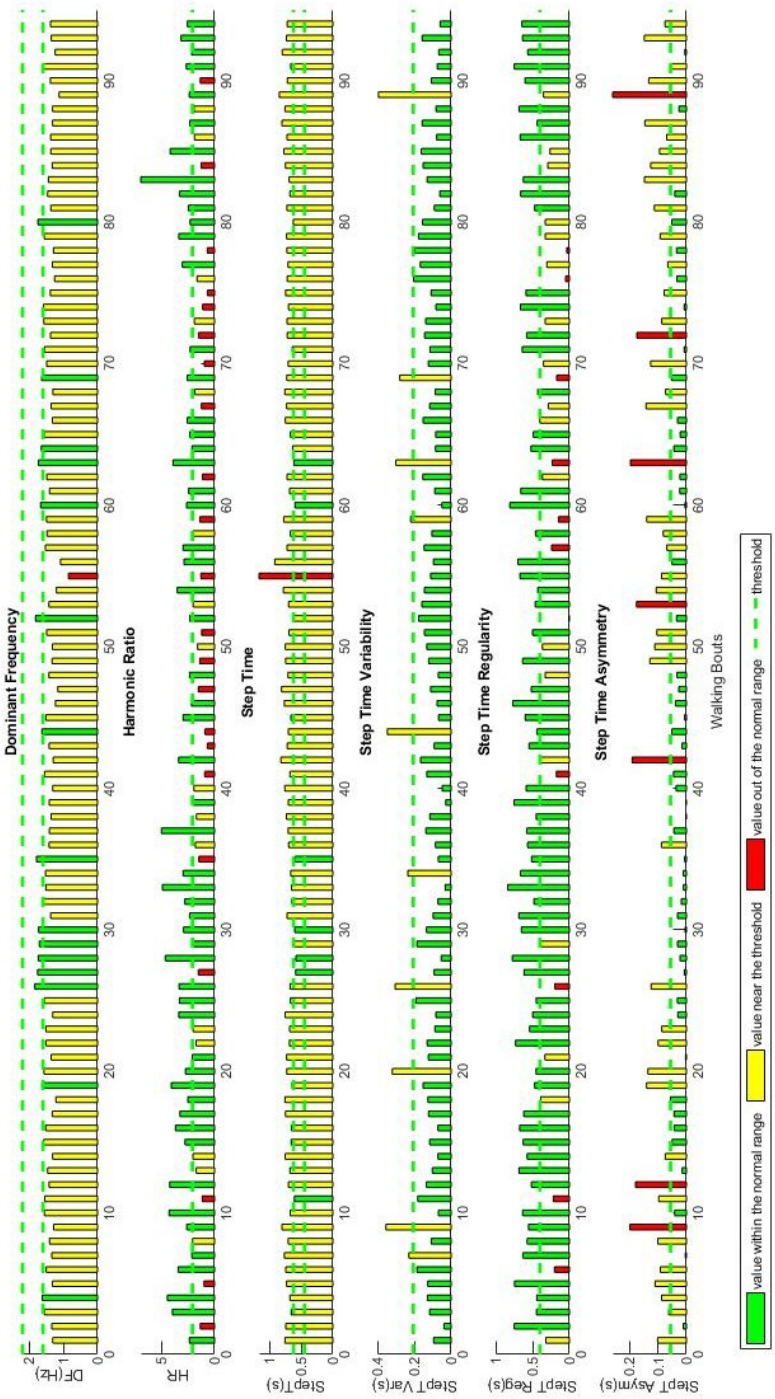

Figure 53: this figure illustrates the first graph composed by six histograms with parameters related to step time extracted from the subject 6 (home recording). Each rectangle represents the value of the parameter computed in a specific walking bout. Green colour means that the value of the parameter is within the normal or non-fallers range; yellow that it is near the threshold; red that it is out of the normal range; the dotted green line is the threshold. In the x-axis there is the number of walking bout, in the y-axis there are the magnitudes of the parameters.

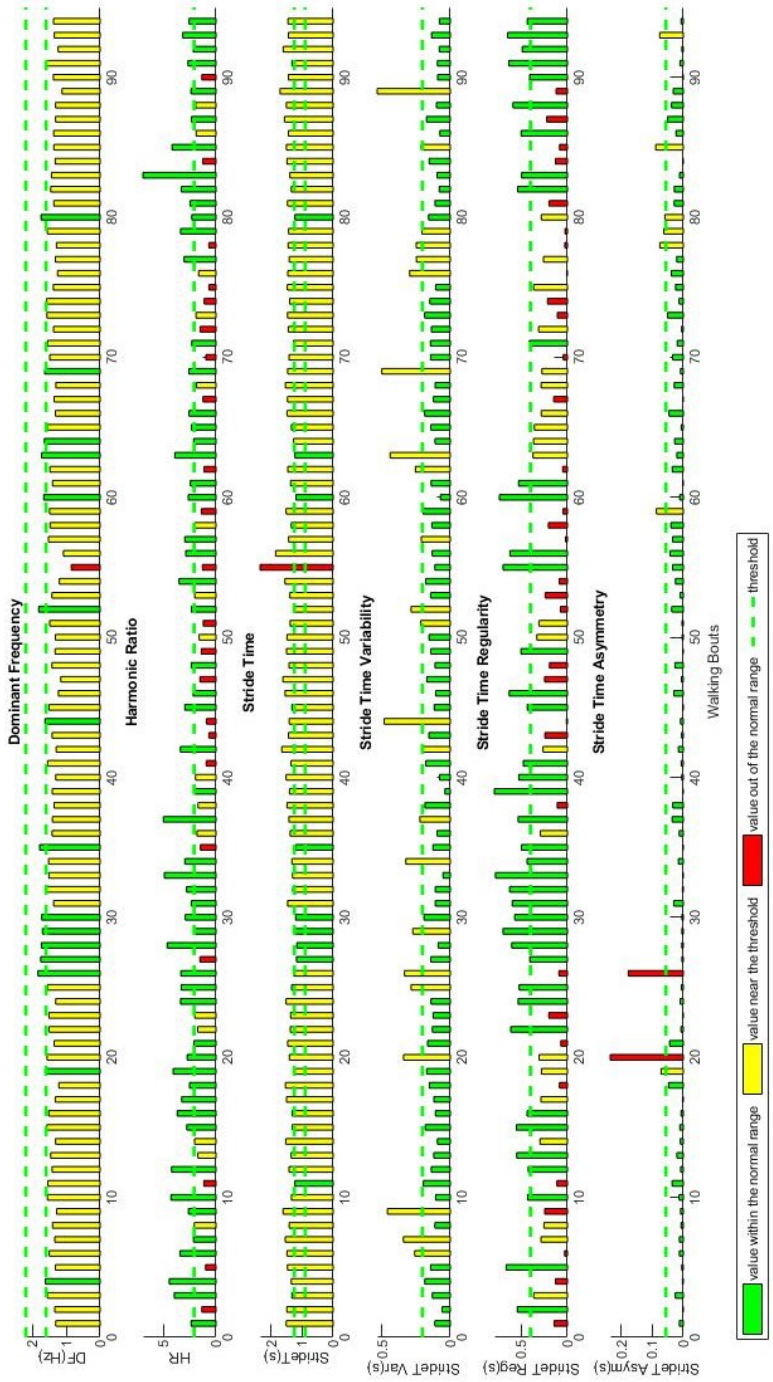

Figure 54: this figure illustrates the second graph composed by six histograms with parameters related to stride time extracted from the subject 6 (home recording). Each rectangle represents the value of the parameter computed in a specific walking bout. Green colour means that value of the parameter is within the normal or non-fallers range; yellow that it is near the threshold; red that it is out of the normal range; the dotted green line is the threshold. In the x-axis there is the number of walking bout, in the y-axis there are the magnitudes of the parameters.

SUBJECT 7

Tables 23 and 24 and figures 55 and 56 illustrates the experimental results from the subject 7 during the home recording.

Table 23: this table lists the values of the gait parameters related to fall risk for the subject 7 during the acquisition performed at home. Legend: s (seconds), min (minutes), Hz (Hertz), psd (power spectral density), rad/s (radians per seconds).

SUBJECT 7 (*home*)	
PARAMETERS	**VALUES**
PARAMETERS RELATED TO THE QUANTITY OF WALKING	
Total Number of Walking Bouts (TWB)	54 *bouts*
Total Walking Duration as a Percentage (TWDp)	5,5500 *%*
Total Number of Steps (TNS)	3624 *steps*
Median Walking Bout Duration (MWBD)	37,5438 *s*
Median Number of Steps per Bouts (MNSB)	69,6923 *steps/bout*
Cadence (Cad)	111,3775 *steps/min*
PARAMETERS RELATED TO THE QUALITY OF WALKING (averaged and weighted)	
Frequency measures	
Dominant Frequency	1,9231 *Hz*
Amplitude	0,0100 *psd (power/rad/s)*
Width	0,0838 *Hz*
Slope	0,6276 p*sd/Hz*
Harmonic Ratio	2,8104 *(unitless)*
Temporal measures	
Step Time	0,5573 *s*
Stride Time	1,1064 *s*
Stance Time	0,8559 *s*
Swing Time	0,2505 *s*
Double Support Time	0,3018 *s*
Single Support Time	0,8046 *s*
Step Time Variability	0,1993 *s*
Stride Time Variability	0,2743 *s*
Stance Time Variability	0,2353 *s*
Double Support Time Variability	0,1323 *s*
Step Regularity	0,5148 *(unitless)*
Stride Regularity	0,3798 *(unitless)*
Asymmetry Step Time	0,0587 *(unitless)*
Asymmetry Stride Time	0,0290 *(unitless)*
Asymmetry Stance Time	0,0770 *(unitless)*
Asymmetry Double Support Time	0,0274 *(unitless)*

Table 24: this table lists the values of some gait parameters expressed in time and as a percentage of the gait cycle for the subject 7 during the home recording. These values are compared with percentages found in literature. Legend: s (seconds).

SUBJECT 7 (*home*)				
GAIT PARAMETERS	**EXPERIMENTAL PARAMETERS AS A PERCENTAGE OF GAIT CYCLE**	**LITERATURE PARAMETERS AS A PERCENTAGE OF GAIT CYCLE [22]**	**EXPERIMENTAL PARAMETERS IN SECONDS (s)**	**GAIT CYCLE DURATION IN SECONDS (s)**
Stance Time	77,3594 *%*	60 *%*	0,8559 *s*	1,1064 s
Swinge Time	22,6406 *%*	40 *%*	0,2505 *s*	
Double Support Time	27,2804 *%*	20 *%*	0,3018 *s*	
Single Support Time	72,7196 *%*	80 *%*	0,8046 *s*	

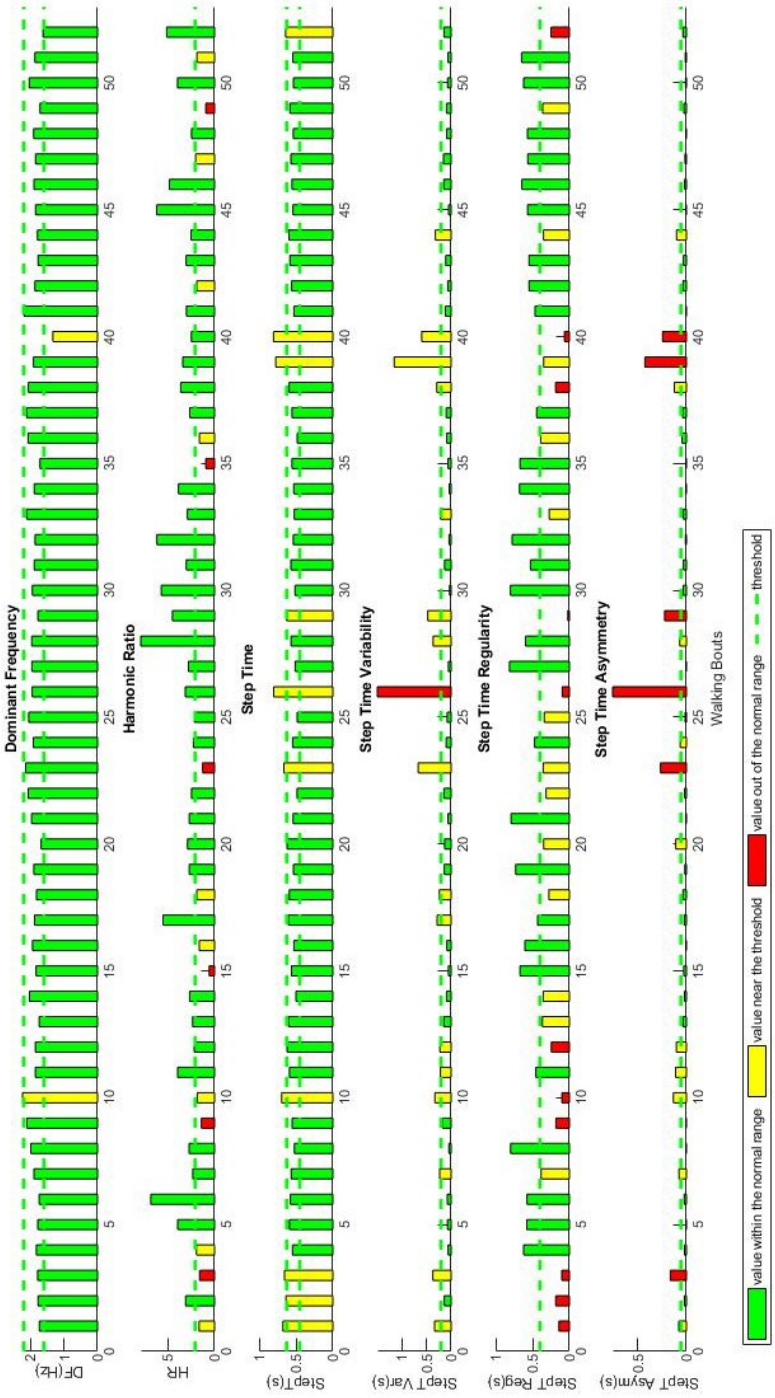

Figure 55: this figure illustrates the first graph composed by six histograms with parameters related to step time extracted from the subject 7 (home recording). Each rectangle represents the value of the parameter computed in a specific walking bout. Green colour means that the value of the parameter is within the normal or non-fallers range; yellow that it is near the threshold; red that it is out of the normal range; the dotted green line is the threshold. In the x-axis there is the number of walking bout, in the y-axis there are the magnitudes of the parameters.

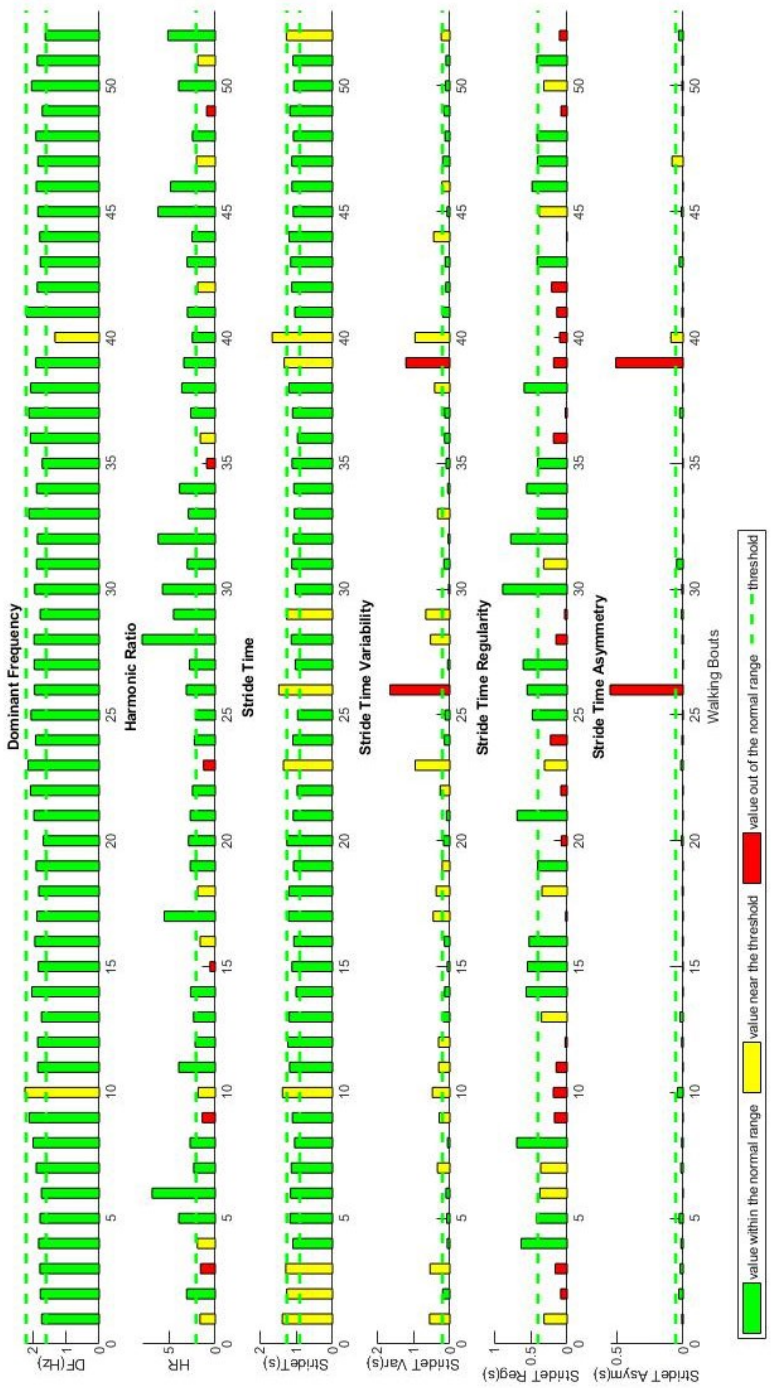

Figure 56: this figure illustrates the second graph composed by six histograms with parameters related to stride time extracted from the subject 7 (home recording). Each rectangle represents the value of the parameter computed in a specific walking bout. Green colour means that value of the parameter is within the normal or non-fallers range; yellow that it is near the threshold; red that it is out of the normal range; the dotted green line is the threshold. In the x-axis there is the number of walking bout, in the y-axis there are the magnitudes of the parameters.

6.4 THE PERCENTAGE ERROR OF THE ALGORITHM

The performance of the algorithm was inspected by controlling the capacity of the algorithm in the identification of steps in the supervised laboratory trial performed by subject 1. The correct number of steps was observed from video recordings and it was compared with the number of steps extracted from the algorithm. Successively, the percentage error was expressed as in the following eq. (15):

$$\varepsilon_{\%} = \frac{|NS_V - NS_A|}{NS_V} \cdot 100 \quad (15)$$

Where, $\varepsilon_{\%}$ is the percentage error of the algorithm, NS_V is the number of steps observed from video recordings, and NS_A is the number of steps extracted from the algorithm.

The performance of the algorithm is reported in table 25.

Table 25: this table describes the performance of the algorithm (expressed as percentage error) as compared to video recordings in the steps identification process. The laboratory trial of subject 1 was used to conduct this analysis. Legend: WB (walking bout), s (seconds), ε% (percentage error).

Walking Bout (WB)	**Duration of Walking Bout in seconds**	**Number of steps seen from video recordings**	**Number of steps extracted from the algorithm**	**Percentage Error (ε%) of the algorithm**
First WB	21,59 s	37 steps	37 steps	0 %
Second WB	10,78 s	19 steps	19 steps	0 %
Third WB	21,50 s	39 steps	39 steps	0 %
Fourth WB	23,69 s	40 steps	40 steps	0 %
Fifth WB	81,66 s	148 steps	146 steps	1,4 %
Sixth WB	75,17 s	132 steps	130 steps	1,5 %
Seventh WB	193,10 s	346 steps	340 steps	1,7 %
Eighth WB	39,96 s	68 steps	67 steps	1,5 %
Ninth WB	185,46 s	310 steps	305 steps	1,6 %

Discussions

The aim of this thesis was to study and fabricate a method for the home assessment of gait parameters related to fall risk in parkinsonian subjects by using a single wearable sensor. The proposed system consists in the extrapolation of meaningful metrics related to gait quantity and quality (both in frequency and temporal domains) and by comparing their experimental outcomes with values found in literature. The latter were used to define non-fallers ("normal") or fallers ("abnormal") ranges and were taken from works conducted on elderly PD people with a similar modality than the one presented in this thesis [48], [52], [80]. In this way, it was possible to study balance properties and relative fall risk of PD individuals while walking during common ADLs in home settings. Since PD is a common and widespread neurodegenerative disorder that affects the motor capacity, this work could be particularly useful in preventing dangerous loss-of-balance episodes and reducing consequent injuries as much as possible. Indeed, doctors could use this system to analyse the gait of PD patients and to optimize the specific medical therapy for each patient to improve their quality of life.

The NGIMU device was adopted to acquire the data used as inputs of the developed algorithm because of its practical and technical properties. In fact, its compactness, ease of use, and high performances in terms of accuracy and reliability together with the long-life battery and the possibility to implement quaternions were found to be particularly advantageous [72]. In literature, there is no consensus about the optimal method to assess gait properties in terms of number, type, and positioning of sensors, but also in terms of features to be extracted and tasks to be performed. Thus, some of the most promising solutions found in literature were adopted in this thesis together with new ones. To increase comfortability and convenience as much as possible, only one device (NGIMU), located at the lumbar region (preferably at the lower back), was used for the analysis. Additionally, the lumbar region, especially the lower back or the waist, was one of the most frequently adopted in these kinds of applications since it is supposed to be the steadiest point of the body in which the COM of all body segments can be enclosed [62]. Data from the tri-axial accelerometer sensor were passed as inputs of the algorithm and were used to extract the gait parameters. However, also data coming from the tri-axial gyroscope were considered to utilize the quaternion function. Although the latter

increased the energy consumption and the software complexity, it was necessary to correct the wrong positioning and orientation of the device in some acquisitions. In fact, some patients preferred to locate the NGIMU in different positions or with a different orientation for reasons of higher comfortability or simply by accident. At the same time, the system proposed in this thesis can dramatically reduce power consumption of the device since, if the device is correctly positioned and oriented, it only requires acceleration data from a single sensor. So, if the patient is sure about the correct location of the accelerometer, data coming from gyroscope and quaternions are not mandatory. This was tested in laboratory trials during which the device was correctly placed, and the usage of quaternions did not effectively change the values of the gait parameters. At the same time, the speed of running of the MATLAB program without quaternions was found to be strongly increased.

Subjects were asked to wear NGIMU while performing ADLs at home because this is the best way to obtain a reliable estimation of gait parameters and relative fall risk. In fact, examinations carried out in laboratory settings are generally more accurate in terms of computation of parameters, but less truthful in terms of “real” validity of their outcomes. This is because participants are forced to perform some activities that are generally thought to induce loss-of-balance events, while common ADLs at home are less associated with these kinds of episodes [11]. This may be the case of subject 2 who during the lab trial walked with stance time, swinge time, double support time, and single support time (expressed as percentages of gait cycle) which were very different to the expected values found in [22]. This study considered the same battery of gait parameters (expressed as a percentage of the gait cycle) extracted from healthy non-fallers and defines the “standard” values of these metrics. Vice versa, the subject 2 showed a more regular walking during home acquisition. Stance time and double support time increased by about 35 % and 25 % from home to lab recording (tables 8 and 14). While swing time and single support time decreased by about 35 % and 25 % from home to lab recording (tables 8 and 14). On the contrary, in some cases, subjects are more focused on the activity to be performed and walk with a higher stability, reducing the risk of FoG and falls [9]. This was probably the case of subject 1 that during laboratory trial (tables 5 and 6) walked with stance time, swinge time, double support

time, and single support time which were very similar to the expected values found in [22]. Instead, the same subject showed different trends of the same parameters during home trials. Stance time and double support time were found to be increased by about 10 %, while swing time and single support time were found to be decreased by about 12 % as compared to lab and literature values. This can be observed in tables 7, 8, 9, and 10. This may also be due to the difference in "complexity" of walking activities between lab and home trials. During home trials, walking activities were probably more complex than lab ones due to interruptions, obstacles, or other factors. Also previous studies introduced the problem of comparing in-home and in-lab results for the same reason [53], [76]. To solve this issue, subject 1 was asked to walk "freely" for 15 minutes during the laboratory trial to simulate a home-like situation and to test the performance of the algorithm also during this motor task (table 25). Additionally, acquisitions performed at home reduce the time consumption and the discomfort for patients as compared to lab examinations [10].

Experimental trials with video recordings and diaries were collected to verify the correct functioning of the algorithm in the extraction of walking windows, in the identification of steps, and in the computation of parameters. The table 25 shows the performance of the algorithm in the identification of steps as compared to video recordings, as also done in [53], [76]. The lab trial of subject 1 was considered. The percentage error of the algorithm was computed for each walking bout and revealed the good functioning of the program. In fact, the error was 0 % in short and simple walking tasks, while it ranged between 1,4 % and 1,7 % in longer and more complex bouts. Thus, the error remained low for all bouts. Most of the thresholds-based filters that were used for the extraction of walking windows were taken from previous works ([48], [76], [77], [79]). While the filter based on periodicity was specifically developed for this work. It was created to focus on walking windows, which are periodic activities ([30]), and to reject other segments that did not include proper walks and which could inevitably compromise the computation of gait parameters. Then literature thresholds were modified to obtain the best accuracy in the outputs and standardized to obtain "universal" values, valid for all subjects. The identification of heel strike and toe off events as minima and maxima of wavelets from AP acceleration was already adopted in [76]. On the contrary, previous

studies like [53], utilised the vertical acceleration to do steps identification with good results. However, this signal reduced its consistency since it generated a more complex pattern especially in data extracted from home trials, as also observed in [76].

All features were taken from the literature (as explained in the paragraph 5.2.6) and were used as gait indicators related to fall risk. The final output consists in the composition of two tables and two graphs. They contain the extracted gait parameters which were compared with some values or ranges observed in literature. Studies conducted with the same modality on the same kind of patients were considered. The two graphs composed by histograms were thought to show the trend of metrics related to step time and to stride time in different walking bouts. In this way, it can be observed how they changed in different moments of the day and whether their dynamics were linked. The subject 1 performed two acquisitions at home in two different days to test the correct functioning of the algorithm by verifying that the parameters were similar, as can be seen in tables 9 and 11. This makes sense because the participant was the same and the acquisitions were performed a day apart from each other.

The first group of metrics were related to the quantity of walking. In [48], [77], [79] they were found to be not significantly different between PD fallers and PD non-fallers. In addition, many of them depend on the length in time of the acquisition and on activities performed by participants. Since the duration of each acquisition was different, it ranged between 8 and 12 hours, these parameters cannot be used for comparisons between subjects or with other studies. So, they can only be used as indicators of the total “amount” of walking activity. However in [30], the cadence, a quantity parameter that belongs to the first group, was used as a meaningful feature in a system that aimed at indicating the fall risk of PD people. In this work, the cadence ranged from about 76 steps/min to about 121 steps/min. It remained within non-faller (or “normal”) range found in [80], except for subject 2, 4, and 6 for whom the cadence was lower than expected but not dramatically low. In fact, it was about 76 steps/min in subject 2, 82 steps/min in subject 4, and 91 steps/min in subject 6.

The second group of metrics were related to quality of walking (in temporal and frequency domains). In [46], they were found to be particularly different between PD fallers and non-fallers. The dominant frequency of the power spectral density and the

harmonic ratio were reported in the tables with all parameters but also in the final graphs due to their important physiological meanings. The dominant frequency indicates the number of steps per second while the cadence indicates the number of steps per minute. So, these metrics are strictly correlated. Indeed, also dominant frequency remained within the non-fallers range for most of the cases, except for subjects 2 (lab), 4, and 6. This is shown by the higher number of yellow rectangles on the first rows of histograms (each rectangle represents a walking bout and the yellow stands for value near the threshold) in figures 39, 49, 56. Dominant frequency and cadence are also correlated with step time and stride time since they describe the time in between two steps or strides. In fact, step time and stride time remained within non-fallers ranges for subjects 1, 2 (home), 3, 5, and 7. Thus, these four parameters followed the same trend. The harmonic ratio, that is an index of whole-body movement, showed a certain oscillation between fallers, non-fallers, and near threshold ranges indicated by red, green, and yellow rectangles. This result is reasonable since this study was conducted on elderly people affected by PD which is a pathology that compromises gait stability, rhythmicity, and smoothness. So, it is possible that the walking stability was differently affected while making specific ADLs or in certain moments of the day. However, the weighted and averaged values of harmonic ratios remained within the normal range for all subjects, except for subject 2 (lab and home). This could be due to the higher number of green rectangles with respect to red and yellow ones in second rows of histograms. Alternatively, when the number of different coloured rectangles was almost the same, it could be due to the greater importance given to longer bouts in case they were green than shorter ones in case they were yellow or red. This probably was the case of subject 5 (table 19, figure 51). Step time variability and stride time variability resulted to be mainly included in the “normal” range. Also in this case subject 2 (lab) was an exception. This was demonstrated by the weighted and averaged values in the tables and by the predominance of green rectangles over yellow and red ones in the histograms. Also stance time variability and double support time variability exhibited values near to zero, which means that they remained into physiological range. Indeed, weighted and mean parameters connected to variability were altogether lower than 0,2 s, excluded subject 2 (table 7). This points out a low variability between steps (left and right steps were combined) during different phases of gait cycle. The weighted and

averaged step time and stride time regularities were found to be out of the “normal” range for subjects 1, 2, 4, and 7 (values lower than 0,4 s). While they were inside the “normal” range (values higher than 0,4 s) for subjects 3, 5, and 6. This result was also confirmed by looking at the trends in fourth rows of histograms. This means that the correlation between left and right steps and left and right strides was not preserved by most participants. The weighted and mean asymmetry-related parameters remained mostly within non-fallers range (lower than 0,056 s). The same result was observed also during walking bouts even if some bouts revealed “abnormal” values. So, some ADLs probably triggered an asymmetric response or in certain moments of the day the symmetry was lost. Thus, in this group of people, PD influenced more the step and stride regularities than other parameters. In summary, measures of dominant frequency, harmonic ratio, variability, regularity, and asymmetry are features of gait that can be associated with fall risk. In fact, the lower is their membership to the non-fallers range, the more compromised is the balance during gait, and so the higher is the probability to experience fall.

The tables 10, 12, 14, 16, 18, 20, 22, 24 demonstrated as some gait parameters computed in home trials were particularly different from expected values found in literature [22]. In fact, stance time and double support time were respectively higher than 20 % and 10 %, while swing time and single support time were lower than 12 % as compared to expected values. As already said, the acquisition of subject 1 (table 6) carried out in laboratory settings was characterized by values that were closer to the ones found in [22]. Instead, subject 2 showed particularly “problematic” outcomes during the laboratory trial (table 8). Indeed, this subject was not able to perform some motor tasks due to precarious stability and revealed marked difficulties in the execution of turns around an obstacle.

At the end, a graphical user interface was fabricated to obtain in a direct way the visualization of final graphs and gait parameters. Through this user-friendly tool, it is possible to reduce the time consumption and to execute the program in a simple way, with no requirement of specialized personnel.

An interesting further step in this work could be the implementation of a machine-learning classifier that can directly estimate the fall risk, maybe giving as output three

(low risk, medium risk, high risk) or more levels of fall risk. In this case, the dataset must be split into training, testing, and validation sets. Generally, 70 % of dataset is used as training set, 15 % as testing set and 15 % as validation set. Subsequently, this classifier could be trained by passing some gait parameters related to fall risk as inputs and patients' fall risk as expected output. The latter could be defined starting from two factors. The subjects' history of falls in the last year and a score extracted from the execution of specific motor tasks while observing the patient (scales based on the observation of the patient). For example, in [30] participants were asked to do the short physical performance battery test. Through these tests, it was possible to evaluate with a score the participants' capacity in maintaining balance while standing still, walking, and getting up from sitting. The metrics considered in this thesis (measures of gait) and other statistical parameters computed from acceleration (signal-based features), together with the level of fall risk, could be used in the learning phase. In [30], the most significant signal-based features were found to be the mean of AP and ML accelerations, the mean amplitude deviation of ML component, the coefficient of variance of ML acceleration, and the correlation coefficient between AP and ML components. The study [54] revealed as another interesting feature could be the total sum vector magnitude given by the root mean square of the three components of acceleration signal. However, it is possible to extract other gait or statistical features, like gait velocity or standard deviation, and to select the best group of metrics for the classification problem. Once this process will be completed, it will be necessary to pass these metrics to the classifier to obtain the index of the subject's fall risk using a testing set and then a validation set. Accuracy, sensitivity, specificity, receiver operating curves, and contingency tables could be used to estimate the performances of the system. Regarding the type of classifier, a support vector machine, a random forest, or a decision tree could be used maybe with a k-folds cross validation procedure to avoid overfitting or underfitting, as also reported in [30]. To conclude, this machine learning classifier could represent a smart and suitable tool to obtain a precise indication about patients' level of fall risk. However, the dataset must be increased before implementing this system.

Conclusions

To resume, the developed system represents a solid platform to be used for the extraction of gait parameters related to fall risk in home settings through a single wearable sensor. However, this work is intended as a starting point since it can be subjected to several possible improvements and future developments. First, the algorithm can be validated by introducing one of the gold standard techniques (electromyography, force platforms, or stereophotogrammetry) to estimate the performances of the system. This can provide a measurement of the system's error and of the standard deviation of the system's error with respect to more accurate and reliable gold standards. This can be also useful for two purposes. First, to sharpen the computation of the thresholds that were used for the filters needed for the extraction of walking windows. Second, to verify the correct detection of HS and TO events which cannot be guaranteed from video recordings. Another possible improvement regards the number of participants (7 subjects were included in the experiment) which can be increased to refine the entire process. Moreover, also elderly healthy subjects with good walking stability could be included in a future analysis to refine the definition of non-fallers ranges, extrapolating it from real acquisitions. Another possibility is to add other significant gait parameters, like step length and gait velocity, to augment the information content of the system. Additionally, this system could be improved through the implementation of a machine-learning classifier that can directly estimate the patients' level of fall risk, as also reported in the previous section. At the end, this apparatus, that is intended to work off-line, could be supported by a real-time fall prediction and detection system. In this way, it would be also possible to prevent falls or to communicate with help centres in case of fall detection. This combined with the indication of the participant's gait characteristics and the knowledge of the level of fall risk.

In conclusion, this thesis presents a promising and non-invasive system for the home assessment of gait parameters related to fall risk in PD subjects through a single wearable sensor. It is unobtrusive, simple to be used, and it can reduce the patients' time consumption of in-clinic examinations. In addition, once improved, it could be considered a reliable system to estimate the walking stability and consequent fall risk of

PD people, allowing doctors to optimize the medical therapy for each patient, and finally improving their quality of life.

REFERENCES

[1] J. M. Beitz, “Parkinson’s disease: a review,” *Front. Biosci.*, vol. 6, no. 3, pp. 65–74, 2014, doi: 10.2741/s415.

[2] M. T. Hayes, “Parkinson’s Disease and Parkinsonism,” *Am. J. Med.*, vol. 132, no. 7, pp. 802–807, 2019, doi: 10.1016/j.amjmed.2019.03.001.

[3] A. Samii, J. G. Nutt, and B. R. Ransom, “Parkinson ’ s disease,” *Lancet*, vol. 363, no. 9423, pp. 1783–1793, 2004, doi: 10.1016/S0140-6736(04)16305-8.

[4] B. Debû, C. De Oliveira Godeiro, J. C. Lino, and E. Moro, “Managing Gait, Balance, and Posture in Parkinson’s Disease,” *Curr. Neurol. Neurosci. Rep.*, vol. 18, no. 5, p. 23, May 2018, doi: 10.1007/s11910-018-0828-4.

[5] R. Rucco *et al.*, “Type and Location of Wearable Sensors for Monitoring Falls during Static and Dynamic Tasks in Healthy Elderly: A Review,” *Sensors*, vol. 18, no. 5, p. 1613, May 2018, doi: 10.3390/s18051613.

[6] J. A. Opara, A. Małecki, E. Małecka, and T. Socha, “Motor assessment in parkinson’s disease,” *Ann. Agric. Environ. Med.*, vol. 24, no. 3, pp. 411–415, 2017, doi: 10.5604/12321966.1232774.

[7] B. R. Bloem *et al.*, “Measurement instruments to assess posture, gait, and balance in Parkinson’s disease: Critique and recommendations,” *Mov. Disord.*, vol. 31, no. 9, pp. 1342–1355, 2016, doi: 10.1002/mds.26572.

[8] C. Ramaker, J. Marinus, A. M. Stiggelbout, and B. J. van Hilten, “Systematic evaluation of rating scales for impairment and disability in Parkinson’s disease,” *Mov. Disord.*, vol. 17, no. 5, pp. 867–876, 2002, doi: 10.1002/mds.10248.

[9] W. Maetzler, J. Domingos, K. Srulijes, J. J. Ferreira, and B. R. Bloem, “Quantitative wearable sensors for objective assessment of Parkinson’s disease,” *Mov. Disord.*, vol. 28, no. 12, pp. 1628–1637, 2013, doi: 10.1002/mds.25628.

[10] M. Mancini *et al.*, “Clinical and methodological challenges for assessing freezing of gait: future perspectives,” *Mov Disord.*, vol. 34, no. 6, pp. 783–790, 2020, doi:

10.1002/mds.27709.Clinical.

[11] J. Hauth *et al.*, “Automated Loss-of-Balance Event Identification in Older Adults at Risk of Falls during Real-World Walking Using Wearable Inertial Measurement Units,” *Sensors*, vol. 21, no. 14, p. 4661, Jul. 2021, doi: 10.3390/s21144661.

[12] N. Hasegawa, V. V. Shah, P. Carlson-Kuhta, J. G. Nutt, F. B. Horak, and M. Mancini, “How to select balance measures sensitive to parkinson’s disease from body-worn inertial sensors—separating the trees from the forest,” *Sensors (Switzerland)*, vol. 19, no. 15, pp. 1–18, 2019, doi: 10.3390/s19153320.

[13] F. Hussain, F. Hussain, M. Ehatisham-Ul-Haq, and M. A. Azam, “Activity-Aware Fall Detection and Recognition Based on Wearable Sensors,” *IEEE Sens. J.*, vol. 19, no. 12, pp. 4528–4536, 2019, doi: 10.1109/JSEN.2019.2898891.

[14] M. Ghislieri, L. Gastaldi, S. Pastorelli, S. Tadano, and V. Agostini, “Wearable Inertial Sensors to Assess Standing Balance: A Systematic Review,” *Sensors*, vol. 19, no. 19, p. 4075, Sep. 2019, doi: 10.3390/s19194075.

[15] “PARKINSON’S SYMPTOMS & COMPLICATIONS,” *Parkinson’s NSW \ In this together*. https://www.parkinsonsnsw.org.au/about-parkinsons-disease/symptoms-and-complications/ (accessed Aug. 16, 2021).

[16] P. C. Fino *et al.*, “Assessment and rehabilitation of central sensory impairments for balance in mTBI using auditory biofeedback: A randomized clinical trial,” *BMC Neurol.*, vol. 17, no. 1, pp. 1–14, 2017, doi: 10.1186/s12883-017-0812-7.

[17] J. S. Perlmutter, “Assessment of Parkinson Disease Manifestations,” *Curr. Protoc. Neurosci.*, vol. 49, no. 1, pp. 1–16, Oct. 2009, doi: 10.1002/0471142301.ns1001s49.

[18] “Activities-Specific Balance Confidence (ABC) Scale,” *Yumpu*. https://www.yumpu.com/en/document/view/11600003/activities-specific-balance-confidence-abc-scale (accessed Aug. 17, 2021).

[19] C. G. Goetz *et al.*, “Movement Disorder Society-Sponsored Revision of the Unified Parkinson’s Disease Rating Scale (MDS-UPDRS): Scale presentation and

clinimetric testing results," *Mov. Disord.*, vol. 23, no. 15, pp. 2129–2170, 2008, doi: 10.1002/mds.22340.

[20] V. Agostini, M. Ghislieri, S. Rosati, G. Balestra, and M. Knaflitz, "Surface Electromyography Applied to Gait Analysis: How to Improve Its Impact in Clinics?," *Front. Neurol.*, vol. 11, no. September, pp. 1–13, Sep. 2020, doi: 10.3389/fneur.2020.00994.

[21] "BerryIMUv2-accelerometer, gyroscope, magnetometer," *tindie*. https://www.tindie.com/products/ozzmaker/berryimuv2-accelerometer-gyroscope-magnetometer/ (accessed Aug. 17, 2021).

[22] "clinicalgate," *assessment of gait*. https://clinicalgate.com/assessment-of-gait/ (accessed Dec. 07, 2021).

[23] M. Pistacchi *et al.*, "Gait analysis and clinical correlations in early Parkinson's disease," *Funct. Neurol.*, vol. 32, no. 1, pp. 28–34, 2017, doi: 10.11138/FNeur/2017.32.1.028.

[24] G. Bonora *et al.*, "Investigation of Anticipatory Postural Adjustments during One-Leg Stance Using Inertial Sensors: Evidence from Subjects with Parkinsonism," *Front. Neurol.*, vol. 8, no. July, pp. 1–12, Jul. 2017, doi: 10.3389/fneur.2017.00361.

[25] C. Curtze, J. G. Nutt, P. Carlson-Kuhta, M. Mancini, and F. B. Horak, "Objective gait and balance impairments relate to balance confidence and perceived mobility in people with parkinson disease," *Phys. Ther.*, vol. 96, no. 11, pp. 1734–1743, 2016, doi: 10.2522/ptj.20150662.

[26] M. F. Gago *et al.*, "The effect of levodopa on postural stability evaluated by wearable inertial measurement units for idiopathic and vascular Parkinson's disease," *Gait Posture*, vol. 41, no. 2, pp. 459–464, 2015, doi: 10.1016/j.gaitpost.2014.11.008.

[27] M. Rigoberto, P. R. Otniel, L. Daniel, and M. Arturo, "Analysis of Subtle Movements Related to Neurodegenerative Diseases Using Wearable Inertial Sensors : A Study in Healthy Subjects," *35th Annu. Int. Conf. IEEE Eng. Med. Biol.*

Soc., pp. 6119–6122, 2013, doi: 10.1109/EMBC.2013.6610949.

[28] J. L.a, O. S. J. . | K. M. M. | L. Susan M.a, | Machado Andre G.a, | Dey Tanujitc, and | Alberts, "Three-dimensional evaluation of postural stability in Parkinson's disease with mobile technology," *NeuroRehabilitation*, vol. 41, pp. 211–218, 2017, doi: 10.3233/NRE-171473.

[29] N. Muthukrishnan, J. J. Abbas, and N. Krishnamurthi, "A Wearable Sensor System to Measure Step-Based Gait Parameters for Parkinson's Disease Rehabilitation," *Sensors*, vol. 20, no. 22, p. 6417, Nov. 2020, doi: 10.3390/s20226417.

[30] A. Hua *et al.*, "Accelerometer-based predictive models of fall risk in older women: a pilot study," *npj Digit. Med.*, vol. 1, no. 1, p. 25, 2018, doi: 10.1038/s41746-018-0033-5.

[31] A. L. Silva de Lima *et al.*, "Freezing of gait and fall detection in Parkinson's disease using wearable sensors: a systematic review," *J. Neurol.*, vol. 264, no. 8, pp. 1642–1654, 2017, doi: 10.1007/s00415-017-8424-0.

[32] N. G. Pozzi *et al.*, "Freezing of gait in Parkinson's disease reflects a sudden derangement of locomotor network dynamics," *Brain*, vol. 142, no. 7, pp. 2037–2050, 2019, doi: 10.1093/brain/awz141.

[33] D. Rodríguez-Martín *et al.*, "Home detection of freezing of gait using support vector machines through a single waist-worn triaxial accelerometer," *PLoS One*, vol. 12, no. 2, p. e0171764, Feb. 2017, doi: 10.1371/journal.pone.0171764.

[34] J. G. Nutt and F. B. Horak, "The impact of freezing of gait on balance perception and mobility in community-living with Parkinson's disease," *Annu Int Conf IEEE Eng Med Biol Soc.*, pp. 3040–3043, 2018, doi: 10.1109/EMBC.2018.8512910.

[35] L. Sigcha *et al.*, "Deep Learning Approaches for Detecting Freezing of Gait in Parkinson ' s Disease Patients through On-Body Acceleration Sensors," *Sensors (Switzerland)*, vol. 20, no. 7, p. 1895, 2020, doi: 10.3390/s20071895.

[36] M. Mancini *et al.*, "Measuring freezing of gait during daily-life: an open-source,

wearable sensors approach," *J. Neuroeng. Rehabil.*, vol. 18, no. 1, p. 1, Dec. 2021, doi: 10.1186/s12984-020-00774-3.

[37] P. Pierleoni, A. Belli, O. Bazgir, L. Maurizi, M. Paniccia, and L. Palma, "A Smart Inertial System for 24h Monitoring and Classification of Tremor and Freezing of Gait in Parkinson ' s Disease," *IEEE Sens. J.*, vol. 19, no. 23, pp. 11612–11623, 2019, doi: 10.1109/JSEN.2019.2932584.

[38] L. Borzì *et al.*, "Home monitoring of motor fluctuations in Parkinson ' s disease patients," *J. Reliab. Intell. Environ.*, vol. 5, no. 3, pp. 145–162, 2019, doi: 10.1007/s40860-019-00086-x.

[39] S. Mazilu *et al.*, "A wearable assistant for gait training for Parkinson's disease with freezing of gait in out-of-the-lab environments," *ACM Trans. Interact. Intell. Syst.*, vol. 5, no. 1, pp. 1–31, Mar. 2015, doi: 10.1145/2701431.

[40] C. Ahlrichs *et al.*, "Detecting freezing of gait with a tri-axial accelerometer in Parkinson's disease patients," *Med. Biol. Eng. Comput.*, vol. 54, no. 1, pp. 223–233, 2016, doi: 10.1007/s11517-015-1395-3.

[41] A. T. Tzallas *et al.*, "PERFORM: A System for Monitoring, Assessment and Management of Patients with Parkinson's Disease," *Sensors*, vol. 14, no. November, pp. 21329–21357, 2014, doi: 10.3390/s141121329.

[42] L. Montesinos, R. Castaldo, and L. Pecchia, "Wearable inertial sensors for fall risk assessment and prediction in older adults: A systematic review and meta-analysis," *IEEE Trans. Neural Syst. Rehabil. Eng.*, vol. 26, no. 3, pp. 573–582, 2018, doi: 10.1109/TNSRE.2017.2771383.

[43] R. Rajagopalan, I. Litvan, and T. P. Jung, "Fall prediction and prevention systems: Recent trends, challenges, and future research directions," *Sensors (Switzerland)*, vol. 17, no. 11, pp. 1–17, 2017, doi: 10.3390/s17112509.

[44] E. Stack *et al.*, "Could In-Home Sensors Surpass Human Observation of People with Parkinson's at High Risk of Falling? An Ethnographic Study," *Biomed Res. Int.*, vol. 2016, pp. 1–10, 2016, doi: 10.1155/2016/3703745.

[45] J. C. Ayena, H. Zaibi, M. J. Otis, and B. J. Ménélas, “Home-Based Risk of Falling Assessment Test Using a Closed-Loop Balance Model,” *IEEE Trans. Neural Syst. Rehabil. Eng.*, vol. 24, no. 12, pp. 1351–1362, 2016, doi: 10.1109/TNSRE.2015.2508960.

[46] L. Haertner *et al.*, “Effect of Fear of Falling on Turning Performance in Parkinson’s Disease in the Lab and at Home,” *Front. Aging Neurosci.*, vol. 10, no. MAR, pp. 1–8, Mar. 2018, doi: 10.3389/fnagi.2018.00078.

[47] M. El-Gohary *et al.*, “Continuous monitoring of turning in patients with movement disability,” *Sensors (Switzerland)*, vol. 14, no. 1, pp. 356–369, 2014, doi: 10.3390/s140100356.

[48] A. Weiss, T. Herman, N. Giladi, and J. M. Hausdorff, “Objective assessment of fall risk in Parkinson’s disease using a body-fixed sensor worn for 3 days,” *PLoS One*, vol. 9, no. 5, 2014, doi: 10.1371/journal.pone.0096675.

[49] T. Iluz *et al.*, “Automated detection of missteps during community ambulation in patients with Parkinson’s disease: a new approach for quantifying fall risk in the community setting,” *J. Neuroeng. Rehabil.*, vol. 11, no. 1, p. 48, 2014, doi: 10.1186/1743-0003-11-48.

[50] A. L. Silva de Lima *et al.*, “Home-based monitoring of falls using wearable sensors in Parkinson’s disease,” *Mov. Disord.*, vol. 35, no. 1, pp. 109–115, 2020, doi: 10.1002/mds.27830.

[51] A. Sturchio *et al.*, “Kinematic but not clinical measures predict falls in Parkinson-related orthostatic hypotension,” *J. Neurol.*, vol. 268, no. 3, pp. 1006–1015, 2021, doi: 10.1007/s00415-020-10240-8.

[52] S. Del Din, A. Godfrey, B. Galna, S. Lord, and L. Rochester, “Free-living gait characteristics in ageing and Parkinson’s disease: Impact of environment and ambulatory bout length,” *J. Neuroeng. Rehabil.*, vol. 13, no. 1, pp. 1–12, 2016, doi: 10.1186/s12984-016-0154-5.

[53] S. Del Din, A. Godfrey, and L. Rochester, “Validation of an Accelerometer to Quantify a Comprehensive Battery of Gait Characteristics in Healthy Older

Adults and Parkinson's Disease: Toward Clinical and at Home Use," *IEEE J. Biomed. Heal. Informatics*, vol. 20, no. 3, pp. 838–847, 2016, doi: 10.1109/JBHI.2015.2419317.

[54] W. Saadeh, S. A. Butt, and S. Member, "A Patient-Specific Single Sensor IoT-Based Wearable Fall Prediction and Detection System," *IEEE Trans. Neural Syst. Rehabil. Eng.*, vol. 27, no. 5, pp. 995–1003, 2019, doi: 10.1109/TNSRE.2019.2911602.

[55] X. Yu, H. Qiu, and S. Xiong, "A Novel Hybrid Deep Neural Network to Predict Pre-impact Fall for Older People Based on Wearable Inertial Sensors," *Front. Bioeng. Biotechnol.*, vol. 8, no. February, pp. 1–10, Feb. 2020, doi: 10.3389/fbioe.2020.00063.

[56] J. Shi, D. Chen, and M. Wang, "Pre-Impact Fall Detection with CNN-Based Class Activation Mapping Method," *Sensors*, vol. 20, no. 17, p. 4750, Aug. 2020, doi: 10.3390/s20174750.

[57] T. H. Kim, A. Choi, H. M. Heo, H. Kim, and J. H. Mun, "Acceleration Magnitude at Impact Following Loss of Balance Can Be Estimated Using Deep Learning Model," *Sensors*, vol. 20, no. 21, p. 6126, Oct. 2020, doi: 10.3390/s20216126.

[58] Y. Wu, Y. Su, R. Feng, N. Yu, and X. Zang, "Wearable-sensor-based pre-impact fall detection system with a hierarchical classifier," *Meas. J. Int. Meas. Confed.*, vol. 140, pp. 283–292, 2019, doi: 10.1016/j.measurement.2019.04.002.

[59] N. F. Ribeiro, J. André, L. Costa, and C. P. Santos, "Development of a Strategy to Predict and Detect Falls Using Wearable Sensors," *J. Med. Syst.*, vol. 43, no. 5, 2019, doi: 10.1007/s10916-019-1252-2.

[60] S. Liang, T. Chu, D. Lin, Y. Ning, H. Li, and G. Zhao, "Pre-impact Alarm System for Fall Detection Using MEMS Sensors and HMM-based SVM Classifier," in *2018 40th Annual International Conference of the IEEE Engineering in Medicine and Biology Society (EMBC)*, Jul. 2018, pp. 4401–4405, doi: 10.1109/EMBC.2018.8513119.

[61] Z. Zhong *et al.*, "A Real-time Pre-impact Fall Detection and Protection System,"

in *2018 IEEE/ASME International Conference on Advanced Intelligent Mechatronics (AIM)*, Jul. 2018, pp. 1039–1044, doi: 10.1109/AIM.2018.8452687.

[62] D. Ajerla, S. Mahfuz, and F. Zulkernine, "A Real-Time Patient Monitoring Framework for Fall Detection," *Wirel. Commun. Mob. Comput.*, vol. 2019, pp. 1–13, Sep. 2019, doi: 10.1155/2019/9507938.

[63] L. Rachakonda, A. Sharma, S. P. Mohanty, and E. Kougianos, "Good-Eye: A Combined Computer-Vision and Physiological-Sensor Based Device for Full-Proof Prediction and Detection of Fall of Adults," *IFIP Adv. Inf. Commun. Technol.*, vol. 574 IFIP, pp. 273–288, 2020, doi: 10.1007/978-3-030-43605-6_16.

[64] N. Zurbuchen, A. Wilde, and P. Bruegger, "A Machine Learning Multi-Class Approach for Fall Detection Systems Based on Wearable Sensors with a Study on Sampling Rates Selection," *Sensors*, vol. 21, no. 3, p. 938, Jan. 2021, doi: 10.3390/s21030938.

[65] C. Hsieh, H. Huang, K. Liu, C. Liu, C. Chan, and S. J. Hsu, "Multiphase Identification Algorithm for Fall Recording Systems Using a Single Wearable Inertial Sensor," *Sensors*, vol. 21, p. 3302, 2021, doi: 10.3390/s21093302.

[66] X. Yu, J. Jang, and S. Xiong, "A Large-Scale Open Motion Dataset (KFall) and Benchmark Algorithms for Detecting Pre-impact Fall of the Elderly Using Wearable Inertial Sensors," *Front. Aging Neurosci.*, vol. 13, no. July, pp. 1–14, 2021, doi: 10.3389/fnagi.2021.692865.

[67] G. Šeketa, L. Pavlaković, D. Džaja, I. Lacković, and R. Magjarević, "Event-Centered Data Segmentation in Accelerometer-Based Fall Detection Algorithms," *Sensors*, vol. 21, no. 13, p. 4335, Jun. 2021, doi: 10.3390/s21134335.

[68] H. Jung, B. Koo, J. Kim, T. Kim, Y. Nam, and Y. Kim, "Enhanced Algorithm for the Detection of Preimpact Fall for Wearable Airbags," *Sensors*, vol. 20, p. 1277, 2020, doi: 10.3390/s20051277.

[69] M. Saleh and R. L. B. Jeannes, "Elderly Fall Detection Using Wearable Sensors: A Low Cost Highly Accurate Algorithm," *IEEE Sens. J.*, vol. 19, no. 8, pp. 3156–3164,

2019, doi: 10.1109/JSEN.2019.2891128.

[70] Y. Harari, N. Shawen, C. K. Mummidisetty, M. V. Albert, K. P. Kording, and A. Jayaraman, “A smartphone-based online system for fall detection with alert notifications and contextual information of real-life falls,” *J. Neuroeng. Rehabil.*, vol. 18, no. 1, pp. 1–13, 2021, doi: 10.1186/s12984-021-00918-z.

[71] G. Serpen and R. H. Khan, “Real-time detection of human falls in progress: Machine learning approach,” *Procedia Comput. Sci.*, vol. 140, pp. 238–247, 2018, doi: 10.1016/j.procs.2018.10.324.

[72] “XIO TECHNOLOGIES,” *NGIMU*. https://x-io.co.uk/ngimu/ (accessed Dec. 07, 2021).

[73] “IGNITEC,” *NGIMU*. https://www.ignitec.com/work/ngimu/ (accessed Dec. 07, 2021).

[74] M. T. Silva, E. T. F. Santos, L. S. Batista, J. M. Araújo, J. M. Araujo, and L. S. Batista, “Alternative analytical solution for position and orientation in electromagnetic motion tracking systems,” *WSEAS Trans. Syst.*, vol. 16, no. August, pp. 225–233, 2017, [Online]. Available: http://www.wseas.org/multimedia/journals/systems/2017/a505802-879.php.

[75] “Villa dei Pini,” *Home Page*. https://www.casadicuravillapini.it/ (accessed Dec. 06, 2021).

[76] M. H. Pham *et al.*, “Validation of a step detection algorithm during straight walking and turning in Patients with Parkinson’s disease and older adults using an inertial measurement unit at the lower back,” *Front. Neurol.*, vol. 8, no. SEP, pp. 1–9, 2017, doi: 10.3389/fneur.2017.00457.

[77] A. Weiss *et al.*, “Does the evaluation of gait quality during daily life provide insight into fall risk? A novel approach using 3-Day accelerometer recordings,” *Neurorehabil. Neural Repair*, vol. 27, no. 8, pp. 742–752, 2013, doi: 10.1177/1545968313491004.

[78] M. Kangas, A. Konttila, P. Lindgren, I. Winblad, and T. Jämsä, “Comparison of

low-complexity fall detection algorithms for body attached accelerometers," *Gait Posture*, vol. 28, no. 2, pp. 285–291, 2008, doi: 10.1016/j.gaitpost.2008.01.003.

[79] A. Weiss, S. Sharifi, M. Plotnik, J. P. P. Van Vugt, N. Giladi, and J. M. Hausdorff, "Toward automated, at-home assessment of mobility among patients with Parkinson disease, using a body-worn accelerometer," *Neurorehabil. Neural Repair*, vol. 25, no. 9, pp. 810–818, 2011, doi: 10.1177/1545968311424869.

[80] J. L. Roche, K. A. Lowry, J. M. VanSwearingen, J. S. Brach, and M. S. Redfern, "Harmonic ratios: A quantification of step to step symmetry," *J. Biomech.*, vol. 46, no. 4, pp. 828–831, Feb. 2013, doi: 10.1016/j.jbiomech.2012.12.008.

[81] J. M. Barden, C. A. Clermont, D. Kobsar, and O. Beauchet, "Accelerometer-based step regularity is lower in older adults with bilateral knee osteoarthritis," *Front. Hum. Neurosci.*, vol. 10, no. DEC2016, pp. 1–9, 2016, doi: 10.3389/fnhum.2016.00625.